IDENTIFICATION AND ANALYSIS OF GOLGI TRANSPORTERS THAT PROVIDE HOMEOSTASIS FOR GLYCOSYLATION AND OTHER GOLGI PROCESSES

by

Nathan A. Snyder

A dissertation submitted to Johns Hopkins University in conformity with the requirements for the degree of Doctor of Philosophy

Baltimore, Maryland

October, 2018

ABSTRACT

The Golgi apparatus of eukaryotes is a critical organizing center that is responsible for protein and lipid maturation, sorting, and trafficking. Because of the diverse population of proteins and lipids being modified at any given time, the Golgi is host to a large collection of resident enzymes and transporters that are required to achieve the necessary modifications. Many of the Golgi resident proteins, accounting for a large portion of the entire genome, are involved in the process and regulation of glycosylation, the process by which complex oligosaccharides are assembled on proteins and lipids. These oligosaccharides assist in folding, stability, and trafficking of the substrate molecule. The complex nature of the reactions and mechanisms taking place within the Golgi require careful maintenance of the homeostatic balance of all substrates, cofactors, and products, because failure of any single component could result in downstream consequences that compound to become very dangerous for the cell. The mechanisms and transporters of the Golgi apparatus are reviewed in Chapter 1. This dissertation aims to elucidate the roles of several transporters involved in Golgi homeostasis, which have roles in regulating the pH as well as concentrations of Ca^{2+}, Mn^{2+}, and inorganic phosphate (Pi), and identify a new method that may be used to screen antifungals for essential protein targets, including those affiliated with Golgi processes.

In the second chapter, I identify a new highly conserved class of reversible H^{+}/Ca^{2+} exchanger in the Golgi of yeast, Gdt1. Through genetic analysis, I demonstrate that Gdt1 functions alongside the secretory pathway Ca^{2+} ATPase, Pmr1, to supply Ca^{2+} to the Golgi apparatus and detoxify high levels of Ca^{2+} in the cytoplasm. I further show that this activity requires the establishment of a pH gradient, generated by the V-ATPase

between the Golgi and cytoplasm. Interestingly, abolishment of this pH gradient by deletion of the V-ATPase resulted in Gdt1 instead removing Ca^{2+}, supplied by Pmr1, from the Golgi, demonstrating the reversibility of the H^{+}/Ca^{2+} exchange. I also identify and characterize another Golgi transporter of yeast, Erd1, which functions to recycle Pi from the Golgi to the cytoplasm, as it is otherwise lost to the environment through the secretory pathway. This Pi was produced from the breakdown of the GDP byproduct of glycosylation into Pi and GMP, which is recycled by Vrg4 for GDP-mannose, needed for further glycosylation reactions.

In Chapter 3, I investigate the mammalian homolog of Gdt1, TMEM165, and its role in lactation in mice. I present evidence that TMEM165, the expression of which is highly upregulated in the mammary gland during lactation, supplies the Golgi with Mn^{2+}, required for activity of lactose synthase, along with Ca^{2+}, secreted into milk as a component of casein micelles, while removing H^{+}, released by lactose synthesis and glycosylation, to prevent acidification of the Golgi. A mouse model, deficient for TMEM165 in the mammary gland, exhibited decreased secretion of lactose into milk, which reduced the osmotic potential of the milk, decreasing its volume, and concentrating the protein and nutritional metals it contains. This ultimately decreased the nutritional quality of the milk, resulting in low weight gain in pups nursed by these mothers.

Chapter 4 develops and examines a new technology that can be used to study essential genes in yeast. A collection of yeast strains containing genes expressing proteins tagged with the auxin-inducible degron (AID) was generated. The AID tag enables proteins to be rapidly ubiquitylated and targeted for degradation after the addition of the drug auxin. I analyze the ability of this system to be used in the screening of tagged yeast

strains for sensitivity or resistance to various drugs and inhibitors. Using co-varied concentrations of auxin and SDZ 90-215, I demonstrated that a yeast strain containing AID-tagged Vrg4 displayed synergistic sensitivity to the combination of drugs. Further analysis demonstrated that SDZ 90-215 inhibits the activity of Vrg4, blocking the transport of GDP-mannose into the Golgi of yeast, preventing glycosylation of proteins and lipids. This inhibition ultimately kills the yeast cell, allowing SDZ 90-215 to function as a fungicide.

The final chapter provides a summary of the implications of the major findings in this work and provides insight into future directions that research into these topics may take.

Thesis Advisor: Dr. Kyle W. Cunningham

Thesis Reader: Dr. Miles Andrew Hoyt

ACKNOWLEDGEMENTS

Thank you to all of the people that have supported me through the process of accomplishing this work. Your insight and assistance have helped me become the scientist that I am today. Without the technical expertise, ideas, and patience all of you have given me, none of this would be possible.

In particular, I would like to thank my mentor, Kyle Cunningham, for all the effort he has put into shaping my scientific intellect and technical ability. You have continually driven me to grow and improve as a researcher, and your excitement and drive in all of our scientific pursuits has always been a great asset toward motivating me to keep working. I would also like to thank the other members of my committee, Trina Schroer, Haiqing Zhao, and Valeria Culotta, for their constructive criticism and direction that has helped drive this work forward to completion. Thank you to the administration of the department, especially to Joan Miller, Cindy Holstein, Barb Birsit, and Chuck Stenley for all of your efforts to keep the department and myself working with efficiently.

Thank you to the members of my lab, especially Adam Kim, Andrew Gale, and Matthew Pavesic. You helped me hone my abilities and maintained a cheerful environment within the lab. Thank you to my friends, whom have always lended me the support, expertise, and even couches (Emily Scott-Solomon) that was necessary to complete this dissertation.

Thank you to my family for helping to shape me into the person I am today and giving me the drive to pursue science and knowledge every day. And of course, thank you to my wife, Yael Gau Snyder. You have stuck by me throughout everything, and provided me with the motivation to move toward a bright future.

TABLE OF CONTENTS

LIST OF TABLES

LIST OF FIGURES

CHAPTER 1

INTRODUCTION

ABSTRACT

The eukaryotic Golgi apparatus functions as the central hub for the maturation, sorting, and trafficking of newly synthesized proteins and lipids. It therefore plays a critical role in providing the machinery required for nearly all cellular processes. The Golgi contains numerous resident enzymes, which carry out the required modifications to proteins and lipids, such as glycosylation, as well as transporters that supply these enzymes with the necessary resources to fulfil this task. There exists a complex and diverse population of proteins in the Golgi, with each enzyme requiring specific conditions, cofactors, and substrates to carry out its function. On account of this, mechanisms have been developed to maintain homeostasis within the Golgi of numerous factors. These homeostatically controlled factors include pH, metal cofactors for enzymes, nucleotide sugars, phosphates, and concentration and localization of the enzymes themselves. Described below is a review of the pathways and mechanisms by which the homeostasis of the Golgi is maintained and the negative downstream effects and disorders that result when this homeostasis is no longer regulated.

GLYCOSYLATION

A major function of the Golgi complex is to decorate proteins and lipids with elaborate oligosaccharide chains through a variety of coordinated glycosylation reactions. This process requires numerous glycosyltransferases of different substrate specificities to be organized within the Golgi and continuously supplied. An estimated 1% of the human genome is devoted to this purpose (Freeze 2006). Almost all secretory proteins receive these post-translational modifications, which contribute to the normal

folding, assembly, stability, solubility, and trafficking of the glycoproteins (Hebert *et al.* 2014). Glycoproteins and glycolipids on the cell surface can aid in cell-cell adhesion, and they are even used for recognition by immune cells (Varki 1993; Lowe 2003; Cobb and Kasper 2005).

GLYCOPROTEINS

Proteins can be glycosylated in several different ways. The two most common forms of glycosylation are N-linked and O-linked (Varki 1993). In N-linked glycosylation, carbohydrates are first added to the amide nitrogen of an asparagine residue within an N-x-S/T motif by an oligosaccharyl transferase in the endoplasmic reticulum (Marshall 1972). In O-linked glycosylation, sugars are instead added to the hydroxyl group of a serine and threonine in O-linked glycosylation (Wilson *et al.* 1991). In both cases, additional glycosyltransferases in the Golgi can elaborate further modifications.

Due to the stereospecificity of glycosyltransferases, the sequence of carbohydrates added to a glycoprotein are dependent on the protein sequence and the sequence of carbohydrates already present, (Stanley 2011; Liang *et al.* 2015). In fact, glycosyltransferases that have the same specificity for donor nucleotide sugars could have unique acceptor specificity, meaning that a single sugar addition could completely alter the potential final sequence of carbohydrates on the glycoprotein (Reynders *et al.* 2011). The carbohydrate sequence is also regulated by the availability of glycosyltransferases present in the Golgi at the time (Reynders *et al.* 2011). This means

that glycosylation can also be regulated at the transcriptional level or by modifications to the glycosyltransferases that alter the localization between the ER and Golgi apparatus.

The process of N-linked glycosylation, outlined in Figure 1.1, begins within the rough ER, where a preformed oligosaccharide is transferred to the asparagine residue of the protein (Waechter and Lennarz 1976). The assembly of the oligosaccharide begins by adding two N-acetyl glucosamine and five mannose molecules to dolichol pyrophosphate embedded within the ER membrane on the cytoplasmic face (Helenius and Aebi 2001). At that point, the oligosaccharide is flipped to the luminal side of the membrane, where an additional four mannose and three glucose molecules are added to complete the oligosaccharide precursor, abbreviated as Glc3Man9(GlcNAc)2 (Hubbard and Robbins 1980). Once this is transferred from the dolichol pyrophosphate to the nascient polypeptide, the glucose molecules and one of the mannose molecules are sequentially removed prior to transport of the glycoprotein to the Golgi, where processing is completed by further additional and/or removal of carbohydrates by Golgi lumen-resident enzymes (Trombetta 2003).

Alternatively, in O-linked glycosylation, all carbohydrates are instead added individually, with each addition being carried out by a unique glycosyltransferase, dependent on the carbohydrate being added (den Steen *et al.* 2008). These glycosyltransferases all operate within the luminal face of either the rough ER or the Golgi (Boulan *et al.* 1978). The initial carbohydrate in these reactions can differ, depending on the tissue in which the synthesis is occurring or the subcellular localization fate of the protein (Roth *et al.* 1986).

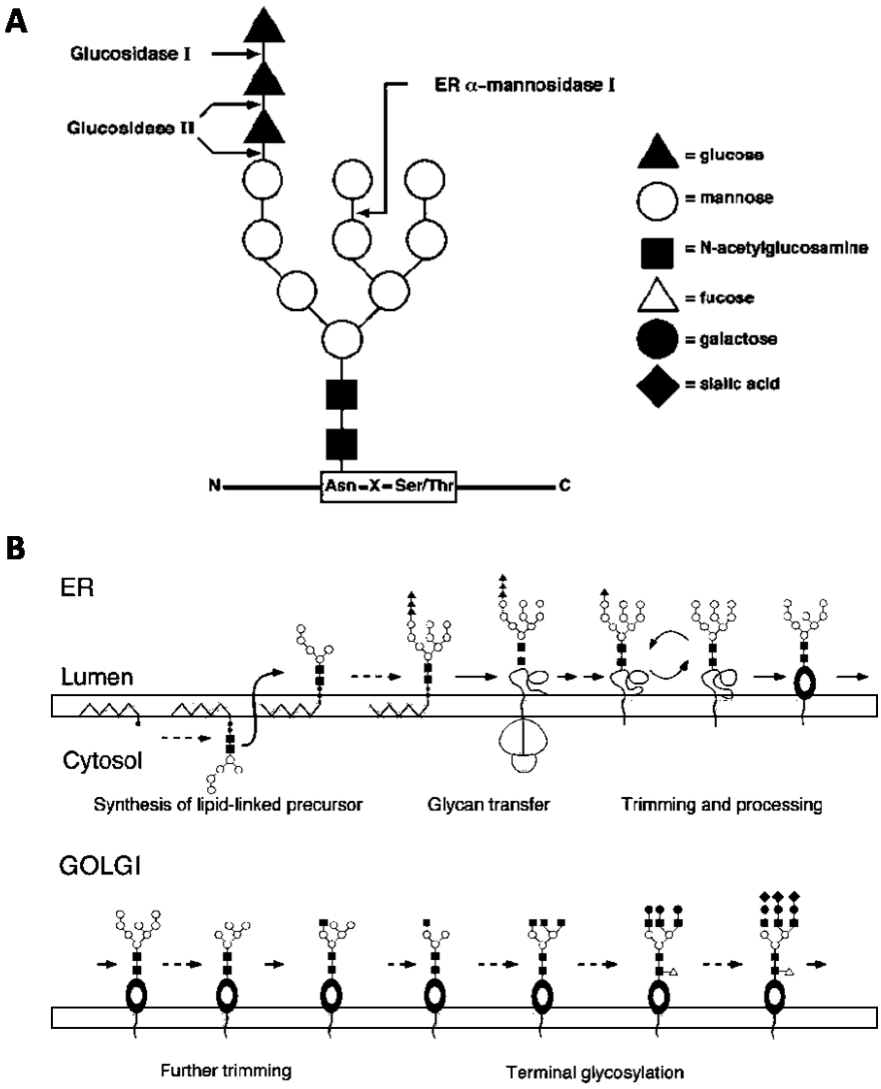

Figure 1.1: N-glycosylation structures within the ER and Golgi apparatus.

The structure of the N-linked core oligosaccharide (A) is comprised of 2 GlcNAc, 9 mannose, and 3 glucose sugars in the orientation shown, bound to the amine nitrogen of an asparagine residue of an N-x-S/T motif. As shown in (B), the assembly of this structure begins on the cytoplasmic face of the ER, prior to moving to the luminal face for completion. The resulting glycopeptide undergoes trimming and processing, prior to being sent to the Golgi apparatus for further modifications. This figure was adapted from Helenius and Aebi (2001).

GLYCOLIPIDS

Sphingolipids are the most abundant molecule in the plasma membrane of both mammals and yeast (Fröhlich *et al.* 2015). In the case of mammals, the major sphingolipids are sphingomyelin and glucosylceramides, while they are inositol phosphorylceramides (IPCs) in yeast (Levine *et al.* 2000). In either case, these sphingolipids are synthesized in the Golgi complex by glycosylation of ceramides that arrive from the ER mainly via vesicular transport (Levine *et al.* 2000). Ceramides are extremely toxic to both yeast and mammalian cells, so *de novo* ceramide synthesis is tightly coupled to ceramide conversion into sphingolipids (Daido *et al.* 2004; Guenther *et al.* 2008; Klug and Daum 2014). Therefore, the glycosylation of ceramides in the Golgi complex can be crucial for cell survival. These modifications assist in targeting these sphingolipids to the plasma membrane and the maintenance of their stability once there (Breslow and Weissman 2010).

GLYCOSYLTRANSFERASES

Glycosyltransferases with different substrate specificities can be differentially localized to the ER, cis-, medial-, and trans-Golgi compartments, and thus generate intricate patterns of glycosylation (Schoberer and Strasser 2011). Almost all glycosyltransferases require Mn^{2+} as an essential cofactor, though Ca^{2+} is also utilized in some cases (Dürr *et al.* 1998). Their activities are also highly sensitive to pH (Rivinoja *et al.* 2009; Hassinen *et al.* 2011). Two categories of sugar transfer mechanism have been established for glycosyltransferases: inverting, where the primary carbon of the donor

sugar changes stereochemistry, and retaining, where the configuration of the sugar is maintained (Lairson *et al.* 2008).

In inverting glycosylation (see Figure 1.2), a catalytic base of the glycosyltransferase (usually from an aspartate, glutamate, or histidine side chain) removes a proton from the functional group of the target acceptor, allowing for it to conduct a nucleophilic attack on the primary carbon of the sugar from the donor nucleotide sugar, thus forming a glycosidic bond and freeing the sugar from the nucleotide phosphate (Krupicka and Tvaroska 2009). The exact mechanism of retaining glycosylation remains a matter of research and debate. One potential mechanism performs a two round of inverting glycosylation, where the sugar initially binds to the transferase in the inverted confirmation before being transferred to the acceptor, reclaiming the original confirmation (Ardevol *et al.* 2016). The other popular hypothesis proposes that there is no catalytic base in these transferases, and therefore glycosyltransferase instead serves to protect the sugar from nucleophilic attack on one side, forcing the acceptor to instead form the glycosidic bond with the sugar retaining its confirmation (Ardevol *et al.* 2016).

NUCLEOTIDE-SUGAR TRANSPORTERS

The key substrates used for glycosylation are nucleotide-sugars, which are synthesized in the cytoplasm and transported to the lumen of the ER and Golgi complex (Stanley 2011; Orellana *et al.* 2016). Mammalian cells utilize a large repertoire of nucleotide-sugar molecules (Table 1.1) while yeast is much simpler (Hirschberg 1997). In the yeast Golgi, only GDP-mannose is utilized by a variety of mannosyltransferases,

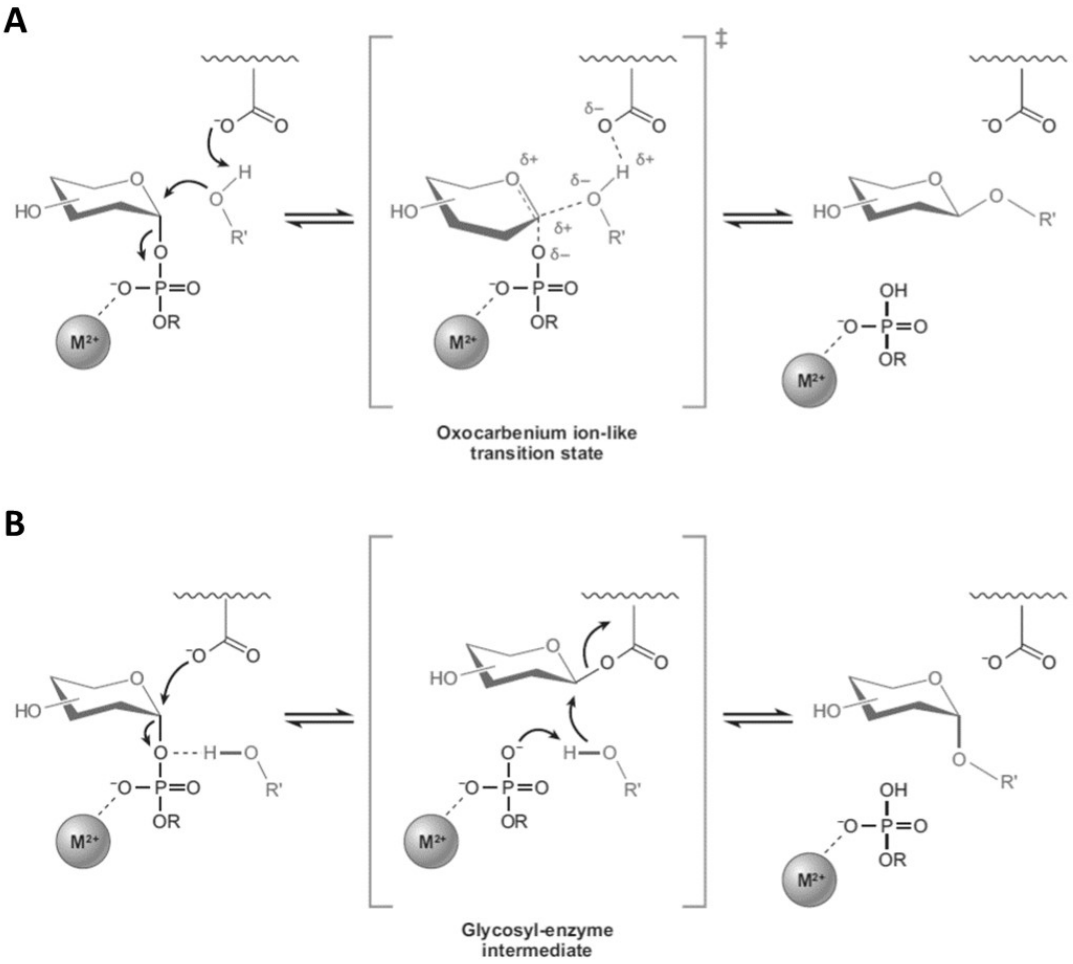

Figure 1.2: Mechanisms of glycosyltransfer during glycosylation.

The direct displacement mechanism used by inverting glycosyltransferases (A) and the hypothesized double-displacement mechanism used by retaining glycosyltransferases (B) are depicted. In either mechanism, a divalent cation, usually Mn^{2+} is utilized as a cofactor to stabilize the negative charge of the phosphate leaving group. This figure was adapted from Lairson, et al. (2008).

Table 1.1: Common nucleotide sugars utilized in glycosylation reactions

Glycans	Abbreviation	Species	Donor
D-Glucose	Glc	Mammals, plants	UDP-sugar
D-Galactose	Gal	Mammals, plants	
N-Acetyl-D-glucosamine	GlcNAc	Yeast, mammals, plants, insects	
N-Acetyl-D-galactosamine	GalNAc	Mammals	
D-Glucouronic Acid	GlcA	Mammals	
D-Xylose	Xyl	Mammals, plants	
D-Mannose	Man	Yeast, mammals, plants, insects	GDP-sugar
L-Fucose	Fuc	Mammals, plants, insects	
Sialic Acid	Sia	Mammals	CMP-Sia

and therefore only one nucleotide-sugar transporter is required in that organelle (Abeijon *et al.* 1989). Nucleotide-sugar transporters (NST's) of appropriate specificity supply the organelles with nucleotide-sugars and also counter-transport the nucleoside monophosphate byproduct of glycosylation. This nucleoside monophosphate is itself a product, along with inorganic phosphate and H^+ byproducts, of the breakdown of nucleoside diphosphates by apyrase-like nucleoside diphosphatases (Figure 1.3) (Perez and Hirschberg 1985; Milla *et al.* 1992). The counter-transport of nucleotide-sugars and nucleoside monophosphates is thought to be electroneutral, and thus both molecules constantly flow down their concentration gradients without the need for an energy source (Capasso and Hirschberg 1984). The main NST of the yeast Golgi, the GDP-mannose/GMP exchanger known as Vrg4, is essential for viability of multiple yeast species including the human pathogens *Candida glabrata* and *Candida albicans* (Poster and Dean 1996; Dean *et al.* 1997; Nishikawa *et al.* 2002a, 2002b). In chapter 4, I identify the first specific inhibitor of Vrg4 and demonstrate its antifungal properties. In mammals, the NSTs are classified into 7 subfamilies of the SLC35 superfamily, based on sequence similarity and then by the type of substrate transported (Hadley *et al.* 2014).

TRANSPORT OF Mn^{2+} AND Ca^{2+}

In order to stabilize the negative charges of the phosphate groups during glycosylation, the glycosyltransferases require a cofactor of Mn^{2+} (Dürr *et al.* 1998). Mn^{2+} is a transition metal used as a cofactor in many redox reactions (Thielges *et al.* 2005). A family of secretory pathway calcium ATPase (SPCA's) that localize to the Golgi complex are responsible for supplying the Golgi with Mn^{2+} in addition to Ca^{2+}

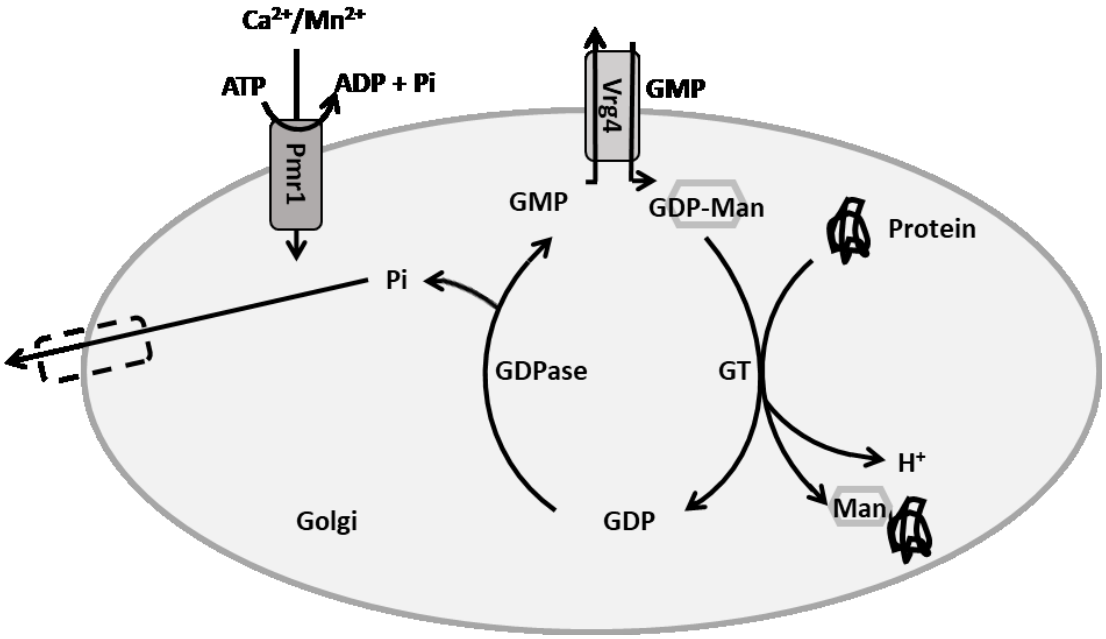

Figure 1.3: Model of transport of cofactors, donors, and byproducts of glycosylation into/out of the Golgi apparatus in yeast

GDP-mannose is utilized as a sugar donor by a galactosyltransferase (GT) to transfer a mannose to modify a glycopeptide. This transfer requires a cofactor of Ca^{2+} or Mn^{2+}, which is supplied by Pmr1, and results in the release of a proton and GDP as a byproduct. This GDP is cleaved to form GMP, which is recycled to the cytoplasm in exchange for GDP-mannose to continue additional glycosylation reaction by Vrg4, and inorganic phosphate, which is hypothesized to be recycled to the cytoplasm as well by an undermined mechanism.

(Lapinskas *et al.* 1995; Dürr *et al.* 1998; Ton *et al.* 2002). There are three SPCA's in human, that each exhibit different patterns of expression, while there is only one in yeast (termed Pmr1) (Ton *et al.* 2002). Unlike the SERCA-family and PMCA-family of Ca^{2+} ATPases that localize to the ER and plasma membrane (or fungal vacuole) respectively, SPCA's cannot countertransport H^+ during Ca^{2+} transport and therefore cannot serve as a channel for proton release from the Golgi lumen (Niggli *et al.* 1982; Dode *et al.* 2006; Hauser and Barth 2007). The dual-ion selectivity of SPCA's can be altered with amino acid substitutions. The Q783A mutation in Pmr1 abolishes Mn^{2+} transport but not Ca^{2+} transport, resulting in glycosylation defects (Wei *et al.* 2000).

In yeast, expression of Pmr1 and Pmc1 (the PMCA-family pump localized to the vacuole) can be up-regulated by the activation of the transcription factor Crz1. Crz1 is activated by the Ca^{2+}/calmodulin-activated protein phosphatase known as calcineurin (Klee *et al.* 1979; Matheos *et al.* 1997). Thus, when cytosolic free Ca^{2+} levels rise, the up-regulation of these Ca^{2+} ATPases helps restore the basal Ca^{2+} levels. The *pmr1*Δ knockout mutant is viable because Pmc1 expression is up-regulated and the Ca^{2+} pump is partially mislocalized to the Golgi (Marchi *et al.* 1999). The *pmr1*Δ *pmc1*Δ double mutant is not viable, suggesting a critical role for Ca^{2+} or Mn^{2+} in the secretory pathway (Cunningham and Fink 1994). Indeed, the *pmr1*Δ mutant responds to depletion of Ca^{2+} and Mn^{2+} by activating a Ca^{2+} influx channel in the plasma membrane that helps resupply the depleted organelles (Locke *et al.* 2000).

When cytoplasmic calcium levels increase, the resulting activation of calcineurin not only induces Pmr1 and Pmc1 expression but also inhibits the activity of the vacuolar H^+/Ca^{2+} exchanger (Vcx1) to help spare Ca^{2+} for use in the Golgi (Cunningham and Fink

1996). The precise mechanism by which calcineurin inhibits the activity of Vcx1 remains to be determined. Recent reports suggest that calcineurin can regulate the localization of the plasma membrane proton exporter, Pma1, decreasing the pH of the cytoplasm, and potentially limiting the pH gradient that Vcx1 utilizes for transport of Ca^{2+} (Velivela and Kane 2017). This also has the potential of developing a double-negative feedback loop, which stabilizes the state in which one pathway or the other is fully active, between calcineurin and Vcx1, since the sequestration of Ca^{2+} into the vacuole by Vcx1 would limit the activation of calcineurin. These regulatory mechanisms ensure proper Ca^{2+} and Mn^{2+} homeostasis in the organelles of yeast over a broad range of environmental conditions.

Unlike the ER, which stores calcium at concentration between 400 and 700 μM, the Golgi apparatus has a gradient of Ca^{2+} storage concentrations, reaching as high as 300 μM at the *cis*-Golgi and as low as 130 μM at the *trans*-Golgi (Pinton *et al.* 1998; Micaroni 2012). The differences in calcium storage within the different Golgi compartments is likely due to differences in localization of Ca^{2+} transporters across the Golgi apparatus (Pizzo *et al.* 2011). Interestingly, Golgi compartments that harbor SPCA1 are uniquely resistant to inositol triphosphate (IP_3) signaling, which stimulates Ca^{2+} release from the ER and *cis*-Golgi compartments, due to a low abundance of the IP_3 receptor (Lissandron *et al.* 2010). Furthermore, when Ca^{2+} is released from both organelles, the release from the Golgi apparatus terminates more quickly than that from the ER (Missiaen *et al.* 2004). These differences in Ca^{2+} retention may be the result of the need to maintain Ca^{2+} stores within the Golgi, particularly at the *trans*-Golgi, for use in vesicular transport and membrane trafficking (Hu *et al.* 2002). A distinct mechanism

operates in mammalian cells to resupply the ER when it is depleted of Ca^{2+} and the responses to Golgi Ca^{2+}/Mn^{2+} depletion have not been studied (Wuytack *et al.* 2002). Though there was no apparent need for any other Ca^{2+} transporter in the Golgi complex, we nonetheless discovered an entirely new class of Golgi-localized H^{+}/Ca^{2+} exchanger that is conserved in yeast and mammals and most other eukaryotes. These studies are described in chapter 2.

The discovery of a Golgi-resident exchanger capable of transporting Ca^{2+} is interesting, because it adds a new dynamic to Ca^{2+} homeostasis. While ATPases like Pmr1 or Pmc1 utilize energy from the hydrolysis of ATP to transport Ca^{2+} unidirectionally across the membrane, exchangers are instead governed by relative concentrations of ions on either side of the membrane, as is the case with Na^{+}/Ca^{2+} exchangers in animals (Harper and Sage, 2016). Exchangers start with the active site exposed to either the luminal or cytoplasmic side of the membrane, where a compatible ion will bind, triggering a confirmation shift that exposes the active site to the opposite side of the membrane, where the ion is released (Hilgemann *et al.*, 1991). Any compatible ion can be transported in either direction across the membrane, so net transport is only positive or negative if there is a concentration gradient that increases the likelihood that one ion will be bound on one side of the membrane. If the concentration of an ion is equivalent on either side of the membrane, it is transported in both directions, results in no net change in the luminal/cytoplasmic concentrations. Low abundance of compatible ions on either side of the membrane halt transport, due to inavailability of substrate. An exchanger capable of transporting three or more different ion species would have the ability to transport the ions in different combinations and directions, adding to

the complexity of the system. In the case of Vcx1, the low luminal pH within the vacuole means that, when the active site is exposed to the vacuolar lumen, it is far more likely to bind a proton than Ca^{2+} (Cunningham and Fink, 1996). The likelihood of binding Ca^{2+} increases when open to the cytoplasmic face, enabling unidirectional transport into the vacuole, against its concentration gradient, utilizing the pH-gradient of the vacuole.

PROTON-ATPases

The glycosylation reactions that occur within the Golgi cisternae require a pH that is more acidic than those of the cytoplasm, requiring the establishment of a pH gradient on either side of the membrane. In most cell types, the primary driver of protons from the cytoplasm to the Golgi is thought to be the V-ATPase (Forgac 2007). V-ATPases are multi-subunit proton pumps driven by the hydrolysis of ATP that acidify the various organelles of the cell, including the Golgi, endosome, and lysosome (or vacuole in fungi and plants) (Nelson and Harvey 1999).

The V-ATPase is comprised of two sectors, each made up of multiple protein components. The catalytic sector, V_1, is responsible for ATP hydrolysis, and the transmembrane sector, V_0, functions as a proton turbine (Nelson and Taiz 1989). There are different isoforms of the V-ATPase that are specific to distinct organelles and/or tissues. In yeast, there are two isoforms for the major subunit of the V_0 domain, Vph1 and Stv1 (Manolson *et al.* 1992, 1994). The Vph1 isoform localizes to the vacuole, while the Stv1 isoform localizes to the Golgi apparatus and endosome (Manolson *et al.* 1992; Kawasaki-Nishi *et al.* 2001). Vph1 is capable of suppressing *stv1Δ* mutations, compensating for the loss to prevent phenotypic presentation, while Stv1 is only able to

mask the effects of *vph1Δ* mutations when overexpressed (Manolson *et al.* 1994). *stv1Δvph1Δ* double knockout strains are viable, but slow-growing, similar to knockout mutants of the other V1 and V0 subunits (Nelson and Nelson 1990). In mammalian cells, all the V-ATPase subunits are essential for survival (Nelson *et al.* 2000; Breton and Brown 2013). The reason why yeast cells can survive without the V-ATPase is because a completely different H^+-pumping ATPase, termed Pma1, becomes partially relocalized from the plasma membrane and serves to weakly acidify the intracellular secretory organelles (Mason *et al.* 1998). Homologs of Pma1 are present in all fungi and plants, but not animals (Møller *et al.* 1996).

The V-ATPase can be regulated by the reversible disassembly of V_0 and V_1 subunits (Kane 1995; Sumner *et al.* 1995). This has been shown to occur in yeast during glucose deprivation, which interestingly does result in alkalization of the vacuole, raising the pH of the vacuolar lumen (Sautin *et al.* 2005). While dissociated, the V1 subunit remains in close proximity to the membrane, but neither ATP hydrolysis nor H^+ transport occur (Zhang *et al.* 1992; Parra *et al.* 2000; Tabke *et al.* 2014). Subsequent re-addition of glucose causes a pH decrease and the reassembly of the V-ATPase (Sautin *et al.* 2005). The mechanism of this regulation is not fully understood. V-ATPase is also regulated by extracellular pH, as it remains assembled in high pH conditions, even during glucose deprivation (Diakov and Kane 2010).

PROTON LEAK

When the V-ATPase is inhibited, such adding the compound concanamycin, the pH of the Golgi increases to become nearly equivalent to that of the cytoplasm (Kim *et*

al. 1996; Schapiro and Grinstein 2000). This demonstrates the existence of a constitutive mechanism by which protons leak from the Golgi, assumedly for the purpose of preventing overacidification of the Golgi by the V-ATPase. The leak was still evident after the cell membrane was permeabilized with streptolycin O (SLO) to remove cytoplasmic contents, demonstrating that it is not due to vesicular traffic, which might have delivered a higher pH buffer from the ER while removing lower pH buffers to the secretory pathway (Schapiro and Grinstein 2000). Instead, the proton leak can be attributed to either the existence of unknown uncouplers, which could dissipate the pH gradient, possibly as a proton channel, or transporters that couple H^+ efflux to transport of other ions or organic molecules (Nakamura *et al.* 2005). In yeast mutants that lack an endosomal Na^+/H^+ exchanger (Nhx1) or a vacuolar H^+/Ca^{2+} exchanger (Vcx1), proton leakage from the Golgi still occurred while proton leakages from those organelles were significantly diminished (Cagnac *et al.* 2010). While the source of the Golgi proton leak is not known, in later chapters I report the discovery and characterization of a novel Golgi-localized H^+/Ca^{2+} exchanger in yeast (Gdt1) and mammals (TMEM165).

GOLAC, AN ANION CHANNEL

The electrogenic transport of protons to the Golgi by the V-ATPase not only creates a pH gradient between the Golgi lumen and the cytoplasm, but it also generates a positive electrical potential, or charge imbalance, that would inhibit further transport of positively charged ions if not corrected (Glickman *et al.* 1983; Rybak *et al.* 1997). This charge imbalance is largely reduced by the Golgi anion channel (GOLAC) (Nordeen *et al.* 2000; Thompson *et al.* 2002). This channel is approximately 6 times more selective

for Cl^- than it is for K^+, and it is open over 95% of the time (Thompson *et al.* 2002). This constitutively open state, combined with a lack of specificity for any particular anion size, has led to the hypothesis that GOLAC serves not only to balance the charge imbalance created by the V-ATPase, but also to allow the release of inorganic phosphate, created as a byproduct of reactions like glycosylation, from the Golgi (Nordeen *et al.* 2000; Hirschberg 2001). This is supported by GOLAC being more permeant to $H_2PO_4^-$ than HPO_4^{2-}, because the acidic environment of the Golgi would make the former species more prevalent in the lumen, while the latter is more prevalent in the cytoplasm (Nordeen *et al.* 2000). GOLAC has even been shown to have the potential to allow movement of ATP into the Golgi lumen where it can be utilized to provide energy to various reactions (Thompson *et al.* 2006).

Fungi do not possess homologs of GOLAC, but do express a voltage-gated chloride channel in the Golgi (Gef1 in yeast) that participates in acidification by dissipating the charge imbalances (Huang *et al.* 1994; Gaxiola *et al.* 1998). As described in chapter 2, I discovered a homolog of phosphate transporters that recycles the Pi, produced in the Golgi through glycosylation reactions, back to the cytoplasm for reuse. This way, the critical nutrient is not lost to the environment through the secretory pathway.

BYPRODUCT REMOVAL

Above, I have reviewed the basic mechanism by which the Golgi complex is supplied with the raw materials that are necessary for glycosylation. The constant 1:1 exchange of nucleotide-sugar with nucleoside monophosphate continuously supplies the

glycosyltransferases, which require an acidic pH and Mn^{2+} (Capasso and Hirschberg 1984; Dürr *et al.* 1998). However, several questions remain about the homeostasis of this system. First, it is not clear how the system can amplify itself during cell growth and proliferation since only stoichiometric exchange reactions are known. What is missing from all textbook accounts is a transporter that increases nucleotide-sugar concentration above the 1:1 exchange to enable duplication of Golgi complex during cell division. Second, while the inorganic phosphate generated in the Golgi can be released to the extracellular fluids in metazoans without loss to the environment, this would be a costly loss of nutrients to yeasts, which often grow naturally in phosphate-poor environments. As mentioned earlier, in chapter 2 I will define a novel Golgi-localized Pi-recycling transporter in yeast, termed Erd1. Third, there are 1 to 2 protons generated during each glycosylation cycle even after considering the buffering by Pi (Persson and Palcic 2008). In professional secretory cells, which function to rapidly synthesize, fold, and secrete numerous functional proteins, the need for glycosylation can be huge, meaning it may be necessary to actively transport H^+ out of the Golgi to ensure proper pH management. In chapters 2 and 3, I define a novel family of H^+/Ca^{2+} exchangers in both yeast and mouse (Gdt1 and TMEM165) that fulfils this role.

LACTATION

Mammals are defined as a group by their ability to produce and secrete milk. Within their mammary glands, polarized alveolar epithelial cells develop and these professional secretory cells generate essentially all the components of milk (Boutinaud *et al.* 2004). The Golgi complex plays a central role in this process because it is the site of

lactose biosynthesis through a modified glycosylation reaction where the sugar from UDP-galactose is attached to glucose that has been imported from the cytoplasm (Coffey and Reithel 1968). Additionally, the Golgi is the site of casein micelle biogenesis (Sasaki *et al.* 1978). Caseins are major milk glycoproteins that receive modifications in the Golgi complex, and also bind to Pi and Ca^{2+} and other materials while aggregating into large nutrient-packed "micelles" (Aoki *et al.* 1987). Biosynthesis of these major milk constituents – lactose and casein micelles – are both highly sensitive to the pH of the Golgi (Permyakov and Kreimer 1986; Liu and Guo 2008). Below I will summarize some key steps in these processes and highlight the potential need for H^+/Ca^{2+} exchange in the Golgi, which in later chapters I show is dependent on TMEM165. I will show that mouse mutants deficient in TMEM165 expression in the mammary gland produce low quality milk with a much reduced concentration of lactose, resulting in nutritional deficiencies in nursing pups.

LACTOSE SYNTHESIS

During the mammalian process of lactation, the Golgi complex collects and produces numerous products that are released into the milk via the secretory pathway (Silcock and Patton 1972). These products include proteins, metals, and fat, but one of the most crucial components is lactose (Silcock and Patton 1972). Lactose is not only the primary supply of sugar to a suckling infant, but it is also the primary osmotic driver of water into milk, providing the appropriate volume and viscosity required for nursing (Holt 1983). The reactions and mechanisms involved in lactose synthesis are not much different from those of glycosylation. SLC35A2 and GLUT1 are transporters responsible

for bringing in UDP-galactose and glucose, the primary substrates of the reaction (Mohammad *et al.* 2012; Zhang *et al.* 2018).

Similar to glycosylation of proteins and lipids, a glycosyltransferase, β4-galactosyltransferase (β4-GALT) frees the galactose from the UDP and attaches it to the glucose, forming a glycosidic bond (Fraser and Mookerjea 1976). The linked glucose and galactose form the disaccharide lactose. This process requires Mn^{2+} as a cofactor during the reaction (Fraser and Mookerjea 1976). Similar to the byproducts of protein glycosylation, UDP that is produced immediately during lactose synthesis reactions is quickly hydrolyzed by apyrases into UMP and Pi (Kuhn and White 1977). The UMP is then recycled into the cytoplasm by SLC35A2, in exchange for cytoplasmic UDP-galactose (Mohammad *et al.* 2012). Because it is present in milk, the Pi byproduct may be incorporated into casein, clusters of protein held together by Ca^{2+}/phosphate bridges, or it too can be recycled into the cytoplasm by an unknown mechanism, possibly through leakage through GOLAC (Nordeen *et al.* 2000). The fate of H^+ byproducts of lactose biosynthesis has never been reported. Because lactose concentrations in milk range from 2 to 7% in different mammals (70 to 250 mM) and milk pH is typically near neutral, a great deal of H^+ transport is likely to occur (Jenness and Holt 1987). In chapter 3, I will show that a novel H^+/Ca^{2+} exchanger termed TMEM165 is strongly up-regulated in the milk producing cells of the mammary gland and is necessary for proper lactose biosynthesis, likely by eliminating H^+ that could feedback inhibit B-GALT.

DISORDERS RELATED TO GOLGI HOMEOSTASIS

There is a homeostatic balance of all the substrates, products, and cofactors of the various reactions within the Golgi apparatus. Disruption of any of these components or the reaction machinery often leads to downstream consequences for the cells. In the case of humans and other mammals, these consequences can manifest as serious disorders. Due to the difficulty of studying the reactions and regulation of the Golgi apparatus, there is still much that is unknown about the pathways and mechanisms involved. Therefore, many of the disorders affiliated with Golgi homeostatic imbalance have no cure and limited treatment, emphasizing the need for further research into the nature of the Golgi and the reactions within it.

CANCER

Alterations to glycosylation is a common identifier of cancerous cells (Kim and Varki 1997; Ono and Hakomori 2003). Some of these alterations are the result of changes in expression or activity of glycosyltransferases and/or NSTs due to mutations in those proteins (Rivinoja *et al.* 2012; Song 2013). Additionally, changes in pH of the Golgi have been found to result in defects in glycosylation (Rivinoja *et al.* 2009; Hassinen *et al.* 2011). In fact, slight pH increases in the Golgi apparatus results in accumulation of some glycosyltransferases and other Golgi-resident proteins in the late endosomes, where they cannot carry out glycoprotein synthesis and other necessary reactions (Rivinoja *et al.* 2009). Changes in pH can also affect protein sorting, which may result in changes in cell polarity (Caplan *et al.* 1987). In the case of hyper-acidification, it has been demonstrated that many chemotherapeutic agents, which are often pH-sensitive, become sequestered

within acidified compartments rather than reaching the cell structures required to trigger cell death (Lucien *et al.* 2017). This means that alterations of pH in the Golgi and other organelles can result in the formation of drug-resistant cancers (Lucien *et al.* 2017).

CONGENITAL DISORDERS OF GLYCOSYLATION

When a patient receives a mutant gene that negatively impacts glycosylation, it is called a congenital disorder of glycosylation (CDG) (Freeze 1998; Grünewald *et al.* 2002). These inherited diseases are broken down into two categories, CDG-I, which results in a defect of assembly of the lipid-linked oligosaccharide and/or its subsequent transfer to a peptide, and CDG-II, which results in a defect of glycan processing after it is bound to a peptide (Grünewald *et al.* 2002). While CDG is rare, the number of identified patients and unique mutations and deficiencies leading to CDG has been increasing rapidly in recent years (Ng and Freeze 2018).

CDG-I typically results from mutations to glycosylation-related genes that localize to the ER or cytoplasm. For example, in the most prevalent form, CDG-Ia, is caused by a mutation in the gene for phosphomannomutase 2 (PMM2), a cytoplasmic protein responsible for converting mannose-6-phosphate to mannose-1-phosphate, allowing it to be subsequently converted to GDP-mannose by Mannose-1-phosphate guanyltransferase beta (GMPPB) (Schollen *et al.* 2000; Cline *et al.* 2012). By blocking synthesis of GDP-mannose, the mutation of PMM2 prevents the formation of the lipid-bound oligosaccharide precursor, stopping N-glycosylation in infancy (Eklund *et al.* 2005). O-glycosylation is also deficient, due to the absence of GDP-mannose. In this form of CDG, symptoms such as low weight gain, insufficient muscle tone, abnormal fat

distribution, strabismus, and retracted nipples present during infancy (Jaeken and Matthijs 2001; Grünewald *et al.* 2002). More severe symptoms may also develop, including underdevelopment of the cerebellum, seizures, pericardial effusion, and blood clotting disorders (Grünewald *et al.* 2002). Of the infants affected, 20% die during the first year of life, due to multiple organ failure (Jaeken and Matthijs 2001).

CDG-II can also result from mutations to genes localized in the ER, but it is far more prevalent for this type of CDG to be derived from mutations to Golgi-resident proteins (Reynders *et al.* 2009). Cutis laxa type II is an autosomal recessive form of CDG-II that results from mutations in the a2 subunit of the V_0 complex of the V-ATPase (Kornak *et al.* 2007). These mutations cause complete loss of activity and therefore block the establishment of a pH gradient between the Golgi and the cytoplasm, as well as deficiencies in glycosylation and vesicular transport (Kornak *et al.* 2007). Ultimately, patients with this disease have severe and premature wrinkling of the skin at an early age (Kornak *et al.* 2007).

Another form of CDG-II arises from a mutation in the gene for TMEM165, a transmembrane protein, localized to the Golgi apparatus that has been proposed to function as an exchanger of Ca^{2+}/Mn^{2+} for H^+ across the Golgi membrane (Foulquier *et al.* 2012; Demaegd *et al.* 2013; Rosnoblet *et al.* 2013; Potelle *et al.* 2016; Dulary *et al.* 2017). Characterization of this gene began recently, as a result of its affiliation with CDG, so further study is required to fully understand its role. However, in addition to N-glycosylation deficiencies, patients identified as having a mutation in *TMEM165* present severe bone dysplasia and growth abnormalities, muscular hypotrophy, excess fat production, increased serum transaminases and LDH, and decreased coagulation factors

(Zeevaert *et al.* 2013). In chapter 3, I will demonstrate that loss of TMEM165 during lactation leads to similar deficiencies in lactose synthesis, further supporting the important role this protein plays in the maintenance of Golgi pH and Ca^{2+}/Mn^{2+} homeostasis.

HAILEY-HAILEY DISEASE

Hailey-Hailey disease is an autosomal dominant disease that arises due to haploinsufficiencies in the SPCA1 gene, *ATP2C1*. These patients have deficiencies in transport of Ca^{2+} and Mn^{2+} into the Golgi (Hu *et al.* 2000; Wuytack *et al.* 2003). The disease presents with low cell-cell adhesion, resulting in itchy and painful skin lesions, particularly in areas of frequent skin-to-skin contact, such as the groin and neck (Burge 1992). This is because the added stress of friction and heat on the cells in these areas exacerbates the phenotypic problems that arise from the haploinsufficiency (Burge 1992; Missiaen *et al.* 2004). The inability to properly regulate the calcium concentrations causes deficiencies in glycosylation as well as protein folding and sorting, leading to improper desmosome and adherens assembly, causing the cells of the epidermis to have poor differentiation and weak contacts with one another (Pillai *et al.* 1990; Vasioukhin *et al.* 2000).

TYPE 2 DIABETES

Because glycosylation is required for appropriate protein sorting from the Golgi to the target membrane, improper glycosylation could result in mislocalization of critical transporters that are needed for signaling and nutrition for the cell (Scheiffele *et al.*

1995). In the case of GLUT2, a transporter responsible for moving glucose into the cytoplasm from the extracellular matrix, proper glycosylation is required to target the protein to the plasma membrane (Ohtsubo *et al.* 2005). If expression and localization of GLUT2 is impaired in pancreatic β cells, the cells are unable to undergo glucose-stimulated insulin secretion (Ohtsubo *et al.* 2005). Expression of one particular glycosyltransferase, N-acetylglucosaminyltransferase-IV isoenzyme A (GnT-IVa), coincides with expression of GLUT2 (Ohtsubo *et al.* 2011). This is because GnT-IVa is required for a critical step in the glycosylation of GLUT2, involving the transfer of GlcNAc from UDP-GlcNAc to the core N-linked oligosaccharide (Minowa *et al.* 1998). In the absence of GnT-IVa, GLUT2 has only 2 terminal sugars of the N-glycan, as opposed to 4 in normal cells (Ohtsubo *et al.* 2005). This change results in decreased stability of the presence of GLUT2 at the cell surface, meaning that the protein is internalized prematurely, decreasing the uptake of glucose (Ohtsubo *et al.* 2005). In mice, this change has been demonstrated to be sufficient for the presentation of type-II diabetes phenotypes (Orci *et al.* 1990).

PERSPECTIVES AND CONCLUSIONS

The Golgi apparatus plays a critical role in cellular dynamics. Central to its function are the glycosyltransferases that carry out the process of glycosylation, as this contributes to the other roles of the Golgi, including protein and lipid maturation and trafficking. Without the activity of the various transporters of the Golgi membrane, which supply the necessary substrates and/or remove the byproducts of glycosylation, the activity of the glycosyltransferases can no longer function optimally. Disruption of any

aspect of transport or mechanistic reactions within the Golgi have the potential to be incredibly detrimental to the cell and the organism as a whole. Even the deletion of a single transmembrane transporter, like TMEM165, can have massive consequences on glycosylation and protein sorting, ultimately throwing off the function of the entire cell, and potentially leading to a number of diseases (Foulquier *et al.* 2012; Zeevaert *et al.* 2013; Bammens *et al.* 2015). Due to the delicate nature of the homeostasis required for the many functions of the Golgi apparatus, it is important to continue to investigate the roles and mechanisms of all the proteins and their processes within the Golgi apparatus.

In Chapter 2, I characterize two Golgi transporters, Gdt1 and Erd1, which regulate the homeostasis of glycosylation byproducts, H^+ and Pi, respectively. Through genetic analysis and growth assays, I demonstrate that Gdt1 removes H^+ from the Golgi in exchange for Ca^{2+}, which is required for glycosylation and protein sorting. I also demonstrate that, in the absence of Erd1, the Pi byproduct of glycosylation is lost to the environment through the secretory pathway. Gdt1 has a mammalian homolog, TMEM165, which carries out a similar function, exchanging H^+ from the Golgi lumen for Ca^{2+} and Mn^{2+}, to support both glycosylation and lactation. This protein is analysed in Chapter 3, where I analyse TMEM165-deficient lactating mothers to determine that in the absence of *TMEM165*, mothers produce milk with a low yield of lactose, leading to an osmotic defect that concentrates other milk components, such as protein and metals, ultimately resulting in decreased nutrition for nursing pups. In chapter 4, I establish a new method that can be utilized for the study of essential genes, many of which have a role in glycosylation, and I identify an inhibitor of the nucleotide sugar transporter Vrg4, which can be utilized to block glycosylation in yeast.

REFERENCES

Abeijon, C., P. Orlean, P. Robbins, and C. Hirschberg, 1989. Topography of glycosylation in yeast: characterization of GDPmannose transport and lumenal guanosine diphosphatase activities in Golgi-like vesicles. Proc National Acad Sci 86: 6935–6939.

Aoki, T., N. Yamada, I. Tomita, Y. Kako, and T. Imamura, 1987. Caseins are cross-linked through their ester phosphate groups by colloidal calcium phosphate. Biochimica Et Biophysica Acta Bba - Protein Struct Mol Enzym 911: 238–243.

Ardevol, A., J. Iglesias-Fernandez, V. Rojas-Cervellera, and C. Rovira, 2016. The reaction mechanism of retaining glycosyltransferases. Biochem Soc T 44: 51–60.

Bammens, R., N. Mehta, V. Race, F. Foulquier, J. Jaeken *et al.*, 2015. Abnormal cartilage development and altered N-glycosylation in Tmem165-deficient zebrafish mirrors the phenotypes associated with TMEM165-CDG. Glycobiology 25: 669–682.

Boulan, R. E., D.D. Sabatini, B. Pereyra, and G. Kreibich, 1978. Spatial orientation of glycoproteins in membranes of rat liver rough microsomes. II. Transmembrane disposition and characterization of glycoproteins. J Cell Biology 78: 894–909.

Boutinaud, M., J. Guinard-Flament, and H. Jammes, 2004. The number and activity of mammary epithelial cells, determining factors for milk production. Reprod Nutr Dev 44: 499–508.

Breslow, D. K., and J. S. Weissman, 2010. Membranes in Balance: Mechanisms of Sphingolipid Homeostasis. Mol Cell 40: 267–279.

Breton, S., and D. Brown, 2013. Regulation of luminal acidification by the V-ATPase. Physiology Bethesda Md 28: 318–29.

Burge, S. M., 1992. Hailey–Hailey disease: the clinical features, response to treatment and prognosis. Brit J Dermatol 126: 275–282.

Cagnac, O., M. Aranda-Sicilia, M. Leterrier, M.-P. Rodriguez-Rosales, and K. Venema, 2010. Vacuolar Cation/H^+ Antiporters of Saccharomyces cerevisiae. J Biol Chem 285: 33914–33922.

Capasso, J., and C. Hirschberg, 1984. Mechanisms of glycosylation and sulfation in the Golgi apparatus: evidence for nucleotide sugar/nucleoside monophosphate and nucleotide sulfate/nucleoside monophosphate antiports in the Golgi apparatus membrane. Proc National Acad Sci 81: 7051–7055.

Caplan, M. J., J. L. Stow, A. P. Newman, J. Madri, C. H. Anderson *et al.*, 1987. Dependence on pH of polarized sorting of secreted proteins. Nature 329: 329632a0.

Cline, A., N. Gao, H. Flanagan-Steet, V. Sharma, S. Rosa *et al.*, 2012. A zebrafish model of PMM2-CDG reveals altered neurogenesis and a substrate-accumulation mechanism for N-linked glycosylation deficiency. Mol Biol Cell 23: 4175–4187.

Cobb, B. A., and D. L. Kasper, 2005. Coming of age: carbohydrates and immunity. Eur J Immunol 35: 352–356.

Coffey, R., and F. Reithel, 1968. The lactose synthetase particles of lactating bovine mammary gland. Characteristics of the particles. Biochem J 109: 177–183.

Cunningham, K., and G. Fink, 1996. Calcineurin inhibits VCX1-dependent H^+/Ca^{2+} exchange and induces Ca^{2+} ATPases in Saccharomyces cerevisiae. Mol Cell Biol 16: 2226–2237.

Cunningham, K., and G. Fink, 1994. Calcineurin-dependent growth control in Saccharomyces cerevisiae mutants lacking PMC1, a homolog of plasma membrane Ca^{2+} ATPases. J Cell Biology 124: 351–363.

Daido, S., T. Kanzawa, A. Yamamoto, H. Takeuchi, Y. Kondo *et al.*, 2004. Pivotal Role of the Cell Death Factor BNIP3 in Ceramide-Induced Autophagic Cell Death in Malignant Glioma Cells. Cancer Res 64: 4286–4293.

Dean, N., Y. B. Zhang, and J. B. Poster, 1997. The VRG4 Gene Is Required for GDP-mannose Transport into the Lumen of the Golgi in the Yeast, Saccharomyces cerevisiae. J Biol Chem 272: 31908–31914.

Demaegd, D., F. Foulquier, A.-S. Colinet, L. Gremillon, D. Legrand *et al.*, 2013. Newly characterized Golgi-localized family of proteins is involved in calcium and pH homeostasis in yeast and human cells. Proc National Acad Sci 110: 6859–6864.

Diakov, T. T., and P. M. Kane, 2010 Regulation of Vacuolar Proton-translocating ATPase Activity and Assembly by Extracellular pH. J Biol Chem 285: 23771–23778.

Dode, L., J. Andersen, J. Vanoevelen, L. Raeymaekers, L. Missiaen *et al.*, 2006. Dissection of the Functional Differences between Human Secretory Pathway Ca^{2+}/Mn^{2+}-ATPase (SPCA) 1 and 2 Isoenzymes by Steady-state and Transient Kinetic Analyses. J Biol Chem 281: 3182–3189.

Dulary, E., S. Potelle, D. Legrand, and F. Foulquier, 2017. TMEM165 deficiencies in Congenital Disorders of Glycosylation type II (CDG-II): Clues and evidences for roles of the protein in Golgi functions and ion homeostasis. Tissue Cell 49: 150–156.

Dürr, G., J. Strayle, R. Plemper, S. Elbs, S. K. Klee *et al.*, 1998. The medial-Golgi Ion Pump Pmr1 Supplies the Yeast Secretory Pathway with Ca^{2+} and Mn^{2+} Required for Glycosylation, Sorting, and Endoplasmic Reticulum-Associated Protein Degradation. Mol Biol Cell 9: 1149–1162.

Eklund, E. A., N. Merbouh, M. Ichikawa, A. Nishikawa, J. M. Clima *et al.*, 2005. Hydrophobic Man-1-P derivatives correct abnormal glycosylation in Type I congenital disorder of glycosylation fibroblasts. Glycobiology 15: 1084–1093.

Pillai, D. D. Bikle, M. Mancianti, P. Cline, and M. Hincenbergs, 1990. Calcium regulation of growth and differentiation of normal human keratinocytes: Modulation of differentiation competence by stages of growth and extracellular calcium. J Cell Physiol 143: 294–302.

Forgac, M., 2007. Vacuolar ATPases: rotary proton pumps in physiology and pathophysiology. Nat Rev Mol Cell Bio 8: 917–929.

Foulquier, F., M. Amyere, J. Jaeken, R. Zeevaert, E. Schollen *et al.*, 2012. TMEM165 Deficiency Causes a Congenital Disorder of Glycosylation. Am J Hum Genetics 91: 15–26.

Fraser, I., and S. Mookerjea, 1976. Studies on the purification and properties of UDP-galactose glycoprotein galactosyltransferase from rat liver and serum. Biochem J 156: 347–355.

Freeze, H. H., 1998. Disorders in protein glycosylation and potential therapy: Tip of an iceberg? J Pediatrics 133: 593–600.

Freeze, H. H., 2006. Genetic defects in the human glycome. Nat Rev Genet 7: nrg1894.

Fröhlich, F., C. Petit, N. Kory, R. Christiano, H.-K. Hannibal-Bach *et al.*, 2015. The GARP complex is required for cellular sphingolipid homeostasis. Elife 4: e08712.

Gaxiola, R. A., D. S. Yuan, R. D. Klausner, and G. R. Fink, 1998. The yeast CLC chloride channel functions in cation homeostasis. Proc National Acad Sci 95: 4046–4050.

Glickman, J., K. Croen, S. Kelly, and Q. Al-Awqati, 1983. Golgi membranes contain an electrogenic H^+ pump in parallel to a chloride conductance. J Cell Biology 97: 1303–1308.

Grünewald, S., G. Matthijs, and J. Jaeken, 2002. Congenital Disorders of Glycosylation: A Review. Pediatr Res 52: pr2002233.

Guenther, G. G., E. R. Peralta, K. Rosales, S. Y. Wong, L. J. Siskind *et al.*, 2008. Ceramide starves cells to death by downregulating nutrient transporter proteins. Proc National Acad Sci 105: 17402–17407.

Hadley, B., A. Maggioni, A. Ashikov, C. J. Day, T. Haselhorst *et al.*, 2014. Structure and function of nucleotide sugar transporters: Current progress. Comput Struct Biotechnology J 10: 23–32.

Harper, A.G., and S.O. Sage, 2016. TRP-Na^+/Ca^{2+} Exchanger Coupling. Adv Exp Med Biol 898, 67-85.

Hassinen, A., F. M. Pujol, N. Kokkonen, C. Pieters, M. Kihlström *et al.*, 2011. Functional Organization of Golgi N- and O-Glycosylation Pathways Involves pH-dependent Complex Formation That Is Impaired in Cancer Cells. J Biol Chem 286: 38329–38340.

Hauser, K., and A. Barth, 2007. Side-Chain Protonation and Mobility in the Sarcoplasmic Reticulum Ca^{2+}-ATPase: Implications for Proton Countertransport and Ca^{2+} Release. Biophys J 93: 3259–3270.

Hebert, D. N., L. Lamriben, E. T. Powers, and J. W. Kelly, 2014. The intrinsic and extrinsic effects of N-linked glycans on glycoproteostasis. Nat Chem Biol 10: 902–910.

Helenius, A., and M. and Aebi, 2001. Intracellular Functions of N-Linked Glycans. Science 291: 2364–2369.

Hilgemann, D.W., D.A. Nicoll, and K.D. Phillipson, 1991. Charge movement during Na^+ translocation by native and cloned cardiac Na^+/Ca^{2+} exchanger. Nature 352: 715-718.

Hirschberg, C. B., 2001. Golgi nucleotide sugar transport and leukocyte adhesion deficiency II. J Clin Invest 108: 3–6.

Hirschberg, C., 1997. The Golgi Apparatus. 163–178.

Holt, C., 1983. Swelling of golgi vesicles in mammary secretory cells and its relation to the yield and quantitative composition of milk. J Theor Biol 101: 247–261.

Hu, Z., J. M. Bonifas, J. Beech, G. Bench, T. Shigihara *et al.*, 2000. Mutations in ATP2C1, encoding a calcium pump, cause Hailey-Hailey disease. Nat Genet 24: 61–65.

Hu, K., J. Carroll, S. Fedorovich, C. Rickman, A. Sukhodub *et al.*, 2002. Vesicular restriction of synaptobrevin suggests a role for calcium in membrane fusion. Nature 415: 646.

Huang, M.-E., J.-C. Chuat, and F. Galibert, 1994. A Voltage-gated Chloride Channel in the Yeast Saccharomyces cerevisiae. J Mol Biol 242: 595–598.

Hubbard, S., and P. Robbins, 1980. Synthesis of the N-linked oligosaccharides of glycoproteins. Assembly of the lipid-linked precursor oligosaccharide and its relation to protein synthesis in vivo. J Biological Chem 255: 11782–93.

Jaeken, J., and G. Matthijs, 2001. Congenital disorders of glycosylation. Genom Hum Genetics 2: 129–151.

Jenness, R., and C. Holt, 1987. Casein and lactose concentrations in milk of 31 species are negatively correlated. Experientia 43: 1015–1018.

Kane, P., 1995. Disassembly and reassembly of the yeast vacuolar H(+)-ATPase in vivo. J Biological Chem 270: 17025–32.

Kawasaki-Nishi, S., K. Bowers, T. Nishi, M. Forgac, and T. H. Stevens, 2001. The Amino-terminal Domain of the Vacuolar Proton-translocating ATPase a Subunit Controls Targeting and in Vivo Dissociation, and the Carboxyl-terminal Domain Affects Coupling of Proton Transport and ATP Hydrolysis. J Biol Chem 276: 47411–47420.

Kim, J., C. Lingwood, D. Williams, W. Furuya, M. Manolson *et al.*, 1996. Dynamic measurement of the pH of the Golgi complex in living cells using retrograde transport of the verotoxin receptor. J Cell Biology 134: 1387–1399.

Kim, Y. J., and A. Varki, 1997. Perspectives on the significance of altered glycosylation of glycoproteins in cancer. Glycoconjugate J 14: 569–576.

Klee, C., T. Crouch, and M. Krinks, 1979. Calcineurin: a calcium- and calmodulin-binding protein of the nervous system. Proc National Acad Sci 76: 6270–6273.

Klug, L., and G. Daum, 2014. Yeast lipid metabolism at a glance. Fems Yeast Res 14: 369–388.

Kornak, U., E. Reynders, A. Dimopoulou, J. van Reeuwijk, B. Fischer *et al.*, 2007. Impaired glycosylation and cutis laxa caused by mutations in the vesicular H^+-ATPase subunit ATP6V0A2. Nat Genet 40: ng.2007.45.

Krupicka, M., and I. Tvaroska, 2009. Hybrid quantum mechanical/molecular mechanical investigation of the beta-1,4-galactosyltransferase-I mechanism. J Phys Chem B 113: 11314–9.

Kuhn, N., and A. White, 1977. The role of nucleoside diphosphatase in a uridine nucleotide cycle associated with lactose synthesis in rat mammary-gland Golgi apparatus. Biochem J 168: 423–433.

Lairson, L. L., B. Henrissat, G. J. Davies, and S. G. Withers, 2008. Glycosyltransferases: Structures, Functions, and Mechanisms. Annu Rev Biochem 77: 521–555.

Lapinskas, P., K. Cunningham, X. Liu, G. Fink, and V. Culotta, 1995 Mutations in PMR1 suppress oxidative damage in yeast cells lacking superoxide dismutase. Mol Cell Biol 15: 1382–1388.

Levine, T. P., C. Wiggins, and S. Munro, 2000. Inositol Phosphorylceramide Synthase Is Located in the Golgi Apparatus of Saccharomyces cerevisiae. Mol Biol Cell 11: 2267–2281.

Liang, D.-M., J.-H. Liu, H. Wu, B.-B. Wang, H.-J. Zhu *et al.*, 2015. Glycosyltransferases: mechanisms and applications in natural product development. Chem Soc Rev 44: 8350–8374.

Lissandron, V., P. Podini, P. Pizzo, and T. Pozzan, 2010. Unique characteristics of Ca^{2+} homeostasis of the trans-Golgi compartment. Proc National Acad Sci 107: 9198–9203.

Liu, Y., and R. Guo, 2008. pH-dependent structures and properties of casein micelles. Biophys Chem 136: 67–73.

Locke, E. G., M. Bonilla, L. Liang, Y. Takita, and K. W. Cunningham, 2000. A Homolog of Voltage-Gated Ca^{2+} Channels Stimulated by Depletion of Secretory Ca^{2+} in Yeast. Mol Cell Biol 20: 6686–6694.

Lowe, J. B., 2003. Glycan-dependent leukocyte adhesion and recruitment in inflammation. Curr Opin Cell Biol 15: 531–538.

Lucien, F., P.-P. Pelletier, R. R. Lavoie, J.-M. Lacroix, S. Roy *et al.*, 2017. Hypoxia-induced mobilization of NHE6 to the plasma membrane triggers endosome hyperacidification and chemoresistance. Nat Commun 8: ncomms15884.

Manolson, M., D. Proteau, R. Preston, A. Stenbit, B. Roberts *et al.*, 1992. The VPH1 gene encodes a 95-kDa integral membrane polypeptide required for in vivo assembly and activity of the yeast vacuolar H^+-ATPase. J Biological Chem 267: 14294–303.

Manolson, M., B. Wu, D. Proteau, B. Taillon, B. Roberts *et al.*, 1994. STV1 gene encodes functional homologue of 95-kDa yeast vacuolar H^+-ATPase subunit Vph1p. J Biological Chem 269: 14064–74.

Marchi, V., A. Sorin, Y. Wei, and R. Rao, 1999. Induction of vacuolar CaZ+-ATPase and H^+/Ca^{2+} exchange activity in yeast mutants lacking Pmrl, the Golgi Ca^{2+}-ATPase. Febs Lett 454: 181–186.

Marshall, R., 1972. Glycoproteins. Annu Rev Biochem 41: 673–702.

Mason, A. B., T. B. Kardos, and B. C. Monk, 1998. Regulation and pH-dependent expression of a bilaterally truncated yeast plasma membrane H^+-ATPase. Biochimica Et Biophysica Acta Bba - Biomembr 1372: 261–271.

Matheos, D. P., T. J. Kingsbury, S. U. Ahsan, and K. W. Cunningham, 1997. Tcn1p/Crz1p, a calcineurin-dependent transcription factor that differentially regulates gene expression in Saccharomyces cerevisiae. Gene Dev 11: 3445–3458.

Micaroni, M., 2012. Calcium Around the Golgi Apparatus: Implications for Intracellular Membrane Trafficking. Adv Exp Med Biol 740: 439–460.

Milla, M., C. Clairmont, and C. Hirschberg, 1992. Reconstitution into proteoliposomes and partial purification of the Golgi apparatus membrane UDP-galactose, UDP-xylose, and UDP-glucuronic acid transport activities. J Biological Chem 267: 103–7.

Minowa, M., S. Oguri, A. Yoshida, T. Hara, A. Iwamatsu *et al.*, 1998. cDNA Cloning and Expression of Bovine UDP-N-Acetylglucosamine:α1,3-d-Mannoside β1,4-N-Acetylglucosaminyltransferase IV. J Biol Chem 273: 11556–11562.

Missiaen, L., V. K. Acker, V. K. Baelen, L. Raeymaekers, F. Wuytack *et al.*, 2004a. Calcium release from the Golgi apparatus and the endoplasmic reticulum in HeLa cells stably expressing targeted aequorin to these compartments. Cell Calcium 36: 479–487.

Missiaen, L., L. Raeymaekers, L. Dode, J. Vanoevelen, K. Baelen *et al.*, 2004b. SPCA1 pumps and Hailey–Hailey disease. Biochem Bioph Res Co 322: 1204–1213.

Mohammad, M. A., D. L. Hadsell, and M. W. Haymond, 2012. Gene regulation of UDP-galactose synthesis and transport: potential rate-limiting processes in initiation of milk production in humans. Am J Physiology Endocrinol Metabolism 303: E365-76.

Møller, J. V., B. Juul, and M. le Maire, 1996. Structural organization, ion transport, and energy transduction of P-type ATPases. Biochimica Et Biophysica Acta Bba - Rev Biomembr 1286: 1–51.

Nakamura, N., S. Tanaka, Y. Teko, K. Mitsui, and H. Kanazawa, 2005. Four Na^+/H^+ Exchanger Isoforms Are Distributed to Golgi and Post-Golgi Compartments and Are Involved in Organelle pH Regulation. J Biol Chem 280: 1561–1572.

Nelson, N., and W. R. Harvey, 1999. Vacuolar and Plasma Membrane Proton-Adenosinetriphosphatases. Physiol Rev 79: 361–385.

Nelson, H., and N. Nelson, 1990. Disruption of genes encoding subunits of yeast vacuolar H^+-ATPase causes conditional lethality. Proc National Acad Sci 87: 3503–3507.

Nelson, N., N. Perzov, A. Cohen, K. Hagai, V. Padler *et al.*, 2000. The cellular biology of proton-motive force generation by V-ATPases. J Exp Biology 203: 89–95.

Nelson, N., and L. Taiz, 1989. The evolution of H^+-ATPases. Trends Biochem Sci 14: 113–116.

Ng, B. G., and H. H. Freeze, 2018. Perspectives on Glycosylation and Its Congenital Disorders. Trends Genetics Tig 34: 466–476.

Niggli, V., E. Sigel, and E. Carafoli, 1982. The purified Ca^{2+} pump of human erythrocyte membranes catalyzes an electroneutral Ca^{2+}-H^+ exchange in reconstituted liposomal systems. J Biological Chem 257: 2350–6.

Nishikawa, A., B. Mendez, Y. Jigami, and N. Dean, 2002a. Identification of a Candida glabrata homologue of the S. cerevisiaeVRG4 gene, encoding the Golgi GDP-mannose transporter. Yeast 19: 691–698.

Nishikawa, A., J. B. Poster, Y. Jigami, and N. Dean, 2002b. Molecular and Phenotypic Analysis of CaVRG4, Encoding an Essential Golgi Apparatus GDP-Mannose Transporter. J Bacteriol 184: 29–42.

Nordeen, M. H., S. M. Jones, K. E. Howell, and J. H. Caldwell, 2000. GOLAC: An Endogenous Anion Channel of the Golgi Complex. Biophys J 78: 2918–2928.

Ohtsubo, K., M. Z. Chen, J. M. Olefsky, and J. D. Marth, 2011. Pathway to diabetes through attenuation of pancreatic beta cell glycosylation and glucose transport. Nat Med 17: 1067.

Ohtsubo, K., S. Takamatsu, M. T. Minowa, A. Yoshida, M. Takeuchi *et al.*, 2005. Dietary and Genetic Control of Glucose Transporter 2 Glycosylation Promotes Insulin Secretion in Suppressing Diabetes. Cell 123: 1307–1321.

Ono, M., and S. Hakomori, 2003. Glycosylation defining cancer cell motility and invasiveness. Glycoconjugate J 20: 71–78.

Orci, L., M. Ravazzola, D. Baetens, L. Inman, M. Amherdt *et al.*, 1990. Evidence that down-regulation of beta-cell glucose transporters in non-insulin-dependent diabetes may be the cause of diabetic hyperglycemia. Proc National Acad Sci 87: 9953–9957.

Orellana, A., C. Moraga, M. Araya, and A. Moreno, 2016. Overview of Nucleotide Sugar Transporter Gene Family Functions Across Multiple Species. J Mol Biol 428: 3150–3165.

Parra, K. J., K. L. Keenan, and P. M. Kane, 2000. The H Subunit (Vma13p) of the Yeast V-ATPase Inhibits the ATPase Activity of Cytosolic V1 Complexes. J Biol Chem 275: 21761–21767.

Perez, M., and C. Hirschberg, 1985. Translocation of UDP-N-acetylglucosamine into vesicles derived from rat liver rough endoplasmic reticulum and Golgi apparatus. J Biological Chem 260: 4671–8.

Permyakov, E., and D. Kreimer, 1986. Effects of pH, temperature and Ca^{2+} content on the conformation of alpha-lactalbumin in a medium modelling physiological conditions. Gen Physiol Biophys 5: 377–89.

Persson, M., and M. M. Palcic, 2008. A high-throughput pH indicator assay for screening glycosyltransferase saturation mutagenesis libraries. Anal Biochem 378: 1–7.

Pinton, P., T. Pozzan, and R. Rizzuto, 1998, The Golgi apparatus is an inositol 1,4,5-trisphosphate-sensitive Ca^{2+} store, with functional properties distinct from those of the endoplasmic reticulum. Embo J 17: 5298–5308.

Pizzo, P., V. Lissandron, P. Capitanio, and T. Pozzan, 2011. Ca^{2+} signalling in the Golgi apparatus. Cell Calcium 50: 184–192.

Poster, J. B., and N. Dean, 1996. The Yeast VRG4 Gene Is Required for Normal Golgi Functions and Defines a New Family of Related Genes. J Biol Chem 271: 3837–3845.

Potelle, S., W. Morelle, E. Dulary, S. Duvet, D. Vicogne *et al.*, 2016. Glycosylation abnormalities in Gdt1p/TMEM165 deficient cells result from a defect in Golgi manganese homeostasis. Hum Mol Genet 25: 1489–1500.

Reynders, E., F. Foulquier, W. Annaert, and G. Matthijs, 2011. How Golgi glycosylation meets and needs trafficking: the case of the COG complex. Glycobiology 21: 853–863.

Reynders, E., F. Foulquier, E. Teles, D. Quelhas, W. Morelle *et al.*, 2009. Golgi function and dysfunction in the first COG4-deficient CDG type II patient. Hum Mol Genet 18: 3244–56.

Rivinoja, A., A. Hassinen, N. Kokkonen, A. Kauppila, and S. Kellokumpu, 2009. Elevated Golgi pH impairs terminal N-glycosylation by inducing mislocalization of Golgi glycosyltransferases. J Cell Physiol 220: 144–154.

Rivinoja, A., F. M. Pujol, A. Hassinen, and S. Kellokumpu, 2012. Golgi pH, its regulation and roles in human disease. Ann Med 44: 542–554.

Rosnoblet, C., D. Legrand, D. Demaegd, H. Hacine-Gherbi, G. de Bettignies *et al.*, 2013. Impact of disease-causing mutations on TMEM165 subcellular localization, a recently identified protein involved in CDG-II. Hum Mol Genet 22: 2914–2928.

Roth, J., D. Taatjes, J. Weinstein, J. Paulson, P. Greenwell *et al.*, 1986. Differential subcompartmentation of terminal glycosylation in the Golgi apparatus of intestinal absorptive and goblet cells. J Biological Chem 261: 14307–12.

Rybak, S. L., F. Lanni, and R. F. Murphy, 1997. Theoretical considerations on the role of membrane potential in the regulation of endosomal pH. Biophys J 73: 674–687.

Sasaki, W. Eigel, and T. Keenan, 1978. Lactose and major milk proteins are present in secretory vesicle-rich fractions from lactating mammary gland. Proc National Acad Sci 75: 5020–5024.

Sautin, Y. Y., M. Lu, A. Gaugler, L. Zhang, and S. L. Gluck, 2005. Phosphatidylinositol 3-Kinase-Mediated Effects of Glucose on Vacuolar H^+-ATPase Assembly, Translocation, and Acidification of Intracellular Compartments in Renal Epithelial Cells. Mol Cell Biol 25: 575–589.

Schapiro, F. B., and S. Grinstein, 2000. Determinants of the pH of the Golgi Complex. J Biol Chem 275: 21025–21032.

Scheiffele, P., J. Peränen, and K. Simons, 1995. N-glycans as apical sorting signals in epithelial cells. Nature 378: 96–98.

Schoberer, J., and R. Strasser, 2011. Sub-Compartmental Organization of Golgi-Resident N-Glycan Processing Enzymes in Plants. Mol Plant 4: 220–228.

Schollen, E., S. Kjaergaard, E. Legius, M. Schwartz, and G. Matthijs, 2000. Lack of Hardy-Weinberg equilibrium for the most prevalent PMM2 mutation in CDG-Ia (congenital disorders of glycosylation type Ia). Eur J Hum Genet 8: 5200470.

Silcock, R. W., and S. Patton, 1972. Correlative secretion of protein, lactose and K^+ in milk of the goat. J Cell Physiol 79: 151–154.

Song, Z., 2013. Roles of the nucleotide sugar transporters (SLC35 family) in health and disease. Mol Aspects Med 34: 590–600.

Stanley, P., 2011. Golgi Glycosylation. Csh Perspect Biol 3: a005199.

Steen, P., P. M. Rudd, R. A. Dwek, and G. Opdenakker, 2008. Concepts and Principles of O-Linked Glycosylation. Crit Rev Biochem Mol 33: 151–208.

Sumner, J.-P., J. A. Dow, F. G. Earley, U. Klein, D. Jäger *et al.*, 1995. Regulation of Plasma Membrane V-ATPase Activity by Dissociation of Peripheral Subunits. J Biol Chem 270: 5649–5653.

Tabke, K., A. Albertmelcher, O. Vitavska, M. Huss, H.-P. Schmitz *et al.*, 2014. Reversible disassembly of the yeast V-ATPase revisited underin vivoconditions. Biochem J 462: 185–197.

Thielges, M., G. Uyeda, A. Cámara-Artigas, L. Kálmán, J. Williams *et al.*, 2005. Design of a Redox-Linked Active Metal Site: Manganese Bound to Bacterial Reaction Centers at a Site Resembling That of Photosystem II†,‡. Biochemistry-us 44: 7389–7394.

Thompson, R. J., H. C. Akana, C. Finnigan, K. E. Howell, and J. H. Caldwell, 2006. Anion channels transport ATP into the Golgi lumen. Am J Physiol-cell Ph 290: C499–C514.

Thompson, R. J., M. H. Nordeen, K. E. Howell, and J. H. Caldwell, 2002. A Large-Conductance Anion Channel of the Golgi Complex. Biophys J 83: 278–289.

Ton, V.-K., D. Mandal, C. Vahadji, and R. Rao, 2002. Functional Expression in Yeast of the Human Secretory Pathway Ca^{2+}, Mn^{2+}-ATPase Defective in Hailey-Hailey Disease. J Biol Chem 277: 6422–6427.

Trombetta, S. E., 2003. The contribution of N-glycans and their processing in the endoplasmic reticulum to glycoprotein biosynthesis. Glycobiology 13: 77R-91R.

Varki, A., 1993. Biological roles of oligosaccharides: all of the theories are correct. Glycobiology 3: 97–130.

Vasioukhin, V., C. Bauer, M. Yin, and E. Fuchs, 2000. Directed Actin Polymerization Is the Driving Force for Epithelial Cell–Cell Adhesion. Cell 100: 209–219.

Velivela, S., and P. M. Kane, 2017. Compensatory Internalization of Pma1 in V-ATPase Mutants in Saccharomyces cerevisiae Requires Calcium- and Glucose-Sensitive Phosphatases. Genetics 208: genetics.300594.2017.

Waechter, C., and W. Lennarz, 1976. The Role of Polyprenol-Linked Sugars in Glycoprotein Synthesis. Annu Rev Biochem 45: 95–112.

Wei, Y., J. Chen, G. Rosas, D. A. Tompkins, P. A. Holt *et al.*, 2000. Phenotypic Screening Of Mutations In Pmr1, the Yeast Secretory Pathway Ca^{2+}/Mn^{2+}-ATPase, Reveals Residues Critical For Ion Selectivity and Transport. J Biol Chem 275: 23927–23932.

Wilson, I., Y. Gavel, and G. von Heijne, 1991. Amino acid distributions around O-linked glycosylation sites. Biochem J 275: 529–534.

Wuytack, F., L. Raeymaekers, and L. Missiaen, 2002. Molecular physiology of the SERCA and SPCA pumps. Cell Calcium 32: 279–305.

Wuytack, F., L. Raeymaekers, and L. Missiaen, 2003. PMR1/SPCA Ca^{2+} pumps and the role of the Golgi apparatus as a Ca^{2+} store. Pflügers Archiv 446: 148–153.

Zeevaert, R., F. de Zegher, L. Sturiale, D. Garozzo, M. Smet *et al.*, 2013. JIMD Reports - Case and Research Reports, 2012/5. Jimd Reports 8: 145–152.

Zhang, J., M. Myers, and M. Forgac, 1992. Characterization of the V0 domain of the coated vesicle H^+-ATPase. J Biological Chem 267: 9773–8.

Zhang, Y., S. Zhang, W. Guan, F. Chen, L. Cheng *et al.*, 2018. GLUT1 and lactose synthetase are critical genes for lactose synthesis in lactating sows. Nutr Metabolism 15: 40.

CHAPTER 2

H^+ AND Pi BYPRODUCTS OF GLYCOSYLATION AFFECT Ca^{2+} HOMEOSTASIS AND ARE RETRIEVED FROM THE GOLGI BY HOMOLOGS OF TMEM165 AND XPR1

Parts of this chapter were published in G3 (Bethesda) in December, 2017

Contributions from Other Authors:

The genetic screen of the Yeast Knockout Collection for Ca^{2+} Hypersensitivity (presented in Figure 2.1B) was conducted by Carlos Evangelista. Christopher P. Stefan, Camille T. Soroudi, and Adam Kim each conducted preliminary experimentation and generation of yeast and plasmid strains, as well as the BAPTA- and Mn^{2+}-sensitivity assays presented in Figure 2.4.

ABSTRACT

Glycosylation reactions in the Golgi complex and the endoplasmic reticulum utilize nucleotide sugars as donors and produce inorganic phosphate (Pi) and acid (H^+) as byproducts. Here we show that homologs of mammalian XPR1 and TMEM165 (termed Erd1 and Gdt1) recycle luminal Pi and exchange luminal H^+ for cytoplasmic Ca^{2+}, respectively, thereby promoting growth of yeast cells in low Pi and low Ca^{2+} environments. As expected for reversible H^+/Ca^{2+} exchangers, Gdt1 also promoted growth in high Ca^{2+} environments when the Golgi-localized V-ATPase was operational but had the opposite effect when the V-ATPase was eliminated. Gdt1 activities were negatively regulated by calcineurin signaling and by Erd1, which recycled the Pi byproduct of glycosylation reactions and prevented the loss of this nutrient to the environment via exocytosis. Thus, Erd1 transports Pi in the opposite direction from XPR1 and other EXS family proteins and facilitates byproduct removal from the Golgi complex together with Gdt1.

INTRODUCTION

Secretory proteins, lipids, and carbohydrates can undergo one or more cycles of glycosylation in the lumens of the Golgi complex and the endoplasmic reticulum, often resulting in elaborate glycan chains (Stanley, 2011). The glycosyltransferases responsible for these reactions consume nucleotide sugars such as GDP-mannose and UDP-glucose and generate nucleoside diphosphates which are rapidly converted by luminal nucleoside triphosphate diphopshohydrolases (NTPDases, or apyrases) to GMP and UMP plus Pi and H^+ as byproducts (Knowles, 2011). Nucleotide sugar transporters embedded in the membranes of these organelles then exchange one luminal nucleoside monophosphate for one cytoplasmic nucleotide sugar to allow additional rounds of glycosylation to occur (Hirschberg *et al.*, 1998). However, the fates of Pi and H^+ byproducts of glycosylation reactions are not fully understood, and it is possible that their buildup in secretory organelles could adversely affects glycosylation reactions, sorting and trafficking of secretory proteins, and cell physiology.

Glycosyltransferases usually depend on Ca^{2+} or Mn^{2+} ions for maximal activity (Dürr *et al.*, 1998). The SPCA-family of P-type ATPases, which is mutated in Hailey-Hailey disease of humans (Hu *et al.*, 2000; Sudbrak *et al.*, 2000), directly transports Ca^{2+} and Mn^{2+} ions from the cytoplasm into the lumen of the Golgi complex to satisfy the needs of most glycosyltransferases, as well as the kexin-family of pro-protein convertases. The first SPCA-family Ca^{2+}/Mn^{2+} pump, termed Pmr1, was discovered in budding yeast (Rudolph *et al.*, 1989) and the *pmr1*Δ knockout mutants exhibited strong defects in glycosylation and processing of secretory proteins in the Golgi complex, inability to proliferate in low Ca^{2+} environments, and hypersensitivity to high Mn^{2+} in the

culture media (Antebi and Fink, 1992; Sorin *et al.*, 1997; Dürr *et al.*, 1998). The *pmr1*Δ mutants also exhibited mild activation of the unfolded protein response, likely because yeast naturally lacks a SERCA-family Ca^{2+} pump that supplies the ER of most other species with Ca^{2+} necessary for folding of secretory proteins (Dürr *et al.*, 1998; Strayle *et al.*, 1999). The deficiency of Ca^{2+} in the Golgi and ER of yeast leads to activation of the cell wall integrity MAP kinase Slt2/Mpk1, which induces expression of the K^{+} transporter Kch1 that depolarizes the cell membrane and activates a voltage-gated Ca^{2+} channel (also called HACS, and composed of Cch1, Mid1, Ecm7) to promote Ca^{2+} influx, elevation of cytosolic free Ca^{2+} concentrations, and replenishment of the secretory Ca^{2+} pools (Locke *et al.*, 2000; Bonilla *et al.*, 2002; Bonilla and Cunningham, 2003; Martin *et al.*, 2011; Stefan and Cunningham, 2013; Stefan *et al.*, 2013). This mechanism of ER and Golgi Ca^{2+} homeostasis in yeast is analogous to, but mechanistically distinct from, store-operated Ca^{2+} entry mechanisms in animals (Smyth *et al.*, 2010). Elevated cytosolic free Ca^{2+} in yeast also activates calmodulin and the serine/threonine protein phosphatase calcineurin, which induces expression of Pmr1 via activation of the Crz1 transcription factor (Matheos *et al.*, 1997; Stathopoulos and Cyert, 1997). Crz1 also induces a PMCA-family Ca^{2+} pump, termed Pmc1 (Cunningham and Fink, 1994), which localizes to the limiting membrane of lysosome-like vacuoles and partially mislocalizes to the Golgi complex and ER in mutants that lack Pmr1(Marchi *et al.*, 1999). Because the vacuole plays a major role in Ca^{2+} detoxification in yeast, mutants that lack Pmc1 or Crz1 exhibit strong growth defects in medium supplemented with high Ca^{2+} (Cunningham and Fink, 1994; Matheos *et al.*, 1997).

The yeast vacuole, like lysosomes in animals, is strongly acidified by the action of the V-ATPase, which directly transports H^+ from the cytoplasm to the lumen (Kane, 2016) The CAX-family H^+/Ca^{2+} exchangers in the vacuolar limiting membrane utilize this pH gradient to power transport of Ca^{2+} from the cytoplasm to the vacuole lumen (Forster and Kane, 2000). The first CAX-family H^+/Ca^{2+} exchanger, termed Vcx1, was discovered in yeast based on its ability to confer Ca^{2+} or Mn^{2+} resistance when overexpressed (Cunningham and Fink, 1996; Pozos *et al.*, 1996). But surprisingly, *vcx1*Δ mutants exhibit little hypersensitivity to Ca^{2+} unless calcineurin was also eliminated with either mutations or inhibitors such as cyclosporine and FK506 (Cunningham and Fink, 1996). These studies suggest that activated calcineurin may somehow inhibit Vcx1 function, while independently inducing Pmc1 and Pmr1 expression via Crz1 activation (see Figure 2.1A). However, the molecular mechanism of Vcx1 inhibition by calcineurin has not been elucidated and the interaction could be indirect.

Here we rule out the V-ATPase as a necessary intermediate in the inhibition of Vcx1 by calcineurin and we search for possible intermediaries through a genome-wide screen of the yeast gene knockout collection. While the *gdt1*Δ mutant closely resembled the *vcx1*Δ mutant in its hypersensitivity to Ca^{2+} when calcineurin was inhibited or mutated, calcineurin-dependent inhibition of Vcx1 still occurred in *gdt1*Δ mutants. Gdt1 localizes to the Golgi complex of yeast, promotes glycosylation in high Ca^{2+} conditions, and transports Ca^{2+} when expressed in heterologous systems (Demaegd *et al.*, 2013; Colinet *et al.*, 2016; Potelle *et al.*, 2016). The sole human ortholog of Gdt1, termed TMEM165, was previously shown to regulate pH and glycosylation in the Golgi complex and to be deficient in individuals with a congenital disorder of glycosylation (Foulquier *et*

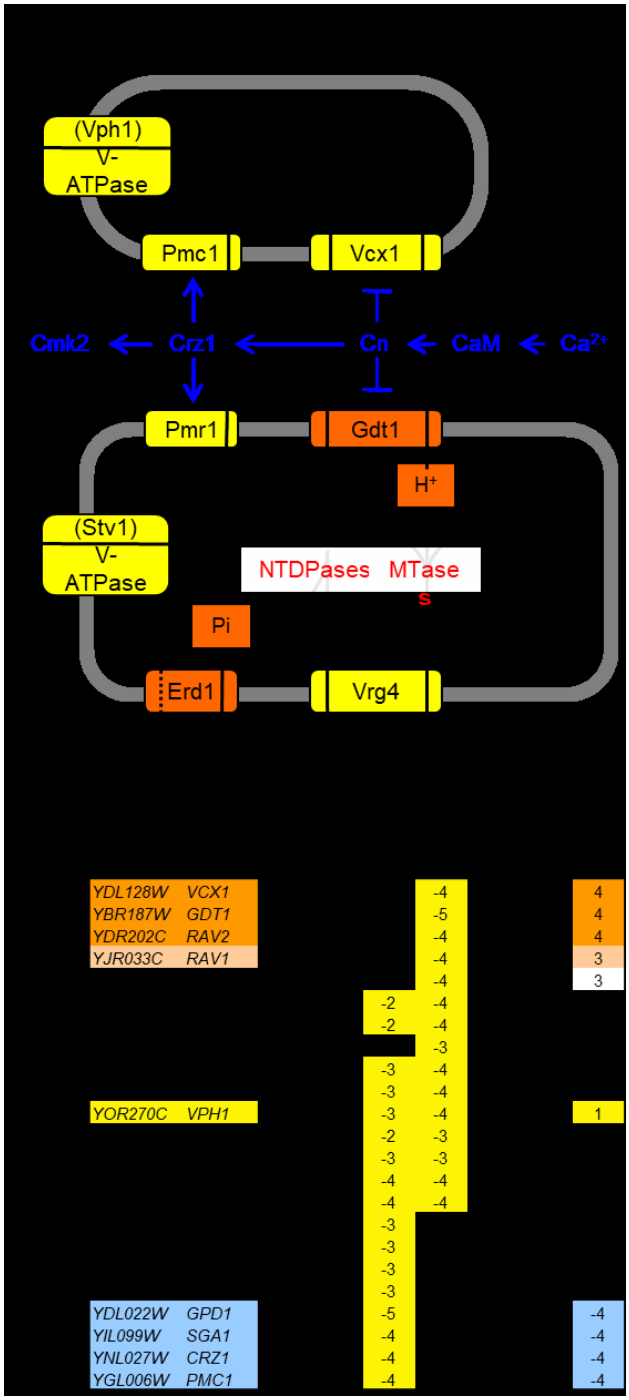

Figure 2.1: Model of Ca2+ homeostasis and Golgi glycosylation, with results from a genome-wide screen.

(A) Model of known ion or nucleotide sugar transporters (yellow) in the vacuole and Golgi complex that are studied here along with modes of regulation (blue) by the Crz1

transcription factor, calcineurin, calmodulin, and high cytosolic Ca^{2+}. Gdt1 and Erd1 (orange) are putative transporters of the byproducts of glycosylation reactions in the Golgi complex such as H^+ (produced by mannosyltransferases [MTases]) and Pi (produced by nucleoside triphosphate diphosphatases [NTDPases]) that were identified in genetic screens. (B) Results of a genetic screen for knockout mutants that specifically exhibit hypersensitivity to elevated Ca^{2+} and/or Ca^{2+} plus FK506 in the growth medium. The numbers indicate growth relative to wild-type controls (smaller numbers indicate slower growth) with the strongest effects highlighted (yellow). The 23 filtered mutants were ranked from *vcx1*Δ-like (orange) to *pmc1*Δ-like (blue) based on the difference between the two Ca^{2+} conditions.

al., 2012; Zeevaert *et al.*, 2013; Potelle *et al.*, 2016). Below we show that Gdt1 and Vcx1 both promote Ca^{2+} sequestration when their organelles are properly acidified by the V-ATPase and both promote Ca^{2+} increases in the cytoplasm when acidification has been disrupted.

To investigate how calcineurin might regulate Gdt1 function, we isolated spontaneous mutations that exhibited elevated Gdt1 function even while calcineurin remained functional. Mutants deficient in Erd1, a polytopic transmembrane protein important for glycosylation and sorting of proteins in the Golgi complex (Hardwick *et al.*, 1990), were recovered. We show evidence that Erd1 recycles Pi byproducts of the glycosylation in the Golgi complex before this important nutrient is lost by exocytosis. Therefore, this study sheds new light on the mechanisms that sustain luminal glycosylation reactions in the Golgi complex and promote Pi, Ca^{2+}, and H^+ homeostasis in the cell.

RESULTS

Genetic screen for mutants with altered Ca^{2+} sensitivity: V-ATPase, Vcx1, and Gdt1.

The ability of yeast cells to proliferate in high Ca^{2+} environments depends mostly on the vacuolar Ca^{2+} ATPase (Pmc1) when calcineurin is functioning and mostly on the vacuolar H^+/Ca^{2+} exchanger (Vcx1) when calcineurin has been inhibited or mutated (Cunningham and Fink, 1996). To search for additional Ca^{2+} transporters or regulators of Vcx1, we screened a collection of 4,848 non-essential gene knockout mutants of yeast strain BY4741 for their ability to proliferate in media containing 200 mM $CaCl_2$ with and without the calcineurin inhibitor FK506 (see methods). A similar genetic screen using

cyclosporine instead of FK506 to inhibit calcineurin yielded partially overlapping results (Zhao *et al.*, 2013). After filtering all the mutants that were hypersensitive to FK506 alone or control osmolyte (200 mM $MgCl_2$), and then filtering out the candidates that had exhibited elevated Ca^{2+} uptake in response to FK506 in a previous study (Martin *et al.*, 2011), a total of 23 mutants were hypersensitive to Ca^{2+}, Ca^{2+} plus FK506, or both while passing the stringent filters. These 23 mutants were ranked on a scale ranging from "*vcx1*Δ-like" to "*pmc1*Δ-like" (Figure 2.1B). As expected, the *crz1*Δ mutant ranked closest to the *pmc1*Δ mutant because the calcineurin-dependent transcription activator Crz1 strongly induces expression of Pmc1 (Matheos *et al.*, 1997; Stathopoulos and Cyert, 1997). Two other mutants (*gpd1*Δ, *sga1*Δ) exhibited hypersensitivity to Ca^{2+} but not Ca^{2+} plus FK506, but were not studied further.

The three mutants closest to *vcx1* (*gdt1*Δ, *rav1*Δ, *rav2*Δ) may be deficient in positive regulators of Vcx1 or in novel Ca^{2+} transporters. Rav2 forms a complex with Rav1 and promotes assembly of V1 and V0 sectors of the vacuolar form of the V-ATPase (Smardon *et al.*, 2014). The low residual vacuolar V-ATPase activity present in *rav1*Δ and *rav2*Δ mutants may be insufficient to power the H^+/Ca^{2+} exchange activity of Vcx1, thereby producing the *vcx1*Δ-like phenotype. Complete loss of all V-ATPase forms, as observed in *vma1*Δ and other *vma* mutants, resulted in hypersensitivity to high Ca^{2+} and Ca^{2+} plus FK506, but these mutants were filtered out because of hypersensitivity to high Mg^{2+} and Mg^{2+} plus FK506. Surprisingly, a mutant that specifically lacks only the vacuolar form of the V-ATPase (*vph1*Δ) while preserving the Golgi/endosomal forms exhibited no hypersensitivity to high Mg^{2+} and strong hypersensitivity to high Ca^{2+} and

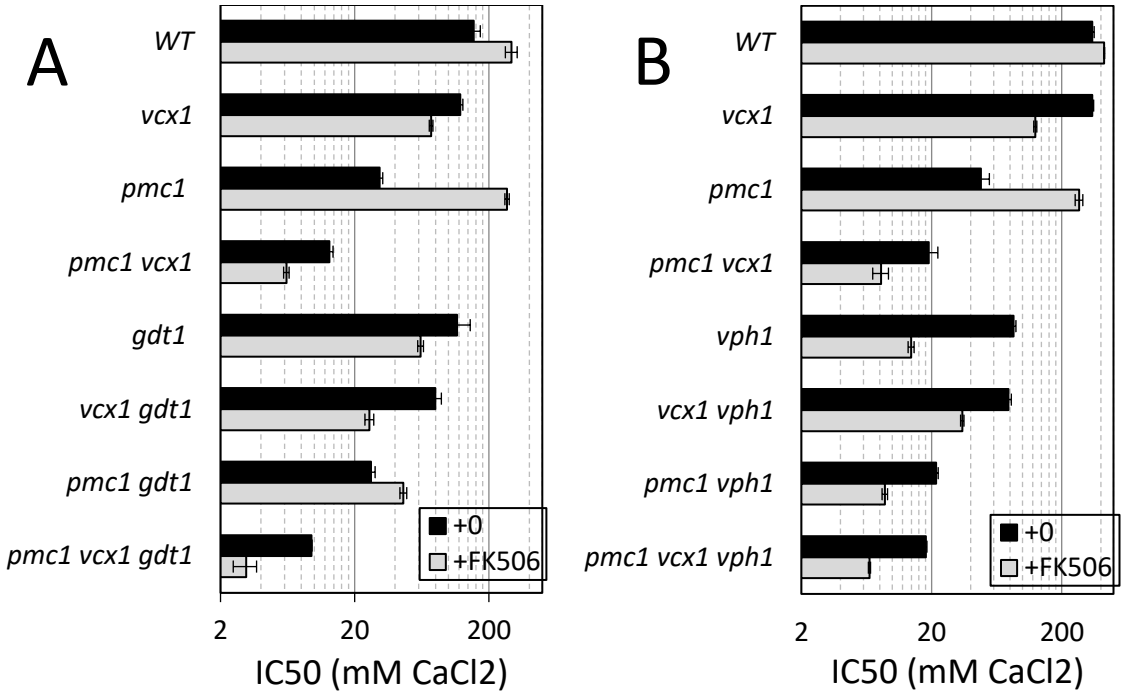

Figure 2.2: Vacuolar V-ATPase determines directionality of Vcx1 operation.

(A) Ca^{2+} tolerance assays were performed in duplicate in YPDS medium (black bars) or in the same medium containing 0.2 μg/mL FK506 (gray bars) as described in Methods, and the derived IC50 values (± S.D.) for the indicated mutants were plotted on a log scale. (B) The indicated strains were transformed with plasmid pKC190 that bears the *PMC1-lacZ* reporter gene (Cunningham and Fink, 1996) and β-galactosidase activity was measured 4 hr after log-phase cells were shifted to YPDS medium containing 100 mM $CaCl_2$. Results from three independent transformants were averaged (± S.D.).

high Ca^{2+} plus FK506 conditions (Figure 2.1B, line 11), as if the functions of Vcx1 and Pmc1 were both compromised.

To investigate how the vacuolar V-ATPase affects Pmc1 and Vcx1 function, a *pmc1*Δ *vcx1*Δ *vph1*Δ triple knockout mutant was constructed in the W303-1A strain background along with all possible double and single knockout mutants and the concentrations of $CaCl_2$ that cause a 50% inhibition of total growth (i.e. the IC50) was compared for all eight strains. Relative to the wild-type parent, the *pmc1*Δ *vcx1*Δ *vph1*Δ triple mutant was ~19-fold more sensitive to Ca^{2+} in the medium (Figure 2.2A, black bars). In the absence of Vph1, restoring Pmc1 increased the IC50 for Ca^{2+} strongly (4.2-fold) whereas restoring Vcx1 had little effect (1.1-fold) in the presence or absence of Pmc1. Restoring Vph1 function had no significant effect in the cells that lack both Pmc1 and Vcx1 (1.05-fold), but had strong effects on cells expressing only Vcx1 (2.2-fold) or Pmc1 (4.4-fold). Therefore, Pmc1 activity was partially dependent on a functional V-ATPase in the vacuolar membrane, and the relatively low Vcx1 activity detectable in *pmc1*Δ mutant backgrounds was totally dependent on the vacuolar V-ATPase.

To test whether the vacuolar V-ATPase mediates the interaction between calcineurin and Vcx1, the same eight mutant strains were reanalyzed in the presence of FK506 (Figure 2.2A, gray bars). The *pmc1*Δ *vcx1*Δ *vph1*Δ triple mutant became 2.7-fold more sensitive to Ca^{2+} in the presence of FK506 than in the absence of FK506, presumably due to diminished function of the Crz1 transcription factor and therefore diminished expression of the Pmr1 Ca^{2+}/Mn^{2+} ATPase in the Golgi complex when calcineurin is inhibited. Restoring Vcx1 function alone had little effect (1.3-fold increase) in the presence of FK506 whereas restoring Pmc1 function alone had strong

effects (5.2-fold increase) despite a lower expression of Pmc1 in the absence of calcineurin (Cunningham and Fink, 1994). Importantly, restoring Vcx1 in the *vph1*Δ mutant actually *lowered* tolerance to environmental Ca^{2+} by a significant degree (2.5-fold decrease) in the absence of both calcineurin and only when Pmc1 was functioning. These findings show, for the first time, that Vcx1 can antagonize the function of Pmc1 when the vacuoles lack acidification by the V-ATPase and when the cytoplasm lacks calcineurin signaling. Such antagonism was expected because H^+/Ca^{2+} exchangers are generally thought to operate in 'reverse-mode' in conditions where the luminal H^+ concentration is low and the Ca^{2+} concentration is high, potentially causing futile cycles between Vcx1 and Pmc1 in the absence of Vph1. Reverse-mode operation of Na^+/Ca^{2+} exchangers is well established (Harper and Sage, 2016). That reverse-mode operation of Vcx1 (observed in *vph1*Δ mutants with FK506) did not occur in the absence of FK506 suggests calcineurin regulates both forward and reverse modes of Vcx1 through a process that is independent of the V-ATPase.

Reverse-mode operation of Vcx1 is predicted to increase cytoplasmic free Ca^{2+} concentrations and enhance calcineurin signaling, while forward-mode operation achieves the opposite effects. To test this prediction, we measured expression of a calcineurin-sensitive reporter gene *PMC1-lacZ* in *vcx1*Δ *vph1*Δ double mutants relative to the single mutants and control strain. This experiment was performed in a *pmc1*Δ mutant background to improve the sensitivity of the reporter and enable detection of forward-mode Vcx1 activity (Cunningham and Fink, 1996). As predicted, the *pmc1*Δ *vcx1*Δ strain expressed *PMC1-lacZ* at significantly higher levels than the *pmc1*Δ strain after exposure to 100 mM $CaCl_2$, whereas the *pmc1*Δ *vph1*Δ *vcx1*Δ triple mutant strain exhibited much

lower levels of expression than the *pmc1*Δ *vcx1*Δ double mutant strain (Figure 2.2B). These findings show that Vcx1 can lower calcineurin signaling when the vacuole is properly acidified and increase calcineurin signaling when the vacuolar V-ATPase is inactivated, thus providing independent evidence that Vcx1 transports Ca^{2+} bi-directionally similar to Na^{+}/Ca^{2+} exchangers in animals.

Calcineurin regulates independent functions of Gdt1 and Vcx1.

The *gdt1*Δ mutant, which lacks a probable Golgi-localized H^{+}/Ca^{2+} exchanger (Demaegd *et al.*, 2013; Colinet *et al.*, 2016), clustered closest to the *vcx1*Δ mutant in our screening conditions (Figure 2.1B) and therefore is a potential regulator of Vcx1. To test whether Gdt1 promotes Ca^{2+} resistance independent of Vcx1, the *gdt1*Δ knockout mutation was introduced into the *pmc1*Δ *vcx1*Δ double mutant and the single mutants in the W303-1A background and the IC50's of Ca^{2+} were quantified in the presence and absence of FK506. The *gdt1*Δ mutation weakly diminished Ca^{2+} tolerance in every strain background when calcineurin was functional (average decline of 1.35 ± 0.15 fold) but strongly diminished Ca^{2+} tolerance in WT, *pmc1*Δ, *vcx1*Δ, and *pmc1*Δ *vcx1*Δ backgrounds when FK506 was present (by 4.8, 2.9, 5.9, and 2.0 fold respectively; Figure 2.3A). Similar results were obtained when calcineurin was inactivated by a *cnb1*Δ knockout mutation (data not shown). Thus, in the absence of calcineurin signaling, Gdt1 strongly promoted Ca^{2+} tolerance independent of both Vcx1 and Pmc1, and likely represents a new class of Ca^{2+} transporter that is partially inhibited by calcineurin.

Calcineurin may directly or indirectly regulate Gdt1 function. To test whether calcineurin inhibits Gdt1 function through its ability to activate Crz1 or to induce

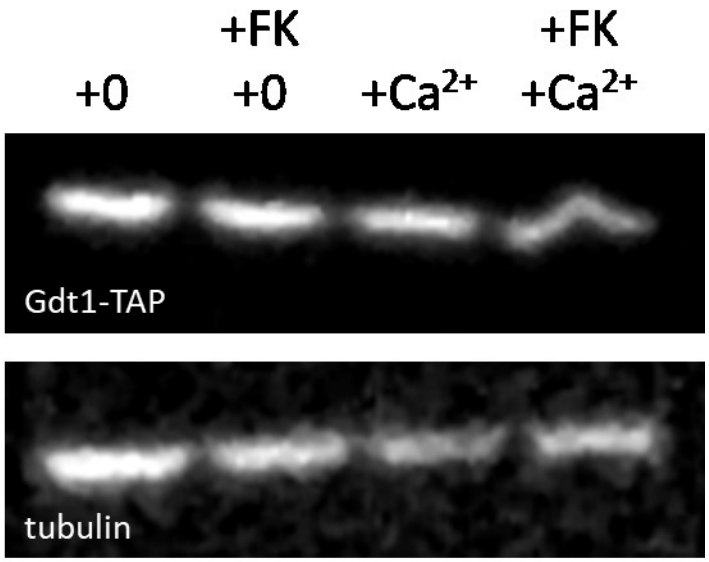

Figure 2.3: Gdt1 promotes Ca2+ detoxification independent of Vcx1 and Pmc1. (A) A panel of *S. cerevisiae* strains lacking Gdt1, Vcx1, and Pmc1 in all possible combinations was assayed for Ca2+ tolerance in the presence (gray bars) or absence (black bars) of FK506 as described in Figure 2.2A. (B) A strain expressing epitope-tagged Gdt1-TAP was grown to log phase in YPDS medium containing 200 mM $CaCl_2$ and/or 1 μg/mL FK506, harvested, lysed, and analyzed by SDS-PAGE and western blotting using anti-TAP polyclonal (top) and anti-tubulin monoclonal (bottom) antibodies.

expression of Cmk2, we repeated the Ca^{2+} tolerance experiments described above in *crz1*Δ *cmk2*Δ double mutant and single mutant backgrounds. This experiment ruled out Crz1 and Cmk2 as possible intermediaries in the inhibition of Gdt1 by calcineurin (see Table 2.1). To test whether calcineurin signaling could diminish expression of Gdt1 or alter its mobility on SDS-PAGE, western blots were performed on cells containing a TAP epitope tag, integrated at the 3' end of the chromosomal *GDT1* gene (Ghaemmaghami *et al.*, 2003), that were exposed to Ca^{2+} with and without FK506. The TAP-tag did not alter the Ca^{2+} tolerance functions of Gdt1 or its responsiveness to FK506 (not shown). After exposure of the cells to 200 mM $CaCl_2$ with or without 1 μg/mL FK506 for 12 hr, the Gdt1-TAP band maintained the same intensity and migration on the gel (Figure 2.3B). Therefore, the inhibitory effects of calcineurin on Gdt1 function were not noticeably associated with changes in Gdt1 expression or modification and possibly dependent on unknown intermediaries.

Gdt1 promotes H^+/Ca^{2+} exchange in the Golgi complex

Recent studies also showed that Gdt1 localized to the Golgi complex of yeast (Demaegd *et al.*, 2013), and we have independently confirmed those findings using immunofluorescence microscopy and sucrose gradient fractionation of a functional Gdt1-3HA fusion protein (data not shown). This finding led us to explore the possible interactions between Gdt1 and Pmr1, the secretory pathway Ca^{2+} ATPase of yeast. To determine whether Gdt1 supplies essential Ca^{2+} or Mn^{2+} to the Golgi complex independent of Pmr1, we quantified the tolerance of *gdt1*Δ *pmr1*Δ double mutant and single mutant strains to either high Mn^{2+} (Figure 2.4A) or a membrane-impermeant

Table 2.1: Sensitivity of mutant strains to added $CaCl_2$ (Experiment A) [a]

	Strain Names		Genotypes and Conditions [b]						CV [c]	avg IC50 [d]	Performance Factor [e]					
LINE	MATa	MATα	PMC1	VCX1	GDT1	CRZ1	CN	CMK2	%	mM	PMC1	VCX1	GDT1	CRZ1	CN	CMK2
1	K1849	K1850	Δ						3	21		0.3	0.2	-0.1	-3.1	-0.3
2	K1851	K1852	Δ			Δ			7	22		0.8	0.3		-3.2	-0.6
3	K1857	K1858	Δ		Δ				0	18		0.6		0.1	-1.0	0.1
4	K1859	K1860	Δ		Δ	Δ			11	18		0.9			-0.9	-0.4
5	K1865	K1866	Δ	Δ					0	18			0.5	0.5	0.3	0.1
6	K1867	K1868	Δ	Δ		Δ			7	12			0.4		0.2	0.4
7	K1873	K1874	Δ	Δ	Δ				12	12				0.3	0.6	-0.2
8	K1875	K1876	Δ	Δ	Δ	Δ			5	9					0.9	0.1
9	K1849	K1850	Δ				+FK		2	179		3.7	2.3	-0.1		0.2
10	K1851	K1852	Δ			Δ	+FK		1	197		4.3	2.6			0.6
11	K1857	K1858	Δ		Δ		+FK		3	36		2.2		0.1		0.1
12	K1859	K1860	Δ		Δ	Δ	+FK		1	33		2.7				0.4
13	K1865	K1866	Δ	Δ			+FK		9	14			0.8	0.4		0.9
14	K1867	K1868	Δ	Δ		Δ	+FK		7	10			1.0			1.3
15	K1873	K1874	Δ	Δ	Δ		+FK		32	8				0.6		0.7
16	K1875	K1876	Δ	Δ	Δ	Δ	+FK		4	5						1.0
17	K1853	K1854	Δ					Δ	4	25		0.6	0.5	-0.4	-2.6	
18	K1855	K1856	Δ			Δ		Δ	14	33		1.8	0.5		-2.0	
19	K1861	K1862	Δ		Δ			Δ	19	18		0.3		-0.4	-0.9	
20	K1863	K1864	Δ		Δ	Δ		Δ	6	23		1.4			-0.1	
21	K1869	K1870	Δ	Δ				Δ	2	16			0.2	0.8	1.2	
22	K1871	K1872	Δ	Δ		Δ		Δ	1	10			0.1		1.2	
23	K1877	K1878	Δ	Δ	Δ			Δ	4	14				0.7	1.5	
24	K1879	K1880	Δ	Δ	Δ	Δ		Δ	4	9					1.8	
25	K1853	K1854	Δ				+FK	Δ	0	156		4.4	2.2	0.2		
26	K1855	K1856	Δ			Δ	+FK	Δ	1	134		5.0	2.4			
27	K1861	K1862	Δ		Δ		+FK	Δ	1	33		2.8		0.4		
28	K1863	K1864	Δ		Δ	Δ	+FK	Δ	15	25		3.3				
29	K1869	K1870	Δ	Δ			+FK	Δ	26	7			0.6	0.8		
30	K1871	K1872	Δ	Δ		Δ	+FK	Δ	7	4			0.7			
31	K1877	K1878	Δ	Δ	Δ		+FK	Δ	14	5				0.9		
32	K1879	K1880	Δ	Δ	Δ	Δ	+FK	Δ	16	3						
33	K1833	K1834							16	70	1.7		0.7	1.1	-1.8	-0.1
34	K1835	K1836				Δ			17	32	0.6		0.1		-2.7	-0.5
35	K1841	K1842			Δ				6	42	1.2			0.5	-0.1	0.0
36	K1843	K1844			Δ	Δ			25	30	0.7				-0.4	-0.3
37	K1833	K1834					+FK		6	244	0.4		2.4	0.2		0.3
38	K1835	K1836				Δ	+FK		4	217	0.1		2.5			0.5
39	K1841	K1842			Δ		+FK		9	45	0.3			0.2		0.3
40	K1843	K1844			Δ	Δ	+FK		12	39	0.2					0.4
41	K1837	K1838						Δ	16	77	1.6		0.9	0.8	-1.3	
42	K1839	K1840				Δ		Δ	12	45	0.4		0.2		-1.8	
43	K1845	K1846			Δ			Δ	29	41	1.2			0.1	0.1	
44	K1847	K1848			Δ	Δ		Δ	6	38	0.7				0.4	
45	K1837	K1838					+FK	Δ	5	192	0.3		2.4	0.3		
46	K1839	K1840				Δ	+FK	Δ	1	156	0.2		2.4			
47	K1845	K1846			Δ		+FK	Δ	13	38	0.2			0.4		
48	K1847	K1848			Δ	Δ	+FK	Δ	32	29	0.2					

Footnotes:

[a] Yeast were inoculated in YPD, supplemented with succinate and containing a dilution series of $CaCl_2$, via a 1:1000 dilution from a saturated culture. Growth was measured by assessment of the optical density (OD_{650}) after 24 hours.

[b] addition of 0.2 µg/mL FK506

[c] coefficient of variation between two strains (in %) or one strain

[d] average of derived IC50 from two strains (in mM $CaCl_2$)

[e] PF = $\log_2$ of (avg IC50 WT strain/avg IC50 Δ strain)

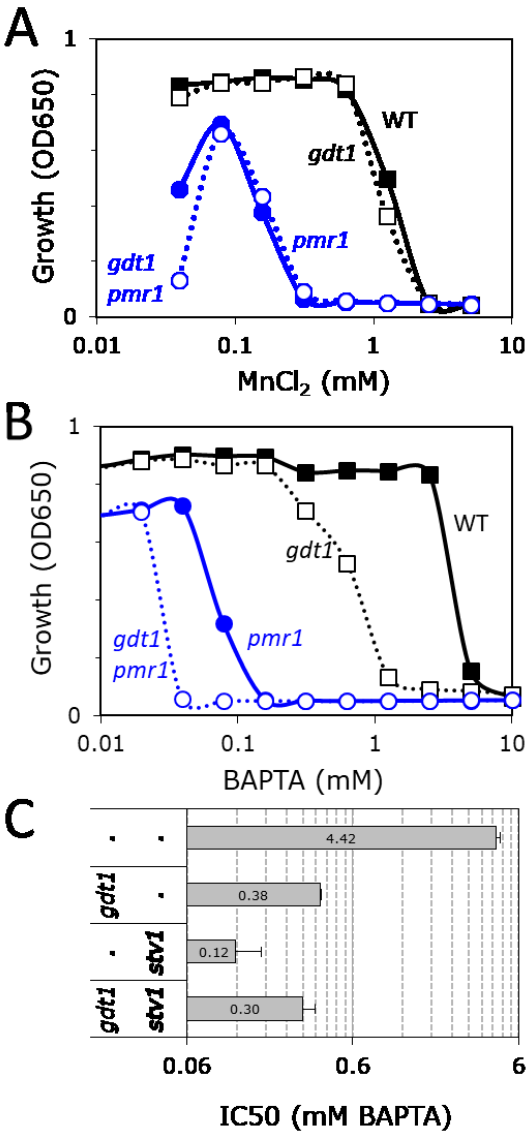

Figure 2.4: Gdt1 supplies essential Ca^{2+} independent of Pmr1 and reverse-mode activity of Gdt1 is blocked by Golgi V-ATPase.

Mn^{2+} (A) and BAPTA (B, C) tolerance assays were performed in YPD medium and raw data (A, B) or derived IC50 values (C; ± S.D.) were plotted on log scales. (D) Expression of *PMC1-lacZ* reporter gene was measured as described in Figure 2.2B except the medium contained either 0 mM (white bars) or 50 mM (grey bars) supplemental $CaCl_2$.

chelator of Ca^{2+}, Mn^{2+}, and other divalent cations (BAPTA, Fig 2.4B) in the culture medium. The Mn^{2+} tolerance of *gdt1*Δ mutants and *gdt1*Δ *pmr1*Δ double mutants were indistinguishable from control strains (wild-type and *pmr1*Δ, respectively), suggesting that Gdt1 cannot remove toxic Mn^{2+} from the cytoplasm. The *gdt1*Δ mutant exhibited a strong hypersensitivity to BAPTA relative to the wild-type parent strain, and the *gdt1*Δ *pmr1*Δ double mutant exhibited extreme hypersensitivity to BAPTA that was significantly greater than the *pmr1*Δ mutant (Figure 2.4B). Thus, Gdt1 appeared to supply essential Ca^{2+} ions to the Golgi complex independent of Pmr1.

Interestingly, FK506 blocked growth of *gdt1*Δ *pmr1*Δ double mutants in all growth media we tested (data not shown). This lethality of FK506 suggests that calcineurin-dependent up-regulation of Pmc1 and relocalization to the Golgi complex (Marchi *et al.*, 1999) is crucial to supply essential Ca^{2+} when Pmr1 and Gdt1 are absent, but further experiments are required to test this hypothesis.

If Gdt1 functions as a H^+/Ca^{2+} exchanger in the Golgi, its contributions to BAPTA tolerance should depend on the Golgi/endosomal forms of the V-ATPase, which employ Stv1 rather than Vph1 in the V0-sector of the enzyme (Manolson *et al.*, 1994). However, *stv1*Δ mutants alone behaved like wild-type in all conditions tested because the remaining Vph1-containing V-ATPase fully acidifies the Golgi even in the absence of Stv1 (Qi and Forgac, 2007). We therefore tested the BAPTA tolerance of *gdt1*Δ and *stv1*Δ mutations in a background that lacks Vph1 (and also Vcx1, which could complicate the analyses). In this *vph1*Δ *vcx1*Δ double mutant background, the loss of Gdt1 caused more than 10-fold decrease in BAPTA tolerance and the further loss of Stv1 had little additional effect (Figure 2.4C). The loss of Stv1 alone caused more than 25-fold

decrease in BAPTA tolerance, and this hypersensitivity was partially reversed (~2.5 fold) by the further loss of Gdt1. Thus, like Vcx1, Gdt1 appeared to function in reverse-mode when the V-ATPase was completely eliminated and in forward-mode when the V-ATPase was functional.

The ability of Gdt1 to decrease and increase cytosolic free Ca2+ was also examined by measuring expression of the calcineurin-dependent *PMC1-lacZ* reporter gene described earlier. In the *vph1*Δ *vcx1*Δ double mutant background that acidifies the Golgi complex, the additional *gdt1*Δ mutation did not significantly alter expression of the reporter gene after addition of 50 mM $CaCl_2$ (Figure 2.4D), and so forward-mode activity of Gdt1 was not detectable above the high influences of Pmc1 and Pmr1 in these conditions. However, reverse-mode activity of Gdt1 was detected in the *vph1*Δ *vcx1*Δ *stv1*Δ triple mutant background because the additional *gdt1*Δ mutation significantly lowered expression of the reporter gene (Figure 2.4D). Together with the earlier findings on Gdt1 and Vcx1 bi-directionality, these findings provide strong support for the hypothesis that Gdt1 functions as a reversible H^+/Ca^{2+} exchanger of the Golgi complex *in vivo*.

Erd1 recycles inorganic phosphate from the ER and Golgi complex and limits the functions of Pmr1 and Gdt1.

If activated calcineurin inhibits Gdt1 function, it may be possible to isolate variants of Gdt1 that are hyperactive when calcineurin is fully functional, similar to the hyperactive Vcx1-D mutants that have been isolated previously (Cunningham and Fink, 1996). To focus on mutants that disrupt the interaction between calcineurin and Gdt1, we

generated strains simultaneously lacking Pmc1, Vcx1, and Crz1 and selected for rare spontaneous mutants that enabled growth in medium supplemented with high concentrations of $CaCl_2$ (see Methods). Of 36 independent spontaneous mutations, 26 were found to be dominant in heterozygous diploids. The *GDT1* coding sequence from all 26 strains was amplified by PCR and sequenced. No mutations were identified in the *GDT1* coding sequences. The mechanism of Gdt1 regulation by calcineurin remains unknown and may involve several unknown intermediary steps (see Discussion).

In addition to the 26 dominant mutants, 10 independent recessive mutants were recovered, and these mutants defined a single complementation group. All of the recessive Ca^{2+}-resistant mutants were found to be hypersensitive to tunicamycin, an inhibitor of N-glycosylation reactions in the ER (Lehle and Tanner, 1976), and we isolated two low-copy plasmids from a library of random genomic DNA fragments that complemented this phenotype. The *ERD1* gene was found to be necessary and sufficient for complementation of both phenotypes, and the *erd1*Δ knockout mutation was found to recapitulate both phenotypes in the starting strain background. Though the precise function of Erd1 has not yet been determined, earlier studies show that Erd1 is a polytopic membrane protein important for two Golgi-localized processes: glycosylation of secretory proteins and for retrieval of escaped HDEL-containing proteins back to the ER (Hardwick *et al.*, 1990). To determine its role in Ca^{2+} homeostasis, the *erd1*Δ mutation was introduced into backgrounds that also lack Pmc1, Vcx1, Gdt1, and Crz1 and the IC50s for $CaCl_2$ were measured as before. These experiments showed that Erd1 significantly decreased Ca^{2+} tolerance of *pmc1*Δ *vcx1*Δ *crz1*Δ triple mutant (1.9 fold decrease), and that this effect was abolished if Gdt1 were eliminated (Table 2.2). Erd1

Table 2.2: Sensitivity of mutant strains to added $CaCl_2$ (Experiment B)[a]

	Strain Names		Genotypes and Conditions [b]							CV [c]	avg IC50 [d]	Performance Factor [e]						
LINE	MATa	MATα	PMC1	VCX1	GDT1	CRZ1	CN	CMK2	ERD1	%	mM	PMC1	VCX1	GDT1	CRZ1	CN	CMK2	ERD1
2	NS132	NS133	Δ			Δ				1	49		2.4	0.7		-2.6		-0.1
3	NS136	NS137	Δ		Δ					4	30		1.0		0.0	-0.5		-0.1
4	NS144	NS145	Δ		Δ	Δ				12	30		1.9			-0.4		0.0
5	NS154	NS155	Δ	Δ						0	27			0.8	1.5	1.4		-0.1
6	NS164	NS165	Δ	Δ		Δ				4	9			0.2		0.2		-0.9
7	NS168	NS169	Δ	Δ	Δ					1	15				0.9	1.6		-0.2
8	NS176	NS177	Δ	Δ	Δ	Δ				*	8					0.9		-0.3
9	NS122	NS123	Δ				+FK			1	298		4.9	2.8	0.0			0.9
10	NS132	NS133	Δ			Δ	+FK			0	297		5.2	2.9				0.9
11	NS136	NS137	Δ		Δ		+FK			5	42		3.0		0.1			1.2
12	NS144	NS145	Δ		Δ	Δ	+FK			11	40		3.2					1.1
13	NS154	NS155	Δ	Δ			+FK			5	10			1.0	0.3			-0.9
14	NS164	NS165	Δ	Δ		Δ	+FK			6	8			0.9				-0.5
15	NS168	NS169	Δ	Δ	Δ		+FK			0	5				0.2			0.0
16	NS176	NS177	Δ	Δ	Δ	Δ	+FK			*	4							0.1
17	NS128	NS129	Δ						Δ	1	33		0.2	0.1	-0.7	-2.3		
18	NS138	NS139	Δ			Δ			Δ	0	53		1.6	0.8		-1.6		
19	NS140	NS141	Δ		Δ				Δ	4	32		0.8		0.1	0.8		
20	NS146	NS147	Δ		Δ	Δ			Δ	1	29		1.6			0.7		
21	NS160	NS161	Δ	Δ					Δ	1	30			0.7	0.8	0.7		
22	NS170	NS171	Δ	Δ		Δ			Δ	0	17			0.8		0.6		
23	NS172	NS173	Δ	Δ	Δ				Δ	8	18				0.9	1.8		
24	NS178	NS179	Δ	Δ	Δ	Δ			Δ	6	10					1.3		
25	NS128	NS129	Δ				+FK		Δ	1	158		3.1	3.1	0.0			
26	NS138	NS139	Δ			Δ	+FK		Δ	7	161		3.8	3.1				
27	NS140	NS141	Δ		Δ		+FK		Δ	1	18		1.8		0.0			
28	NS146	NS147	Δ		Δ	Δ	+FK		Δ	1	18		2.2					
29	NS160	NS161	Δ	Δ			+FK		Δ	0	19			1.8	0.7			
30	NS170	NS171	Δ	Δ		Δ	+FK		Δ	2	11			1.5				
31	NS172	NS173	Δ	Δ	Δ		+FK		Δ	16	5				0.3			
32	NS178	NS179	Δ	Δ	Δ	Δ	+FK		Δ	8	4							
33	NS116	NS117					-			3	245	3.0	0.0	0.3	1.8	-0.4		0.1
34	NS120	NS121				Δ	-			0	70	0.5	0.9	0.3		-2.2		0.3
35	NS124	NS125			Δ		-			*	203	2.8	0.5		1.8	2.2		0.8
36	NS134	NS135			Δ	Δ	-			1	57	0.9	0.8			0.0		0.7
37	NS148	NS149		Δ			-			2	237	3.1		0.7	2.6	1.6		0.1
38	NS152	NS153		Δ		Δ	-			8	38	2.0		0.2		-1.1		0.0
39	NS156	NS157		Δ	Δ		-			6	146	3.2			2.1	2.0		0.2
40	NS166	NS167		Δ	Δ	Δ	-			3	34	2.1				0.5		0.1
41	NS116	NS117					+FK			0	325	0.1	2.0	2.9	0.0			0.4
42	NS120	NS121				Δ	+FK			1	316	0.1	2.0	2.4				1.0
43	NS124	NS125			Δ		+FK			*	44	0.1	0.2		-0.4			1.1
44	NS134	NS135			Δ	Δ	+FK			1	59	0.6	1.3					1.3
45	NS148	NS149		Δ			+FK			1	81	3.0		1.1	0.0			0.1
46	NS152	NS153		Δ		Δ	+FK			4	80	3.3		1.8				0.3
47	NS156	NS157		Δ	Δ		+FK			2	37	2.9			0.7			1.5
48	NS166	NS167		Δ	Δ	Δ	+FK			1	23	2.4						1.1
49	NS118	NS119					-		Δ	2	223	2.8	0.0	1.0	1.9	-0.1		
50	NS126	NS127				Δ	-		Δ	2	59	0.2	0.7	0.7		-1.5		
51	NS130	NS131			Δ		-		Δ	2	116	1.9	-0.2		1.7	2.5		
52	NS142	NS143			Δ	Δ	-		Δ	2	35	0.3	0.2			0.5		

53	**NS150**	**NS151**		**Δ**			**-**		**Δ**	**3**	**219**	**2.9**		**0.8**	**2.6**	**1.6**		
54	**NS158**	**NS159**		**Δ**		**Δ**	**-**		**Δ**	**3**	**37**	**1.1**		**0.2**		**-0.8**		
55	**NS162**	**NS163**		**Δ**	**Δ**		**-**		**Δ**	*****	**128**	**2.9**			**2.0**	**3.3**		
56	**NS174**	**NS175**		**Δ**	**Δ**	**Δ**	**-**		**Δ**	**4**	**31**	**1.7**				**1.6**		
57	**NS118**	**NS119**					**+FK**		**Δ**	**2**	**244**	**0.6**	**1.7**	**3.6**	**0.6**			
58	**NS126**	**NS127**				**Δ**	**+FK**		**Δ**	**4**	**163**	**0.0**	**1.3**	**2.7**				
59	**NS130**	**NS131**			**Δ**		**+FK**		**Δ**	**3**	**20**	**0.1**	**0.6**		**-0.3**			
60	**NS142**	**NS143**			**Δ**	**Δ**	**+FK**		**Δ**	**29**	**24**	**0.4**	**1.2**					
61	**NS150**	**NS151**		**Δ**			**+FK**		**Δ**	**1**	**74**	**2.0**		**2.5**	**0.2**			
62	**NS158**	**NS159**		**Δ**		**Δ**	**+FK**		**Δ**	**3**	**64**	**2.5**		**2.6**				
63	**NS162**	**NS163**		**Δ**	**Δ**		**+FK**		**Δ**	*****	**13**	**1.3**			**0.3**			
64	**NS174**	**NS175**		**Δ**	**Δ**	**Δ**	**+FK**		**Δ**	**9**	**11**	**1.4**						

Footnotes:

[a] Yeast were inoculated in YPD, supplemented with succinate and containing a dilution series of $CaCl_2$, via a 1:1000 dilution from a saturated culture. Growth was measured by assessment of the optical density (OD_{650}) after 24 hours.

[b] addition of 0.2 µg/mL FK506

[c] coefficient of variation between two strains (in %) or one strain

[d] average of derived IC50 from two strains (in mM $CaCl_2$)

[e] PF = $\log_2$ of (avg IC50 WT strain/avg IC50 Δ strain)

actually increased Ca^{2+} tolerance or was neutral in most other conditions. These results are consistent with models where Erd1 selectively diminishes the forward function of Gdt1 in the Golgi complex.

Erd1 contains an EXS domain similar to that of human XPR1 and plant PHO1 proteins, which recently have been shown to export inorganic phosphate (Pi) from the cell (Hamburger *et al.*, 2002; Giovannini *et al.*, 2013). Because Pi is produced in the lumen of the Golgi complex and ER as a byproduct of glycosylation reactions (Figure 2.1A), it is possible that *erd1*Δ mutants fail to recycle Pi to the cytoplasm and the backlog of Pi in the lumen increases the buffer capacity for Ca^{2+} while also interfering with normal glycosylation and sorting reactions. To test the hypothesis that Erd1 recycles the Pi byproduct of glycosylation from the lumen of secretory organelles, several experiments were performed.

First, because Pi is an important nutrient to yeast, we explored the possibility that Erd1 is important for growth in low Pi environments. Interestingly, the concentration of Pi in the medium required for 50% maximal growth (i.e. the ED50) was about 1.5-fold higher for *erd1*Δ mutants as compared to the wild-type control strain (Figure 2.5A). The *erd1*Δ mutation caused a similar increase in the requirement for Pi when introduced into a *pho84*Δ mutant background, which lacks a high-affinity Pi transporter in the plasma membrane (Bun-Ya *et al.*, 1991) and requires approximately 3-fold higher concentrations of Pi than wild-type for growth (Figure 2.5A). The *erd1*Δ mutation strongly increased the ED50 of Pi nearly 3-fold when introduced into a *pho84*Δ *pho87*Δ *pho89*Δ *pho90*Δ *pho91*Δ quintuple mutant background (Figure 2.5B) that lacks all five of the known Pi transporters in yeast (Wykoff and O'Shea, 2001; Samyn and Persson, 2016). Therefore,

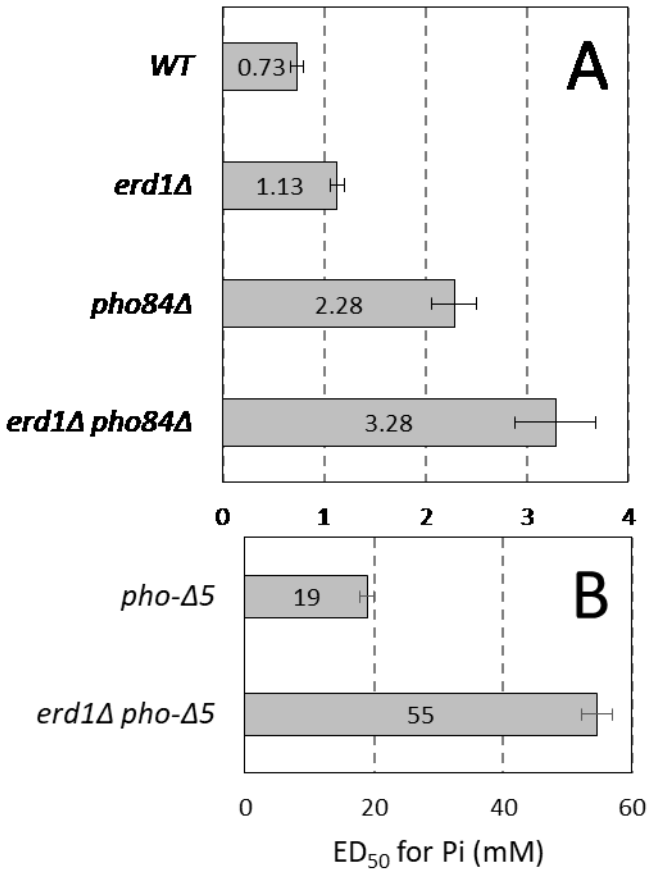

Figure 2.5: Erd1 supplies essential Pi.

The indicated mutant strains were washed and inoculated into in SC medium containing various concentrations of Pi. After 24 hr incubation, the concentration of Pi that enabled 50% maximal growth (i.e. ED50) was derived and the averages (± S.D.) of triplicate measurements are plotted. The *erd1*Δ mutation increased the ED50 by 1.5-fold, 1.4-fold, and 2.9-fold respectively in the wild-type, the *pho84*Δ, and the *pho-*Δ*5* (*pho84*Δ *pho87*Δ *pho89*Δ *pho90*Δ *pho91*Δ) backgrounds.

Erd1 supplies essential Pi to the cytoplasm of yeast cells through a process that does not rely on any of the other Pi transporters.

Second, we tested whether *erd1*Δ mutants exhibited higher rates of Pi export into the culture medium via exocytosis, which would be predicted if Erd1 normally recycles this nutrient from the Golgi complex. For this experiment, the *erd1*Δ and wild-type strains were cultivated for more than 10 generations in standard synthetic medium (7.35 mM Pi) supplemented with tracer amounts of ^{32}Pi, chilled, and the cells were washed extensively in fresh medium lacking Pi. The temperature was then raised to 30°C and aliquots were removed at different times, centrifuged to pellet the cells, and the cell-free supernatants were collected and analyzed by liquid scintillation counting and by thin layer chromatography. In the first 0.25 hr of incubation at 30°C, both *erd1*Δ and wild-type strains exported similar amounts of radioactivity. However, the *erd1*Δ mutant exported strikingly more Pi than wild-type over the next 1.75 hr of incubation (Figure 2.6A, black curves). Similar trends were obtained in the *pho84*Δ background (Figure 2.6A, red curves), though these strains started with less than 30% of the wild-type levels of Pi due to their defect in Pi accumulation prior to the start of the experiment. The large majority of radioactivity exported to the culture medium co-migrated with Pi standards on thin layer chromatography (Figure 2.6B). When the chase experiment is repeated in SC medium containing 7.35 mM Pi, the influx of non-radioactive Pi permits sustained efflux of 32-Pi from wild-type cells for several hours and still the *erd1*Δ mutant exports more 32-Pi (Figure 2.6C). If this Erd1-sensitive Pi efflux depends on exocytosis, such efflux may be diminished in a *sec1-1^{ts}* mutant background, which quickly accumulates post-Golgi secretory vesicles when shifted to the non-permissive temperature of 37°C

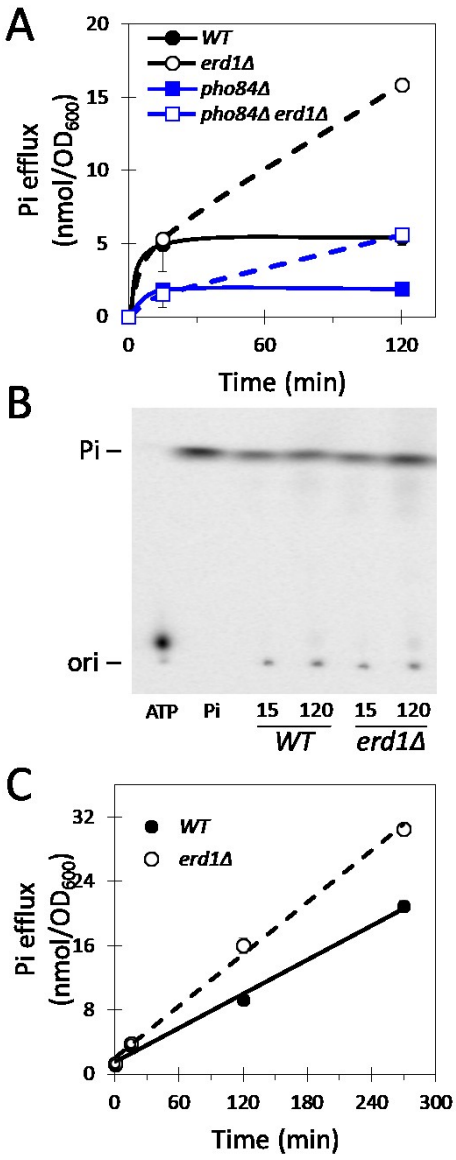

Figure 2.6: Erd1 prevents Pi loss to the environment.

The indicated mutant strains were grown to log phase in SC medium containing tracer levels of 32-Pi radioisotope, washed extensively in Pi-free SC medium, and then in the same medium (A, B) or in SC medium (C). At the indicated times of incubation at 30°C, aliquots were removed and cell-free supernatants were analyzed by liquid scintillation counting (A, C) or by thin layer chromatography (B). Charts illustrate the averages (± S.D.) of three biological replicates.

due to defects in the exocytotic machinery (Novick *et al.*, 1981). Remarkably, the Erd1-sensitive efflux of Pi was markedly diminished in the *sec1-1*^{ts} strain at 37°C but not the wild-type control strain (Figure 2.7A). These data suggest that Erd1 normally limits the export of Pi from cells via exocytosis.

If glycosylation reactions in the Golgi complex produce the Pi that is recycled by Erd1, the Erd1-sensitive Pi efflux may be diminished by inactivation of Vrg4, the main nucleotide sugar transporter of the Golgi complex that primarily supplies GDP-mannose in exchange for luminal GMP (Dean *et al.*, 1997). Vrg4 is essential for yeast growth and is not inhibited by any known molecules. To render Vrg4 druggable, we introduced an auxin-inducible degron tag at its C-terminus along with a flag tag and an expression cassette for osTIR, an auxin-sensitive E3 ubiquitin ligase (Nishimura *et al.*, 2009; Morawska and Ulrich, 2013). Strains bearing Vrg4-AID-FLAG fusion protein grew as well as wild-type in the absence of auxin, but grew much more slowly than wild-type in the presence of 100 μM auxin (data not shown) suggesting that Vrg4 expression became growth-limiting in these conditions. Indeed, just 1 hr exposure to 100 μM auxin resulted in 70% decline of Vrg4-AID-FLAG expression (Figure 2.7B). The *erd1*Δ mutation was introduced into the Vrg4-AID-FLAG and wild-type control strains and Erd1-sensitive Pi efflux was measured as above. After a 2 hr chase period in Pi-free culture medium, the Erd1-sensitive Pi efflux from wild-type cells was unaffected by exposure to auxin (Figure 2.7C). The Erd1-sensitive Pi efflux from the Vrg4-AID-FLAG strain was similar to wild-type in the absence of auxin, and was greatly reduced when the cells were exposed to auxin beginning 1 hr before the washes and continuously during the chase period

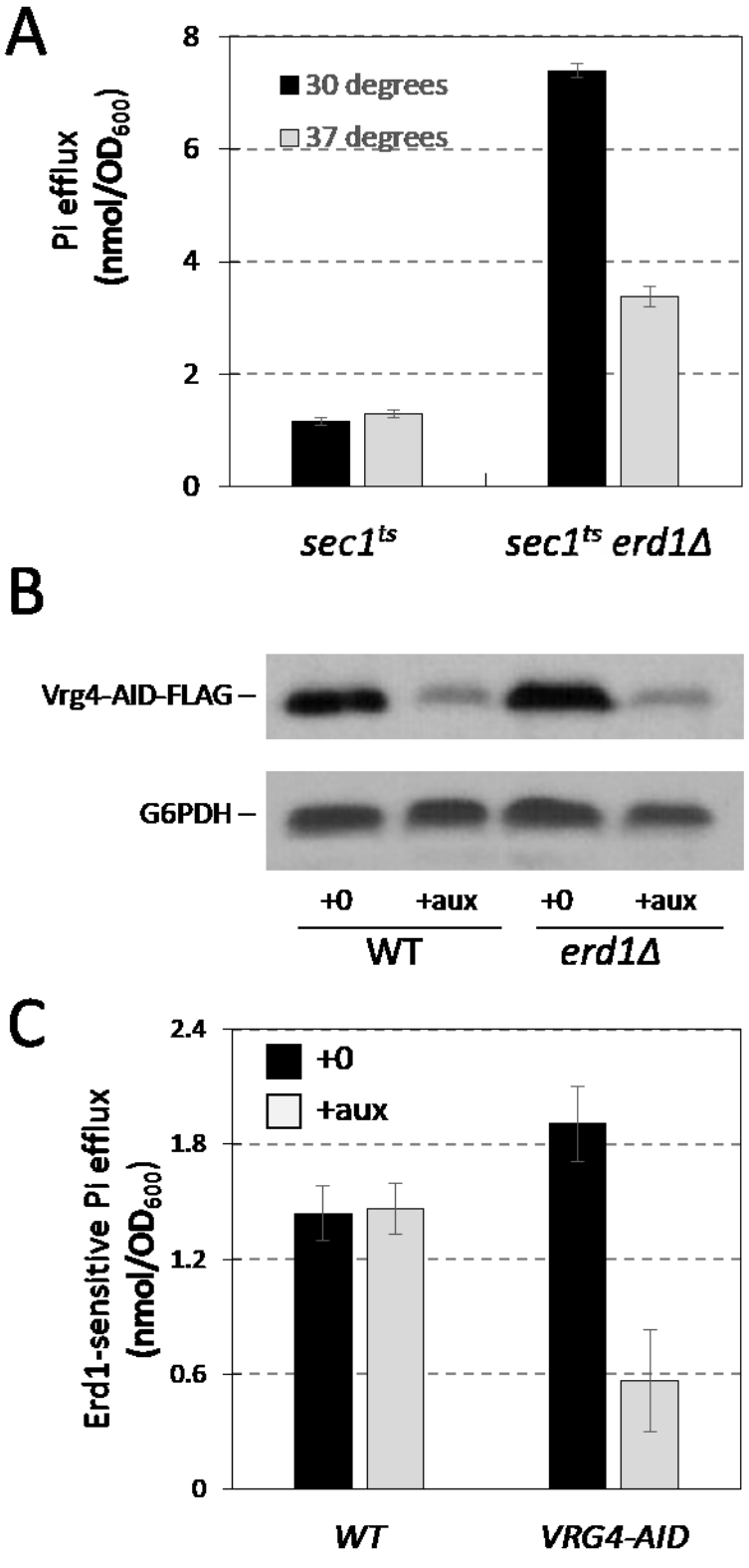
A
Pi efflux
(nmol/OD600)
8
6
4
2
0
30 degrees
37 degrees
sec1ts
sec1ts erd1Δ
B
Vrg4-AID-FLAG –
G6PDH –
+0
+aux
+0
+aux
WT
erd1Δ
C
Erd1-sensitive Pi efflux
(nmol/OD600)
2.4
1.8
1.2
0.6
0
+0
+aux
WT
VRG4-AID

Figure 2.7: Erd1-sensitive losses of Pi depend on exocytosis and on transport of GDP-mannose into the Golgi complex.

(A) Pi losses were measured after 2 hr incubation as in Figure 2.6A except that *sec1-1*^{ts} and *sec1-1*^{ts} *erd1*Δ mutant strains were used at a permissive temperature (30°C; black bars) or a non-permissive temperature (37°C; gray bars) during the incubation in Pi-free medium. (B) Western blot of Vrg4-AID-FLAG strains after 1 hr exposure to 100 μM auxin in SC medium. (C) Erd1-sensitive losses of Pi (i.e. the difference between *erd1*Δ and *ERD1* pairs of strains) were measured for wild-type and Vrg4-AID-FLAG strain backgrounds that were exposed to 100 μM auxin (grey bars) or not (black bars) starting 1 hr before the shifts to Pi-free medium.

(Figure 2.7C). These findings show that the GDP-mannose transporter Vrg4 is a major source of the Pi that is lost to the environment in *erd1*Δ mutants. Altogether the results indicate that Erd1 recycles the Pi byproduct of glycosylation in the Golgi complex, which alters buffering of Ca^{2+} and performance of Gdt1.

DISCUSSION

The Golgi complex of all eukaryotes is a hub for glycosylation, sorting, and processing of secreted proteins, transmembrane proteins, ceramides, and other lipids. In yeast, the glycosylation system of the Golgi complex is essential for viability, as mutations that eliminate the major nucleotide-sugar transporter (Vrg4) or the luminal nucleoside triphosphate diphosphatases (Gda1 and Ynd1) are lethal (Dean *et al.*, 1997; Gao *et al.*, 1999). While the nucleoside monophosphate byproduct of glycosylation is exchanged from the Golgi complex for another nucleotide sugar molecule, the fate of the other byproducts, Pi and H^+, were elusive until now. Our findings above suggest that Erd1 facilitates transport of the luminal Pi to the cytoplasm where it can be reutilized and that Gdt1 transports luminal H^+ to the cytoplasm in exchange for cytoplasmic Ca^{2+}. Because neither protein has been purified to homogeneity and analyzed in reconstituted liposomes, it remains possible that Erd1 and Gdt1 do not directly transport these byproducts of glycosylation and instead regulate unknown transporters that have these properties. Nevertheless, the simplest model of inorganic ion homeostasis in the Golgi complex (summarized in Figure 2.1A) is consistent with numerous genetic observations in both yeast and humans, and it also raises several new questions as well as new

opportunities for treating a congenital disorder of glycosylation in humans (Dulary *et al.*, 2017).

Pi homeostasis in the Golgi complex

Our findings that Erd1 decreases the loss of Pi from the Golgi complex to the environment and promotes growth of yeast cells in low-Pi environments independent of all known Pi transporters suggest that yeast normally recycles this byproduct of glycosylation for reuse in the cytoplasm. This function is somewhat surprising because XPR1, a homolog of Erd1 in the basolateral plasma membrane of humans, has been shown to promote export of cytoplasmic Pi from the cytoplasm rather than import (Giovannini *et al.*, 2013). XPR1 orthologs in zebra fish may have similar roles in Pi export, as knockout mutations resulted in failure to produce osteoclasts (Meireles *et al.*, 2014), which are thought to experience massive Pi uptake and efflux during resorption of bone. PHO1, an ortholog of XPR1 in the plant *Arabidopsis thaliana*, has also been shown to promote Pi export from root stelar cells to the xylem, resulting in Pi deficiencies in the shoots (Hamburger *et al.*, 2002; Wege and Poirier, 2014). PHO1 localizes primarily to the Golgi complex rather than the plasma membrane and thus may export Pi through exocytosis pathways (Arpat *et al.*, 2012). The transmembrane topologies of Erd1 (Kim *et al.*, 2006) and PHO1 (Wege *et al.*, 2016) are similar, so the directionality of net Pi transport by members of the ESX family may depend on other factors such as unknown ions or molecules that could be co- or counter-transported with Pi.

Though absent from Erd1, SPX domains are found at the N-termini of XPR1 and PHO1 and many other proteins that regulate Pi homeostasis (Secco *et al.*, 2012). Deletion of the SPX domain did not diminish Pi transport activity or alter directionality (Wege *et al.*, 2016). The SPX domain can also be found at the N-termini of numerous other proteins involved in Pi homeostasis in yeast such as Pi transporters of the SL13 family (Pho87, Pho90, Pho91), subunits of the vacuolar poly-Pi synthase (Vtc2, Vtc3, Vtc4, Vtc5), a cyclin-dependent kinase (Pho85) and its inhibitor (Pho81) that govern the response to Pi starvation, glycerophosphocholine phosphodiesterase 1 (Gde1), and another ESX domain protein of unknown function (Syg1) (Secco *et al.*, 2012). Several SPX domains have now been shown to bind inositol polyphosphates such as IP6 and IP7 (Lee *et al.*, 2007; Wild *et al.*, 2016), which have important regulatory effects on Pi homeostasis. The lack of an SPX domain in Erd1, and the inability of Pho4 to stimulate transcription of the *ERD1* gene in Pi-limiting conditions, suggest that Erd1 may escape the conventional regulation imposed on other Pi homeostasis regulators.

The evolutionary origins of Erd1 also may be instructive about its functions in cell physiology. Our searches of protein databanks and multiple sequence alignments (not shown) reveal orthologs of Erd1 in virtually all species of fungi, in a unicellular relative of fungi (the nucleariid *Fonticula alba*), and in a unicellular relative of metazoans (the choanoflagellate *Monosiga brevicollis*), but not in metazoans. This suggests that Erd1-subfamily of ESX-domain proteins originated prior to the divergence of fungi and animals but were uniquely lost from the metazoan lineage. This loss in metazoans could have been enabled by the gain of another Pi transporter in the Golgi complex. Alternatively, the benefits of Pi recycling from the Golgi complex may have diminished

in metazoans where the loss of Pi to the extracellular fluids is not harmful or potentially even beneficial for Pi storage, for pH buffering, or for creating extracellular structures.

In addition to defects in Pi recycling, *erd1*Δ mutants of yeast exhibit striking deficiencies of secretory protein glycosylation and of sorting by the H/KDEL receptor (Erd2), which ordinarily retrieves many ER resident molecular chaperones and enzymes that have escaped the ER (Hardwick *et al.*, 1990). How elevated Pi in the lumen of Golgi complex can cause such disparate effects is not clear. Conceivably, high luminal Pi may competitively inhibit the activities of NTPDases that produce it or the glycosyltransferases, nucleotide sugar transporters, other factors involved directly in promoting glycosylation. The binding of H/KDEL peptides to their receptor is highly sensitive to the luminal pH (Wilson *et al.*, 1993), which might be altered in *erd1*Δ mutants through accumulation of $H_2PO_4^-$ and dissociation to H^+ and HPO_4^{2-}. An inability of *erd1*Δ mutants to transport Pi out of the Golgi complex may increase the buffering of Ca^{2+}, Mn^{2+}, Mg^{2+} in the lumen as well, perhaps altering the structure of the organelle or decreasing the performance of glycosylation and ER retrieval systems. Lastly, the concentration of some other molecules in the Golgi complex could be directly disrupted in *erd1*Δ mutants if Erd1 (or possibly its associated catalytic partner) also co- or counter-transports some other molecule together with Pi. Direct transport studies using liposomes with purified and reconstituted Erd1 protein and other biochemical experiments will be needed to test these possibilities.

Ca^{2+} homeostasis in the Golgi complex and vacuole.

Here we show that Gdt1 promotes growth of yeast cells in both low and high Ca^{2+} environments independent of the known Ca^{2+} transporters (Pmr1, Pmc1, Vcx1) and only when the Golgi complex receives sufficient acidification from the V-ATPase. In the absence of all V-ATPase activity, Gdt1 seemed to partially undo the work of the other transporters and to have the opposite effects on cell growth and on calcineurin activation in the cytoplasm. By showing Gdt1 can operate in reverse mode when the V-ATPase is eliminated, we add strong experimental support to the hypothesis that Gdt1 catalyzes H^+/Ca^{2+} exchange in the Golgi complex (Demaegd *et al.*, 2013; Colinet *et al.*, 2016). But unlike Pmr1, which transports both Ca^{2+} and Mn^{2+} to the Golgi complex, we did not detect any hypersensitivity of *gdt1*Δ mutants to elevated Mn^{2+} in the medium even in the absence of Pmr1 (data not shown), suggesting that Gdt1 may not transport significant levels of Mn^{2+}. Consistent with these findings, the partial rescue of glycosylation defects in *pmr1*Δ mutants by supplemental Ca^{2+} depended on Gdt1 but the partial rescue by supplemental Mn^{2+} occurred independent of Gdt1 (Colinet *et al.*, 2016). While these findings suggest that Gdt1 does not play a direct role in Mn^{2+} transport into the Golgi complex, direct transport of Mn^{2+} by Gdt1 was proposed to explain the observation that *gdt1*Δ mutants exhibit glycosylation defects in high Ca^{2+} conditions that can be rescued by supplemental Mn^{2+} and Pmr1 function (Potelle *et al.*, 2016). Our demonstration of reverse-mode operation of Gdt1 strengthens an alternative hypothesis to explain this observation: in high Ca^{2+} conditions, Gdt1 may normally promote net Ca^{2+} efflux from the Golgi complex and thereby allows Pmr1 to cycle more rapidly and effectively transport more Mn^{2+} for stimulation of glycosyltransferases.

Findings from mammalian cells indicate broad conservation of Gdt1 and TMEM165 function in the Golgi complex. Simultaneous knockouts of TMEM165 and SPCA1 genes (a homolog of Pmr1 encoded by *ATP2C1*) result in synthetic lethality in the human HAP1 cell line (Blomen *et al.*, 2015), suggesting these Golgi proteins share important functions. Deficiency of TMEM165 in human cells disrupts pH homeostasis of lysosomes and late endosomes (Demaegd *et al.*, 2013), as expected if TMEM165 normally catalyzes H^+/Ca^{2+} exchange in the forward-mode in these cells. Interestingly, knockdown of TMEM165 in human cell lines resulted in glycosylation defects that could be rescued by low concentrations of Mn^{2+} (Potelle *et al.*, 2016). Such rescue provides clues for therapies to treat rare deficiencies of TMEM165 in humans, which cause a type-II congenital disorder of glycosylation that manifest with glycosylation defects, bone dysplasias, and other abnormalities (Dulary *et al.*, 2017). TMEM165 appears to be expressed in virtually all tissues, so understanding how such specific developmental abnormalities arise from defects in a housekeeping gene function will require much more work. The recent identification of TMEM165 splice variants localized to the ER, rather than the Golgi, raises the possibility of additional functions of TMEM165 that have yet to be identified (Krzewinski-Recchi *et al.*, 2017).

We also provide evidence that activated calcineurin can inhibit the forward mode activity of Gdt1 *in vivo*, similar to that of Vcx1: in the presence of the calcineurin inhibitor FK506, *gdt1*Δ and *vcx1*Δ mutants were far more hypersensitive to Ca^{2+} than in the absence of the calcineurin inhibitor, even when Pmc1 and Crz1 were eliminated. Gdt1 did not mediate the inhibition of Vcx1 by calcineurin, and Vcx1 did not mediate the inhibition of Gdt1 by calcineurin, as calcineurin still retains its inhibitory effects when

one or the other transporter has been eliminated. The molecular mechanism(s) by which calcineurin regulates the function of Gdt1 and Vcx1 remain unknown, as neither protein undergoes changes in expression or mobility on SDS-page upon activation/inhibition of calcineurin. Our finding that calcineurin still inhibited reverse-mode activity of Vcx1 in the absence of Vph1 suggests that neither the vacuolar V-ATPase nor luminal H^+ are key mediators of this regulation. We also ruled out Erd1 as an intermediary of Gdt1 inhibition by calcineurin, as this regulation persisted in *erd1*Δ *vcx1*Δ strains (Table 2.2). Because Gdt1 and Vcx1 both seem to promote H^+/Ca^{2+} exchanger, it is tempting to speculate that calcineurin regulates pH of the cytoplasm or organelles in high Ca^{2+} conditions, which would alter the ability of transporters to bind Ca^{2+}. Indeed, new evidence suggests that calcineurin may down-regulate the plasma membrane H^+ pump Pma1 (Patricia Kane, personal communication), potentially causing acidification of the cytoplasm and diminishing forward Ca^{2+} transport by H^+/Ca^{2+} exchangers.

Because Gdt1 and Vcx1 may also inhibit calcineurin activation by removing Ca^{2+} from the cytoplasm, both proteins have the potential to form double-negative feedback loops with calcineurin (Figure 2.1A). Double-negative feedback loops generate positive feedback in signaling networks, and tend to promote switch-like transitions between two stable states (Ferrell, 2002). In such a scenario, calcineurin is less likely to become activated when Gdt1 and Vcx1 are fully functional, but as cytosolic Ca^{2+} concentrations rise and calcineurin becomes activated both Gdt1 and Vcx1 may become progressively inhibited, thus accelerating the activation of calcineurin and the further inhibition of H^+/Ca^{2+} exchangers. Double-negative feedback loops can contribute to heterogeneity in clonal cell populations and a form of cellular memory (hysteresis), as observed

previously during the switching between high and low affinity Pi transporters in yeast (Wykoff *et al.*, 2007). In addition to these advantages, yeast cells may also inhibit the H^+/Ca^{2+} exchangers in high Ca^{2+} conditions to avoid reverse-mode operation of Vcx1 and Gdt1 and possible futile cycling with the Ca^{2+} ATPases (Pmc1 and Pmr1, which are up-regulated by calcineurin signaling). It will be interesting to determine precisely how and why calcineurin inhibits Gdt1 and Vcx1 functions *in vivo*, and whether such regulation contributes to the unexplained "bursts" of free Ca^{2+} elevation and calcineurin signaling that have been observed through real-time imaging in single yeast cells (Cai *et al.*, 2008; Carbo *et al.*, 2017).

A better understanding of H^+, Ca^{2+}, and Pi homeostasis in the Golgi complex may help explain how this organelle can operate so differently in different tissues of humans. In addition to a general housekeeping function in non-secretory cells, specialized secretory cells may require huge increases in glycosylation and corresponding increases in byproduct production. In the case of alveolar epithelial cells of mammary gland, which can produce massive quantities of lactose (a product of glycosylation) and casein micelles (rich in Ca^{2+} and Pi) in the Golgi complex during lactation (Neville, 2005), retrieval of the Pi byproduct may not be beneficial and removal of the H^+ byproduct in exchange for Ca^{2+} may be exceptionally important. Interestingly, to potentially meet this demand, expression of TMEM165 mRNA and protein becomes massively increased in alveolar epithelial cells just as milk production begins (Reinhardt *et al.*, 2014). The full repertoire of functions carried out by the Gdt1 and the Erd1 families of proteins will be fascinating to unravel in the many different species and cellular situations.

MATERIALS AND METHODS

Yeast strains and genetic screens

The yeast knockout collection in strain BY4741 background (Giaever *et al.*, 1999) was inoculated into 200 µL YPD medium in 96-well dishes and grown to stationary phase (2 days incubation at 30°C). Dishes were vortexed briefly to suspend the settled cells, then pinned onto noble agar medium containing YPD medium plus 5 mM succinic acid and supplemented with either 200 mM $CaCl_2$, 200 mM $MgCl_2$, 1 µg/mL FK506, or combinations of thereof. After incubation for 3 days at 30°C, each strain was scored manually for growth relative to wild-type controls that were included in the arrays, using a scale ranged from $^{+}2$ (increased growth) to 0 (wild-type growth) to -5 (greatly decreased or no growth). The screen was repeated twice independently. Of the 107 mutant strains that consistently exhibited a significant response to at least one condition, 84 were found to exhibit elevated Ca^{2+} influx in YPD medium or YPD medium plus FK506 (Martin *et al.*, 2011). The remaining 23 mutants contained *vcx1*Δ and *pmc1*Δ and were ranked on a scale from *vcx1*Δ-*like* to *pmc1*Δ-*like* based on their distinct behaviors in media containing Ca^{2+} and Ca^{2+} plus FK506. A *gdt1*Δ mutation was generated in W303-1A strain background and crossed with strains bearing *vcx1*Δ, *pmc1*Δ, *crz1*Δ, and *pmr1*Δ to produce a panel of isogenic strains bearing many combinations of these mutations in both mating types. Genotypes were confirmed by marker analyses and by PCR confirmations.

To identify spontaneous mutants that increase Ca^{2+} tolerance of *crz1*Δ *pmc1*Δ *vcx1*Δ triple mutants, two strains of opposite mating types and with different selectable markers (DDY19 and K1357) were streaked for single colonies on agar YPD medium,

and 36 single colonies were picked, grown further on the same medium to allow spontaneous mutations to accumulate, and then incubated on noble agar YPD medium containing 5 mM succinic acid and 111 mM $CaCl_2$ for several days. A single Ca^{2+}-tolerant colony was picked in each case, purified by re-streaking, and then mated with one another in all possible combinations. The resulting diploids were reanalyzed for Ca^{2+} tolerance. This complementation test indicated 26 haploid strains contained dominant mutations in unknown genes and 10 haploid strains contained recessive mutations all in the same gene. The 10 recessive mutants were fortuitously found to exhibit hypersensitivity to tunicamycin. One recessive mutant was transformed with a low-copy plasmid library containing fragments of yeast genomic DNA and 9 transformants were replica plated to YPD plus 2 μg/mL tunicamycin to select for strains bearing complementing plasmids. Two different plasmids overlapping the *ERD1* gene and several nearby genes were recovered and found to reverse both tunicamycin hypersensitivity and the Ca^{2+} tolerance phenotypes upon retransformation into the recessive mutant strains. *ERD1* was identified as the defective gene in the recessive mutants by (1) introducing an *erd1*Δ null mutation into the K1357 strain and obtaining both tunicamycin hypersensitivity and Ca^{2+} resistance phenotypes and (2) demonstrating non-complementation between the *erd1*Δ null strain and the spontaneous recessive mutant strains. Similar *erd1*Δ knockout mutations were also introduced by transformation into several other strains, and all strains utilized here are listed in Table 2.2.

Ion tolerance and Pi dependence assays

Yeast strains were grown to saturation at 30°C, typically overnight, in YPD medium for ion tolerance assays or in SC medium for Pi dependence assays. They were then diluted 1:1000 into fresh media containing 5 mM succinic acid and various concentrations of $CaCl_2$ in 96-well dishes without 1 μg/mL FK506, mixed, and incubated at 30°C for 24 hr without shaking. The cells were resuspended by vortex mixing and optical density was measured at 650 nm using a microplate spectrophotometer (Molecular Devices). The concentration of Ca^{2+} causing a 50% decrease in maximal optical density (the IC50) and the concentration of Pi causing permitting growth to 50% maximal optical density (the ED50) were calculated for each strain by non-linear regression using the sigmoid equation with 4 parameters (maximum OD650, minimum OD650, IC50 or ED50, and slope factor). The averages from two independently generated strains of the same genotype (± S.D.) were calculated and plotted.

PMC1-lacZ expression assays

The *PMC1-lacZ* reporter gene carried on the high copy plasmid pKC190 (Cunningham and Fink, 1996) was transformed into the indicated strains and three independent transformants were grown to log-phase in SC-ura medium, pelleted briefly, and suspended in YPD medium with 5 mM succinic acid containing 0, 50, or 100 mM $CaCl_2$. After 4 hr incubation at 30°C, cells were pelleted, resuspended in Z-buffer, permeabilized with SDS and chloroform, and assayed for β-galactosidase activity using o-nitrophenyl-β-galactoside as substrate as described previously (Cunningham and Fink, 1996).

Pi export assays

Yeast strains were grown overnight to saturation in SC medium (7.35 mM Pi) and then diluted 1000-fold into fresh SC medium containing tracer quantities (~30 μCi per mL) of fresh 32-Pi (Perkin Elmer). After 12 hr of incubation with shaking, the log-phase cells were pelleted and washed 5 times with 5 mL of ice-cold Pi-free SC media to remove all unincoprated 32-Pi from the medium. The cells were then resuspended in Pi-free SC media and incubated on ice or at 30°C and sampled at various times. After centrifugation at 15,000 rpm for 1 min, the cell-free supernatant was analyzed by liquid scintillation counting and by thin layer chromatography, by spotting 3 μL of sample supernatant onto polyethylenimine (PEI)-cellulose TLC plates, which was then developed in 1 M LiCl with 10 mM HEPES, pH 7.5. The TLC plate was imaged by autoradiography.

Antibodies and Western Blotting

Cells were lysed via fast alkaline lysis in 0.5 M NaOH with 1.85% beta-mercaptoethanol (BME) in ice water for 10 minutes. The protein was then isolated through precipitation by addition of trichloracetic acid (TCA) to a final concentration of 10% (w/w). Equal volumes of protein isolate and 2X SDS sample buffer (0.1 M Tris-HCl, pH 6.8, 4% SDS, 0.2% bromophenol blue, 20% glycerol, 2% BME) were then combined, and the samples were incubated at 37 °C for 30 minutes. Proteins were processed by separation on a 10% SDS/PAGE gel and western blotting, as described previously (Mehta, 2009). Blots were probed with anti-TAP polyclonal antibodies from rabbit at 1:10,000 dilution (ThermoFisher, CAB1001) or anti-FLAG polyclonal antibodies from rabbit at 1:10,000 dilution (Sigma, F7425). Protein standards were

probed with anti-glucose-6-phosphate dehydrogenase polyclonal antibodies from rabbit at 1:10,000 dilution (Sigma, A9521), or anti-tubulin monoclonal antibodies at 1:10,000 dilution (EMD Millipore, MAB1864).

Table 2.3: Strains used in Chapter 2

Strain	Background	Genotype	Source
K601	W303 [a]	*MATa*	Cunningham and Fink (1996)
K605	W303	*MATa pmc1::TRP1*	Cunningham and Fink (1996)
K661	W303	*MATa vcx1Δ*	Cunningham and Fink (1996)
K665	W303	*MATa pmc1::TRP1 vcxΔ*	Cunningham and Fink (1996)
AK053	W303	*MATa vph1::NatR*	This Study
AK054	W303	*MATa pmc1::TRP1 vph1::NatR*	This Study
AK055	W303	*MATa vcx1Δ vph1::NatR*	This Study
AK056	W303	*MATa pmc1::TRP1 vcxΔ vph1::NatR*	This Study
K1811	W303	*MATa vcx1Δ vph1::NatR*	This Study
K1812	W303	*MATa vcx1Δ vph1::NatR stv1::KanR*	This Study
K1815	W303	*MATa vcx1Δ gdt1::HIS3 vph1::NatR*	This Study
K1816	W303	*MATa vcx1Δ gdt1::HIS3 vph1::NatR stv1::KanR*	This Study
K1827	W303	*MATα vcx1Δ vph1::NatR*	This Study
K1828	W303	*MATα vcx1Δ vph1::NatR stv1::KanR*	This Study

K1831	W303	*MATα vcx1Δ gdt1::HIS3 vph1::NatR*	This Study
K1832	W303	*MATα vcx1Δ gdt1::HIS3 vph1::NatR stv1::KanR*	This Study
K1833	W303	*MATa*	This Study
K1834	W303	*MATα*	This Study
K1835	W303	*MATa crz1::KanR*	This Study
K1836	W303	*MATα crz1::KanR*	This Study
K1837	W303	*MATa cmk2::TRP1*	This Study
K1838	W303	*MATα cmk2::TRP1*	This Study
K1839	W303	*MATa crz1::KanR cmk2::TRP1*	This Study
K1840	W303	*MATα crz1::KanR cmk2::TRP1*	This Study
K1841	W303	*MATa gdt1::HIS3*	This Study
K1842	W303	*MATα gdt1::HIS3*	This Study
K1843	W303	*MATa gdt1::HIS3 crz1::KanR*	This Study
K1844	W303	*MATα gdt1::HIS3 crz1::KanR*	This Study
K1845	W303	*MATa gdt1::HIS3 cmk2::TRP1*	This Study
K1846	W303	*MATα gdt1::HIS3 cmk2::TRP1*	This Study
K1847	W303	*MATa gdt1::HIS3 crz1::KanR cmk2::TRP1*	This Study
K1848	W303	*MATα gdt1::HIS3 crz1::KanR cmk2::TRP1*	This Study

K1849	W303	*MATa pmc1::LEU2*	This Study
K1850	W303	*MATα pmc1::LEU2*	This Study
K1851	W303	*MATa pmc1::LEU2 crz1::KanR*	This Study
K1852	W303	*MATα pmc1::LEU2 crz1::KanR*	This Study
K1853	W303	*MATa pmc1::LEU2 cmk2::TRP1*	This Study
K1854	W303	*MATα pmc1::LEU2 cmk2::TRP1*	This Study
K1855	W303	*MATa pmc1::LEU2 crz1::KanR cmk2::TRP1*	This Study
K1856	W303	*MATα pmc1::LEU2 crz1::KanR cmk2::TRP1*	This Study
K1857	W303	*MATa pmc1::LEU2 gdt1::HIS3*	This Study
K1858	W303	*MATα pmc1::LEU2 gdt1::HIS3*	This Study
K1859	W303	*MATa pmc1::LEU2 gdt1::HIS3 crz1::KanR*	This Study
K1860	W303	*MATα pmc1::LEU2 gdt1::HIS3 crz1::KanR*	This Study
K1861	W303	*MATa pmc1::LEU2 gdt1::HIS3 cmk2::TRP1*	This Study
K1862	W303	*MATα pmc1::LEU2 gdt1::HIS3 cmk2::TRP1*	This Study
K1863	W303	*MATa pmc1::LEU2 gdt1::HIS3 crz1::KanR cmk2::TRP1*	This Study

K1864	W303	*MATα pmc1::LEU2 gdt1::HIS3 crz1::KanR cmk2::TRP1*	This Study
K1865	W303	*MATa vcx1Δ pmc1::LEU2*	This Study
K1866	W303	*MATα vcx1Δ pmc1::LEU2*	This Study
K1867	W303	*MATa vcx1Δ pmc1::LEU2 crz1::KanR*	This Study
K1868	W303	*MATα vcx1Δ pmc1::LEU2 crz1::KanR*	This Study
K1869	W303	*MATa vcx1Δ pmc1::LEU2 cmk2::TRP1*	This Study
K1870	W303	*MATα vcx1Δ pmc1::LEU2 cmk2::TRP1*	This Study
K1871	W303	*MATa vcx1Δ pmc1::LEU2 crz1::KanR cmk2::TRP1*	This Study
K1872	W303	*MATα vcx1Δ pmc1::LEU2 crz1::KanR cmk2::TRP1*	This Study
K1873	W303	*MATa vcx1Δ pmc1::LEU2 gdt1::HIS3*	This Study
K1874	W303	*MATα vcx1Δ pmc1::LEU2 gdt1::HIS3*	This Study
K1875	W303	*MATa vcx1Δ pmc1::LEU2 gdt1::HIS3 crz1::KanR*	This Study
K1876	W303	*MATα vcx1Δ pmc1::LEU2 gdt1::HIS3 crz1::KanR*	This Study
K1877	W303	*MATa vcx1Δ pmc1::LEU2 gdt1::HIS3 cmk2::TRP1*	This Study
K1878	W303	*MATα vcx1Δ pmc1::LEU2 gdt1::HIS3 cmk2::TRP1*	This Study

K1879	W303	*MATa vcx1Δ pmc1::LEU2 gdt1::HIS3 crz1::KanR cmk2::TRP1*	This Study
K1880	W303	*MATα vcx1Δ pmc1::LEU2 gdt1::HIS3 crz1::KanR cmk2::TRP1*	This Study
CTS05	W303	*MATa*	This Study
CTS06	W303	*MATα*	This Study
CTS09	W303	*MATa gdt1::HIS3*	This Study
CTS10	W303	*MATα gdt1::HIS3*	This Study
CTS13	W303	*MATa pmr1::LEU2*	This Study
CTS14	W303	*MATα pmr1::LEU2*	This Study
CTS17	W303	*MATa pmr1::LEU2 gdt1::HIS3*	This Study
CTS18	W303	*MATα pmr1::LEU2 gdt1::HIS3*	This Study
NS001	W303	*MATa vcx1Δ*	This Study
NS002	W303	*MATα vcx1Δ*	This Study
NS009	W303	*MATa vcx1Δ gdt1::HIS3*	This Study
NS010	W303	*MATα vcx1Δ gdt1::HIS3*	This Study
NS116	W303	*MATa*	This Study
NS117	W303	*MATα*	This Study
NS118	W303	*MATa erd1::NatR*	This Study
NS119	W303	*MATα erd1::NatR*	This Study
NS120	W303	*MATa crz1::KanR*	This Study

NS121	W303	*MATα crz1::KanR*	This Study
NS122	W303	*MATa pmc1::LEU2*	This Study
NS123	W303	*MATα pmc1::LEU2*	This Study
NS124	W303	*MATa gdt1::HIS3*	This Study
NS125	W303	*MATα gdt1::HIS3*	This Study
NS126	W303	*MATa crz1::KanR erd1::NatR*	This Study
NS127	W303	*MATα crz1::KanR erd1::NatR*	This Study
NS128	W303	*MATa pmc1::LEU2 erd1::NatR*	This Study
NS129	W303	*MATa pmc1::LEU2 erd1::NatR*	This Study
NS130	W303	*MATα gdt1::HIS3 erd1::NatR*	This Study
NS131	W303	*MATα gdt1::HIS3 erd1::NatR*	This Study
NS132	W303	*MATa pmc1::LEU2 crz1::KanR*	This Study
NS133	W303	*MATα pmc1::LEU2 crz1::KanR*	This Study
NS134	W303	*MATa gdt1::HIS3 crz1::KanR*	This Study
NS135	W303	*MATα gdt1::HIS3 crz1::KanR*	This Study
NS136	W303	*MATa pmc1::LEU2 gdt1::HIS3*	This Study
NS137	W303	*MATα pmc1::LEU2 gdt1::HIS3*	This Study
NS138	W303	*MATa pmc1::LEU2 crz1::KanR erd1::NatR*	This Study
NS139	W303	*MATα pmc1::LEU2 crz1::KanR erd1::NatR*	This Study

NS140	W303	*MATa pmc1::LEU2 gdt1::HIS3 erd1::NatR*	This Study
NS141	W303	*MATα pmc1::LEU2 gdt1::HIS3 erd1::NatR*	This Study
NS142	W303	*MATa gdt1::HIS3 crz1::KanR erd1::NatR*	This Study
NS143	W303	*MATα gdt1::HIS3 crz1::KanR erd1::NatR*	This Study
NS144	W303	*MATa pmc1::LEU2 gdt1::HIS3 crz1::KanR*	This Study
NS145	W303	*MATα pmc1::LEU2 gdt1::HIS3 crz1::KanR*	This Study
NS146	W303	*MATa pmc1::LEU2 gdt1::HIS3 crz1::KanR erd1::NatR*	This Study
NS147	W303	*MATα pmc1::LEU2 gdt1::HIS3 crz1::KanR erd1::NatR*	This Study
NS148	W303	*MATa vcx1Δ*	This Study
NS149	W303	*MATα vcx1Δ*	This Study
NS150	W303	*MATa vcx1Δ erd1::NatR*	This Study
NS151	W303	*MATα vcx1Δ erd1::NatR*	This Study
NS152	W303	*MATa vcx1Δ crz1::KanR*	This Study
NS153	W303	*MATα vcx1Δ crz1::KanR*	This Study

NS154	W303	*MATa vcx1Δ pmc1::LEU2*	This Study
NS155	W303	*MATα vcx1Δ pmc1::LEU2*	This Study
NS156	W303	*MATa vcx1Δ gdt1::HIS3*	This Study
NS157	W303	*MATα vcx1Δ gdt1::HIS3*	This Study
NS158	W303	*MATa vcx1Δ crz1::KanR erd1::NatR*	This Study
NS159	W303	*MATα vcx1Δ crz1::KanR erd1::NatR*	This Study
NS160	W303	*MATa vcx1Δ pmc1::LEU2 erd1::NatR*	This Study
NS161	W303	*MATα vcx1Δ pmc1::LEU2 erd1::NatR*	This Study
NS162	W303	*MATa vcx1Δ gdt1::HIS3 erd1::NatR*	This Study
NS163	W303	*MATα vcx1Δ gdt1::HIS3 erd1::NatR*	This Study
NS164	W303	*MATa vcx1Δ pmc1::LEU2 crz1::KanR*	This Study
NS165	W303	*MATα vcx1Δ pmc1::LEU2 crz1::KanR*	This Study
NS166	W303	*MATa vcx1Δ gdt1::HIS3 crz1::KanR*	This Study
NS167	W303	*MATα vcx1Δ gdt1::HIS3 crz1::KanR*	This Study
NS168	W303	*MATa vcx1Δ pmc1::LEU2 gdt1::HIS3*	This Study
NS169	W303	*MATα vcx1Δ pmc1::LEU2 gdt1::HIS3*	This Study
NS170	W303	*MATa vcx1Δ pmc1::LEU2 crz1::KanR erd1::NatR*	This Study
NS171	W303	*MATα vcx1Δ pmc1::LEU2 crz1::KanR erd1::NatR*	This Study

NS172	W303	*MATa vcx1Δ pmc1::LEU2 gdt1::HIS3 erd1::NatR*	This Study
NS173	W303	*MATα vcx1Δ pmc1::LEU2 gdt1::HIS3 erd1::NatR*	This Study
NS174	W303	*MATa vcx1Δ gdt1::HIS3 crz1::KanR erd1::NatR*	This Study
NS175	W303	*MATα vcx1Δ gdt1::HIS3 crz1::KanR erd1::NatR*	This Study
NS176	W303	*MATa vcx1Δ pmc1::LEU2 gdt1::HIS3 crz1::KanR*	This Study
NS177	W303	*MATα vcx1Δ pmc1::LEU2 gdt1::HIS3 crz1::KanR*	This Study
NS178	W303	*MATa vcx1Δ pmc1::LEU2 gdt1::HIS3 crz1::KanR erd1::NatR*	This Study
NS179	W303	*MATα vcx1Δ pmc1::LEU2 gdt1::HIS3 crz1::KanR erd1::NatR*	This Study
NS185	W303	*MATa pho84::TRP1*	This Study
NS186	W303	*MATα pho84::TRP1*	This Study
NS187	W303	*MATa erd1::NatR pho84::TRP1*	This Study
NS188	W303	*MATα erd1::NatR pho84::TRP1*	This Study

EY916	W303	*MATa pho84Δ::HIS3 pho87Δ::CgHIS3 pho89Δ::CgHIS3 pho90Δ::CgHIS3 pho91Δ::KlURA3*	Wykoff and O'Shea (2001)
NS229	W303	*MATa pho84Δ::HIS3 pho87Δ::CgHIS3 pho89Δ::CgHIS3 pho90Δ::CgHIS3 pho91Δ::KlURA3 erd1::NatR*	This Study
TSA36	BY4741 [b]	*MATa sec1-1::KanR*	Li et al. (2011)
NS227	BY4741	*MATa sec1-1::KanR erd1::NatR*	This Study
LM001	BY4741	*MATa VRG4-TAP-AID-6xFLAG::TIR1::URA3*	This Study
NS228	BY4741	*MATa VRG4-TAP-AID-6xFLAG::TIR1::URA3 erd1::NatR*	This Study
YSC1178-202229973	BY4741	*MATa GDT1-TAP::HIS3MX6*	Ghaemmaghami *et al.* (2003)

Footnotes

[a] background mutations in W303 (leu2-3,112 trp1-1 can1-100 ura3-1 ade2-1 his3-11,15)

[b] background mutations in BY4741 (his3Δ1 leu2Δ0 met15Δ0 ura3Δ0)

REFERENCES

Antebi, A., and Fink, G.R., 1992. The yeast Ca^{2+}-ATPase homologue, *PMR1*, is required for normal Golgi function and localizes in a novel Golgi-like distribution. Mol Biol Cell 3: 633-654.

Arpat, A.B., Magliano, P., Wege, S., Rouached, H., Stefanovic, A., and Poirier, Y., 2012. Functional expression of PHO1 to the Golgi and trans-Golgi network and its role in export of inorganic phosphate. Plant J 71: 479-491.

Blomen, V.A., Majek, P., Jae, L.T., Bigenzahn, J.W., Nieuwenhuis, J., Staring, J., Sacco, R., van Diemen, F.R., Olk, N., Stukalov, A., Marceau, C., Janssen, H., Carette, J.E., Bennett, K.L., Colinge, J., Superti-Furga, G., and Brummelkamp, T.R., 2015. Gene essentiality and synthetic lethality in haploid human cells. Science 350: 1092-1096.

Bonilla, M., and Cunningham, K.W., 2003. Mitogen-activated protein kinase stimulation of Ca^{2+} signaling is required for survival of endoplasmic reticulum stress in yeast. Mol Biol Cell 14: 4296-4305.

Bonilla, M., Nastase, K.K., and Cunningham, K.W., 2002. Essential role of calcineurin in response to endoplasmic reticulum stress. Embo J 21: 2343-2353.

Bun-Ya, M., Nishimura, M., Harashima, S., and Oshima, Y., 1991. The PHO84 gene of Saccharomyces cerevisiae encodes an inorganic phosphate transporter. Mol Cell Biol 11: 3229-3238.

Cai, L., Dalal, C.K., and Elowitz, M.B., 2008. Frequency-modulated nuclear localization bursts coordinate gene regulation. Nature 455: 485-490.

Carbo, N., Tarkowski, N., Ipina, E.P., Dawson, S.P., and Aguilar, P.S., 2017. Sexual pheromone modulates the frequency of cytosolic Ca^{2+} bursts in Saccharomyces cerevisiae. Mol Biol Cell 28: 501-510.

Colinet, A.S., Sengottaiyan, P., Deschamps, A., Colsoul, M.L., Thines, L., Demaegd, D., Duchene, M.C., Foulquier, F., Hols, P., and Morsomme, P., 2016. Yeast Gdt1 is a Golgi-localized calcium transporter required for stress-induced calcium signaling and protein glycosylation. Sci Rep 6: 24282.

Cunningham, K.W., and Fink, G.R., 1994. Calcineurin-dependent growth control in *Saccharomyces cerevisiae* mutants lacking *PMC1*, a homolog of plasma membrane Ca^{2+} ATPases. J Cell Biol 124: 351-363.

Cunningham, K.W., and Fink, G.R., 1996. Calcineurin inhibits VCX1-dependent H^{+}/Ca^{2+} exchange and induces Ca^{2+} ATPases in *Saccharomyces cerevisiae*. Mol Cell Biol 16: 2226-2237.

Dean, N., Zhang, Y.B., and Poster, J.B., 1997. The VRG4 gene is required for GDP-mannose transport into the lumen of the Golgi in the yeast, Saccharomyces cerevisiae. J Biol Chem 272: 31908-31914.

Demaegd, D., Foulquier, F., Colinet, A.S., Gremillon, L., Legrand, D., Mariot, P., Peiter, E., Van Schaftingen, E., Matthijs, G., and Morsomme, P., 2013. Newly characterized Golgi-localized family of proteins is involved in calcium and pH homeostasis in yeast and human cells. Proc Natl Acad Sci U S A 110: 6859-6864.

Dulary, E., Potelle, S., Legrand, D., and Foulquier, F., 2017. TMEM165 deficiencies in Congenital Disorders of Glycosylation type II (CDG-II): Clues and evidences for

roles of the protein in Golgi functions and ion homeostasis. Tissue Cell 49: 150-156.

Dürr, G., Strayle, J., Plemper, R., Elbs, S., Klee, S.K., Catty, P., Wolf, D.H., and Rudolph, H.K., 1998. The medial-Golgi ion pump Pmr1 supplies the yeast secretory pathway with Ca^{2+} and Mn^{2+} required for glycosylation, sorting, and endoplasmic reticulum-associated protein degradation. Mol Biol Cell 9: 1149-1162.

Ferrell, J.E., Jr., 2002. Self-perpetuating states in signal transduction: positive feedback, double-negative feedback and bistability. Curr Opin Cell Biol 14: 140-148.

Forster, C., and Kane, P.M., 2000. Cytosolic Ca^{2+} homeostasis is a constitutive function of the V-ATPase in *Saccharomyces cerevisiae*. J Biol Chem 275(49): 38245-53.

Foulquier, F., Amyere, M., Jaeken, J., Zeevaert, R., Schollen, E., Race, V., Bammens, R., Morelle, W., Rosnoblet, C., Legrand, D., Demaegd, D., Buist, N., Cheillan, D., Guffon, N., Morsomme, P., Annaert, W., Freeze, H.H., Van Schaftingen, E., Vikkula, M., and Matthijs, G., 2012. TMEM165 deficiency causes a congenital disorder of glycosylation. Am J Hum Genet 91: 15-26.

Gao, X.D., Kaigorodov, V., and Jigami, Y., 1999. YND1, a homologue of GDA1, encodes membrane-bound apyrase required for Golgi N- and O-glycosylation in Saccharomyces cerevisiae. J Biol Chem 274: 21450-21456.

Ghaemmaghami S, Huh WK, Bower K, Howson RW, Belle A, Dephoure N, O'Shea EK, Weissman JS., 2003. Global Analysis of Protein Expression in Yeast. *Nature* 425: 737-741.

Giaever, G., Shoemaker, D.D., Jones, T.W., Liang, H., Winzeler, E.A., Astromoff, A., and Davis, R.W., 1999. Genomic profiling of drug sensitivities via induced haploinsufficiency. Nat Genet 21: 278-283.

Giovannini, D., Touhami, J., Charnet, P., Sitbon, M., and Battini, J.L., 2013. Inorganic phosphate export by the retrovirus receptor XPR1 in metazoans. Cell reports 3: 1866-1873.

Hamburger, D., Rezzonico, E., MacDonald-Comber Petetot, J., Somerville, C., and Poirier, Y., 2002. Identification and characterization of the Arabidopsis PHO1 gene involved in phosphate loading to the xylem. Plant Cell 14: 889-902.

Hardwick, K.G., Lewis, M.J., Semenza, J., Dean, N., and Pelham, H.R., 1990. ERD1, a yeast gene required for the retention of luminal endoplasmic reticulum proteins, affects glycoprotein processing in the Golgi apparatus. EMBO J 9: 623-630.

Harper, A.G., and Sage, S.O., 2016. TRP-Na^+/Ca^{2+} Exchanger Coupling. Adv Exp Med Biol 898: 67-85.

Hirschberg, C.B., Robbins, P.W., and Abeijon, C., 1998. Transporters of nucleotide sugars, ATP, and nucleotide sulfate in the endoplasmic reticulum and Golgi apparatus. Annu Rev Biochem 67: 49-69.

Hu, Z., Bonifas, J.M., Beech, J., Bench, G., Shigihara, T., Ogawa, H., Ikeda, S., Mauro, T., and Epstein, E.H., Jr., 2000. Mutations in ATP2C1, encoding a calcium pump, cause Hailey-Hailey disease. Nat Genet 24: 61-65.

Kane, P.M., 2016. Proton Transport and pH Control in Fungi. Adv Exp Med Biol 892: 33-68.

Kim, H., Melen, K., Osterberg, M., and von Heijne, G., 2006. A global topology map of the *Saccharomyces cerevisiae* membrane proteome. Proc Natl Acad Sci U S A 103: 11142-11147.

Knowles, A.F., 2011. The GDA1_CD39 superfamily: NTPDases with diverse functions. Purinergic Signal 7: 21-45.

Krzewinski-Recchi, M.A., Potelle, S., Mir, A.M., Vicogne, D., Dulary, E., Duvet, S., Morelle, W., de Bettignies, G., and Foulquier, F., 2017. Evidence for splice transcript variants of TMEM165, a gene involved in CDG. Biochim Biophys Acta 1861: 737-748.

Lee, Y.S., Mulugu, S., York, J.D., and O'Shea, E.K., 2007. Regulation of a cyclin-CDK-CDK inhibitor complex by inositol pyrophosphates. Science 316: 109-112.

Lehle, L., and Tanner, W., 1976. The specific site of tunicamycin inhibition in the formation of dolichol-bound N-acetylglucosamine derivatives. FEBS Lett 72: 167-170.

Li, Z., F. J. Vizeacoumar, S. Bahr, J. Li, J. Warringer, F.S. Vizeacoumar, R. Min, B. VanderSluis, J. Bellay, M. DeVit, J.A. Fleming, A. Stephens, J. Haase, Z. Lin, A. Baryshnikova, H. Lu, Z. Yan, K. Jin, S. Barker, A. Datti, G. Giaever, C. Nislow, C. Bulawa, C.L. Myers, M. Costanzo, A. Ginras, Z. Zhang, A. Blomberg, K. Bloom, B. Andrews, and C. Boone, 2011. Systematic exploration of essential yeast gene function with temperature-sensitive mutants. Nat Biotechnol 29: 361.

Locke, E.G., Bonilla, M., Liang, L., Takita, Y., and Cunningham, K.W., 2000. A homolog of voltage-gated Ca^{2+} channels stimulated by depletion of secretory Ca^{2+} in yeast. Mol Cell Biol 20: 6686-6694.

Manolson, M.F., Wu, B., Proteau, D., Taillon, B.E., Roberts, B.T., Hoyt, M.A., and Jones, E.W., 1994. STV1 gene encodes functional homologue of 95-kDa yeast vacuolar H^+-ATPase subunit Vph1p. J Biol Chem 269: 14064-14074.

Marchi, V., Sorin, A., Wei, Y., and Rao, R., 1999. Induction of vacuolar Ca^{2+}-ATPase and H^+/Ca^{2+} exchange activity in yeast mutants lacking Pmr1, the Golgi Ca^{2+}-ATPase. FEBS Lett 454: 181-186.

Martin, D.C., Kim, H., Mackin, N.A., Maldonado-Baez, L., Evangelista, C.C., Beaudry, V.G., Dudgeon, D.D., Naiman, D.Q., Erdman, S.E., and Cunningham, K.W., 2011. New regulators of a high affinity Ca^{2+} influx system (HACS) revealed through a genome-wide screen in yeast. J Biol Chem 286: 10744-10754.

Matheos, D.P., Kingsbury, T.J., Ahsan, U.S., and Cunningham, K.W., 1997. Tcn1p/Crz1p, a calcineurin-dependent transcription factor that differentially regulates gene expression in *Saccharomyces cerevisiae*. Genes Dev 11: 3445-3458.

Meireles, A.M., Shiau, C.E., Guenther, C.A., Sidik, H., Kingsley, D.M., and Talbot, W.S., 2014. The phosphate exporter xpr1b is required for differentiation of tissue-resident macrophages. Cell reports 8: 1659-1667.

Morawska, M., and Ulrich, H.D., 2013. An expanded tool kit for the auxin-inducible degron system in budding yeast. Yeast 30: 341-351.

Neville, M.C., 2005. Calcium secretion into milk. J Mammary Gland Biol Neoplasia 10: 119-128.

Nishimura, K., Fukagawa, T., Takisawa, H., Kakimoto, T., and Kanemaki, M., 2009. An auxin-based degron system for the rapid depletion of proteins in nonplant cells. Nat Methods 6: 917-922.

Novick, P., Ferro, S., and Schekman, R., 1981. Order of events in the yeast secretory pathway. Cell 25: 461-469.

Potelle, S., Morelle, W., Dulary, E., Duvet, S., Vicogne, D., Spriet, C., Krzewinski-Recchi, M.A., Morsomme, P., Jaeken, J., Matthijs, G., De Bettignies, G., and Foulquier, F., 2016. Glycosylation abnormalities in Gdt1p/TMEM165 deficient cells result from a defect in Golgi manganese homeostasis. Hum Mol Genet 25: 1489-1500.

Pozos, T.C., Sekler, I., and Cyert, M.S., 1996. The product of *HUM1*, a novel yeast gene, is required for vacuolar Ca^{2+}/H^{+} exchange and is related to mammalian Na^{+}/Ca^{2+} exchangers. Mol Cell Biol 16: 3730-3741.

Qi, J., and Forgac, M., 2007. Cellular environment is important in controlling V-ATPase dissociation and its dependence on activity. J Biol Chem 282: 24743-24751.

Reinhardt, T.A., Lippolis, J.D., and Sacco, R.E., 2014. The Ca^{2+}/H^{+} antiporter TMEM165 expression, localization in the developing, lactating and involuting mammary gland parallels the secretory pathway Ca^{2+}-ATPase (SPCA1). Biochem Biophys Res Commun 445(2): 417-421.

Rudolph, H.K., Antebi, A., Fink, G.R., Buckley, C.M., Dorman, T.E., LeVitre, J., Davidow, L.S., Mao, J.I., and Moir, D.T., 1989. The yeast secretory pathway is perturbed by mutations in *PMR1*, a member of a Ca^{2+} ATPase family. Cell 58: 133-145.

Samyn, D.R., and Persson, B.L., 2016. Inorganic Phosphate and Sulfate Transport in S. cerevisiae. Adv Exp Med Biol 892: 253-269.

Secco, D., Wang, C., Shou, H., and Whelan, J., 2012. Phosphate homeostasis in the yeast Saccharomyces cerevisiae, the key role of the SPX domain-containing proteins. FEBS Lett 586: 289-295.

Smardon, A.M., Diab, H.I., Tarsio, M., Diakov, T.T., Nasab, N.D., West, R.W., and Kane, P.M., 2014. The RAVE complex is an isoform-specific V-ATPase assembly factor in yeast. Mol Biol Cell 25: 356-367.

Smyth, J.T., Hwang, S.Y., Tomita, T., DeHaven, W.I., Mercer, J.C., and Putney, J.W., 2010. Activation and regulation of store-operated calcium entry. J Cell Mol Med 14: 2337-2349.

Sorin, A., Rosas, G., and Rao, R. , 1997. PMR1, a Ca^{2+}-ATPase in yeast Golgi, has properties distinct from sarco/endoplasmic reticulum and plasma membrane calcium pumps. J Biol Chem 272: 9895-9901.

Stanley, P., 2011. Golgi glycosylation. Cold Spring Harb Perspect Biol 3.

Stathopoulos, A.M., and Cyert, M.S., 1997. Calcineurin acts through the *CRZ1/TCN1* encoded transcription factor to regulate gene expression in yeast. Genes Dev 11: 3432-3444.

Stefan, C.P., and Cunningham, K.W., 2013. Kch1 family proteins mediate essential responses to endoplasmic reticulum stresses in the yeasts Saccharomyces cerevisiae and Candida albicans. J Biol Chem 288: 34861-34870.

Stefan, C.P., Zhang, N., Sokabe, T., Rivetta, A., Slayman, C.L., Montell, C., and Cunningham, K.W., 2013. Activation of an essential calcium signaling pathway

in Saccharomyces cerevisiae by Kch1 and Kch2, putative low-affinity potassium transporters. Eukaryot Cell 12: 204-214.

Strayle, J., Pozzan, T., and Rudolph, H.K., 1999. Steady-state free Ca^{2+} in the yeast endoplasmic reticulum reaches only 10 μM and is mainly controlled by the secretory pathway pump Pmr1. EMBO J 18: 4733-4743.

Sudbrak, R., Brown, J., Dobson-Stone, C., Carter, S., Ramser, J., White, J., Healy, E., Dissanayake, M., Larregue, M., Perrussel, M., Lehrach, H., Munro, C.S., Strachan, T., Burge, S., Hovnanian, A., and Monaco, A.P., 2000. Hailey-Hailey disease is caused by mutations in ATP2C1 encoding a novel Ca^{2+} pump. Hum Mol Genet 9: 1131-1140.

Wege, S., Khan, G.A., Jung, J.Y., Vogiatzaki, E., Pradervand, S., Aller, I., Meyer, A.J., and Poirier, Y., 2016. The EXS Domain of PHO1 Participates in the Response of Shoots to Phosphate Deficiency via a Root-to-Shoot Signal. Plant Physiol 170: 385-400.

Wege, S., and Poirier, Y., 2014. Expression of the mammalian Xenotropic Polytropic Virus Receptor 1 (XPR1) in tobacco leaves leads to phosphate export. FEBS Lett 588: 482-489.

Wild, R., Gerasimaite, R., Jung, J.Y., Truffault, V., Pavlovic, I., Schmidt, A., Saiardi, A., Jessen, H.J., Poirier, Y., Hothorn, M., and Mayer, A., 2016. Control of eukaryotic phosphate homeostasis by inositol polyphosphate sensor domains. Science 352: 986-990.

Wilson, D.W., Lewis, M.J., and Pelham, H.R., 1993. pH-dependent binding of KDEL to its receptor in vitro. J Biol Chem 268: 7465-7468.

Wykoff, D.D., and O'Shea, E.K., 2001. Phosphate transport and sensing in Saccharomyces cerevisiae. Genetics 159: 1491-1499.

Wykoff, D.D., Rizvi, A.H., Raser, J.M., Margolin, B., and O'Shea, E.K., 2007. Positive feedback regulates switching of phosphate transporters in S. cerevisiae. Mol Cell 27: 1005-1013.

Zeevaert, R., de Zegher, F., Sturiale, L., Garozzo, D., Smet, M., Moens, M., Matthijs, G., and Jaeken, J., 2013. Bone dysplasia as a key feature in three patients with a novel congenital disorder of glycosylation (CDG) Type II due to a deep intronic splice mutation in TMEM165. JIMD Rep 8: 145-152.

Zhao, Y., Du, J., Zhao, G., and Jiang, L., 2013. Activation of calcineurin is mainly responsible for the calcium sensitivity of gene deletion mutations in the genome of budding yeast. Genomics 101: 49-56.

CHAPTER 2 APPENDICES

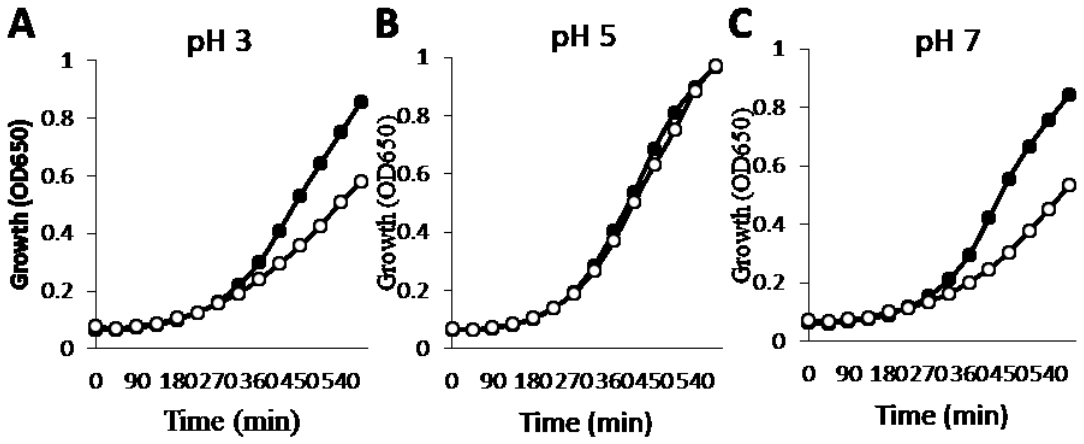

Appendix 2.1: Gdt1 is required for growth in acidic or neutral pH.

Growth of wild-type (black circles) and *gdt1Δ* (white circles) yeast was measured by comparing the optical density (OD650) every 45 minutes for 9 hours in YPD media buffered with HEPES and succinic acid to pH 3 (A), pH 5 (B), and pH 7 (C). Mid-log phase cultures were diluted to a starting OD of 0.05 to begin the time course. At both pH 3 and pH 7, the *gdt1Δ* strain grew at a slower rate than wild-type, while at pH 5, the growth was comparable to that of wild-type.

Appendix 2.2: Sensitivity of mutant strains to added $ZnCl_2$ in YPD

The data demonstrate that *GDT1* is required for tolerance of high concentrations of Zn^{2+}, independent of the two known major Zn^{2+} transporters, Cot1 and Zrc1. This effect is surprisingly also independent of calcineurin activity.

Genotypes and Conditions [a]				IC50 [b]	CV [c]	Performance Factor (PF) [d]			
GDT1	**COT1**	**ZRC1**	**FK506**	**(mM)**	**(%)**	***GDT1* (+/Δ)**	***COT1* (+/Δ)**	***ZRC1* (+/Δ)**	***FK506* (-/+)**
.	.	.	-	1.02	0.2	1.3	1.1	3.5	1.1
Δ	.	.	-	0.81	2.1		1.1	2.7	1.6
.	Δ	.	-	0.89	1.1	1.2		85.1	1.1
Δ	Δ	.	-	0.76	2.2			133.5	1.7
.	.	Δ	-	0.29	1.2	1.0	27.8		1.0
Δ	.	Δ	-	0.30	2.9		52.4		1.3
.	Δ	Δ	-	0.011	2.8	1.8			1.0
Δ	Δ	Δ	-	0.006	10.9				1.1
.	.	.	+	0.95	2.1	1.9	1.2	3.4	
Δ	.	.	+	0.50	4.7		1.1	2.2	
.	Δ	.	+	0.82	2.4	1.8		77.5	
Δ	Δ	.	+	0.45	5.1			84.8	
.	.	Δ	+	0.28	3.4	1.3	26.8		
Δ	.	Δ	+	0.22	6.3		42.0		
.	Δ	Δ	+	0.011	0.3	2.0			
Δ	Δ	Δ	+	0.005	7.7				

Footnote

[a] addition of 0.2 µg/mL FK506

[b] average of derived IC50 from two strains (in mM $ZnCl_2$), determined by measurement of the optical density (OD_{650}) after 24 hours of growth from a 1:1000 dilution of saturated culture.

[c] coefficient of variation (CV) between two strains (in %)

[d] PF = $\log_2$ of (avg IC50 WT strain/avg IC50 Δ strain)

CHAPTER 3

TMEM165 DEFICIENCY IN LACTATING MAMMARY GLAND CAUSES DECREASED LACTOSE SYNTHESIS AND LOW MILK YIELD IN MICE

Outside contributions:

Histological analysis was conducted by Mitchell V. Palmer and TUNEL staining and determination of milk creamatocrit concentrations were conducted by Timothy A. Reinhardt at the USDA/ARS National Animal Disease Center in Ames, IA.

ABSTRACT

Milk is a hallmark of mammals that is critical for normal growth and development of offspring. Here we demonstrate that TMEM165, a Golgi-localized ion exchanger, is required for normal lactose biosynthesis in the lactating mammary gland of mice. Mutant mice lacking TMEM165 in the mammary gland produced milk that was unable to sustain normal growth rates of litters. The milk contained elevated concentrations of fat, protein, calcium, iron, and zinc likely caused by decreased biosynthesis of lactose and diminished dilution by osmosis. Manganese/protein ratios were significantly lower in this milk, suggesting TMEM165 supplies essential Mn^{2+} to lactose synthase in the Golgi complex, which may be driven by counter-transport of H^{+} that is a byproduct of lactose synthesis and other glycosylation reactions.

INTRODUCTION

Deficiencies in the Golgi transmembrane protein TMEM165 cause a type-II congenital disorder of glycosylation in humans (Foulquier *et al.* 2012). Recent reports have shown that this protein, along with its yeast homolog Gdt1, can transport Ca^{2+} *in vitro* and promote normal homeostasis of Ca^{2+}, Mn^{2+} and H^{+} in the Golgi complex (Colinet *et al.* 2016; Potelle *et al.* 2016; Thines *et al.* 2018). These findings suggest that TMEM165 supports glycosylation by maintaining proper pH and supplying Mn^{2+} and Ca^{2+} that are required as cofactors in the glycosyltransferases responsible for protein and lipid glycosylation (Kaufman *et al.* 1994; Dürr *et al.* 1998). Disruption of the homeostasis of pH or the concentrations of Ca^{2+} or Mn^{2+} have been demonstrated to result in deficiencies in glycosylation (Dürr *et al.* 1998; Axelsson *et al.* 2001; Kornak *et al.* 2007; Park *et al.* 2015). The incidence of identified cases of congenital disorders of glycosylation (CDG) among humans is increasing, now including more than 125 unique disorders (Ng and Freeze 2018).

TMEM165 mRNA, formerly Tpar1, is expressed in virtually all tissues and cell types, including the mammary gland (BioGPS). However, TMEM165 mRNA and protein levels increase dramatically, by 7- and 25-fold respectively, in the mammary gland during the secretory activation phase of lactation (Stein *et al.* 2003; Reinhardt *et al.* 2014). TMEM165 protein levels accumulate in the Golgi complexes of alveolar epithelial cells (Reinhardt *et al.* 2014) along with α-lactalbumin subunit of lactose synthase, which together with β4-galactosyltransferase I (β4-GALT-I) synthesizes lactose in the lumen from transported UDP-galactose and glucose (Fraser and Mookerjea 1976). β4-GALT-I requires Mn^{2+} as a co-factor for its catalytic activities (Fraser and Mookerjea

1976). The secretory pathway Ca^{2+}/Mn^{2+} ATPase 1 (SPCA1) supplies the Golgi with much of the Mn^{2+} required for lactose synthase and other glycosyltransferases (Ton *et al.* 2002; Reinhardt *et al.* 2000) and much of the Ca^{2+} that is complexed with inorganic phosphate and casein proteins to form micelles in the Golgi complex (Aoki *et al.* 1987). While there is no obvious requirement for a $H^+/Ca^{2+}/Mn^{2+}$ exchanger in this scheme of milk production in Golgi complex, H^+ is produced as a byproduct of all glycosylation reactions including lactose biosynthesis, and there is no known mechanism for eliminating excess H^+ from the Golgi and maintaining pH within a physiological range. In milk producing cells, TMEM165 may deacidify the Golgi while supplying Ca^{2+} and Mn^{2+} as both enzyme cofactors and nutrients.

In this study, we test the role of TMEM165 in the lactating mammary gland of mice by examining mouse mutants bearing a conditional knockout of TMEM165. Using a Cre-recombinase that is driven by the whey acid protein (WAP) promoter, which is only expressed in milk producing alveolar epithelial cells during late pregnancy, an 85% depletion of TMEM165 protein was achieved and strong defects in milk quality were observed. Unexpectedly, calcium, iron, zinc, fat, and total protein concentrations were elevated in the milk of TMEM165-deficient animals. However, lactose accumulation was strongly diminished, and this likely resulted in decreased osmosis and concentrated other components of in the milk. We show that the catalytic subunit of lactose synthase, *in vitro*, is highly sensitive to acidic pH, and we propose that the reduced quality of milk in TMEM165-deficient animals is due to a failure to remove the H^+ byproduct of lactose biosynthesis, a diminished supply of Mn^{2+} in the Golgi, or both, which then diminishes lactose synthase activity and osmosis. These findings highlight the importance of ion

homeostasis in the Golgi complex of professional secretory cells and the unique role of TMEM165 in exchanging H^+, Ca^{2+}, and Mn^{2+}.

RESULTS

Conditional knockout mouse displays normal histology in the lactating mammary gland

A condition-ready TMEM165 knockout mouse was generated by transfecting embryonic stem cells with a recombinant plasmid from EUCOMM, blastocyst injecting, germ-line screening, and cross-breeding to C57BL/6 wild-type mice, as described in Materials and Methods. In order to study the effect of TMEM165 on lactation, we crossed this mouse line to a mouse line expressing Cre recombinase under control by the whey acid protein (WAP) promoter (Wagner *et al.* 1997). In the experiments below, all nursing mice were heterozygous for WAP-Cre (i.e. $WAP^{+/Cre}$) and either homozygous or heterozygous for the floxed allele of TMEM165 (henceforth referred to as $TMEM165^{\Delta/\Delta}$ and $TMEM165^{\Delta/+}$) or homozygous for the natural allele ($TMEM165^{ctrl}$). To determine the efficacy of this TMEM165 conditional knockout, western blots were performed on mammary tissue harvested from mothers after 12 days of lactation. The $TMEM165^{\Delta/\Delta}$ mice demonstrated an 85% knockdown of TMEM165 expression in mammary tissue, and there was a 43% knockdown in $TMEM165^{\Delta/+}$ mammary tissue, relative to $TMEM165^{ctrl}$ tissue (Figures 3.1A and 3.1B). Histological analysis via H&E sections of mammary tissue from these mothers demonstrated no significant visible difference between genotypes (Figure 3.1C). However, TUNEL staining of mammary tissue sections demonstrated a small but significant increase in apoptotic cells in both $TMEM165^{\Delta/\Delta}$ and $TMEM165^{\Delta/+}$ mice, relative to $TMEM165^{ctrl}$ mice (Figures 3.2A and 3.2B). This suggests

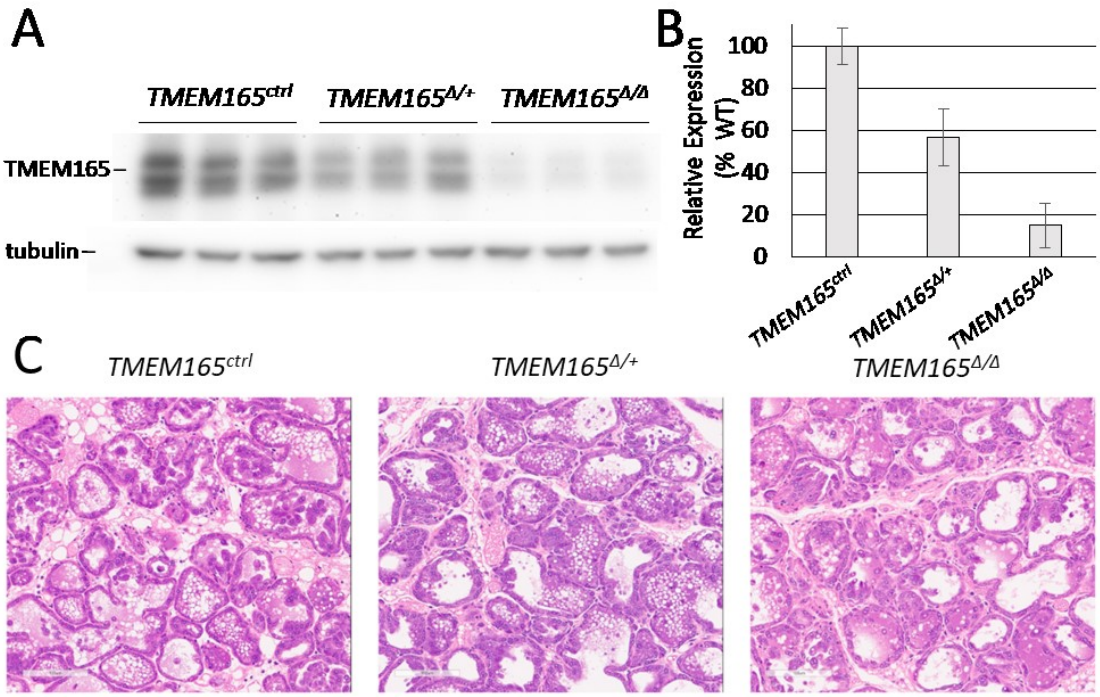

Figure 3.1: *TMEM165*$^{\Delta/\Delta}$ Mammary Gland Displays Normal Histology.

(A) Western blots of total protein extracted from mammary glands on day 12 of lactation were performed using anti-TMEM165 and anti-tubulin antibodies. (B) The ratios of TMEM165 to tubulin were calculated from quantified bands, averaged among replicates, and the heterozygous and homozygous samples were normalized to TMEM165^{ctrl} animals (±S.D.). (C) Representative images H&E stained tissue from these mothers.

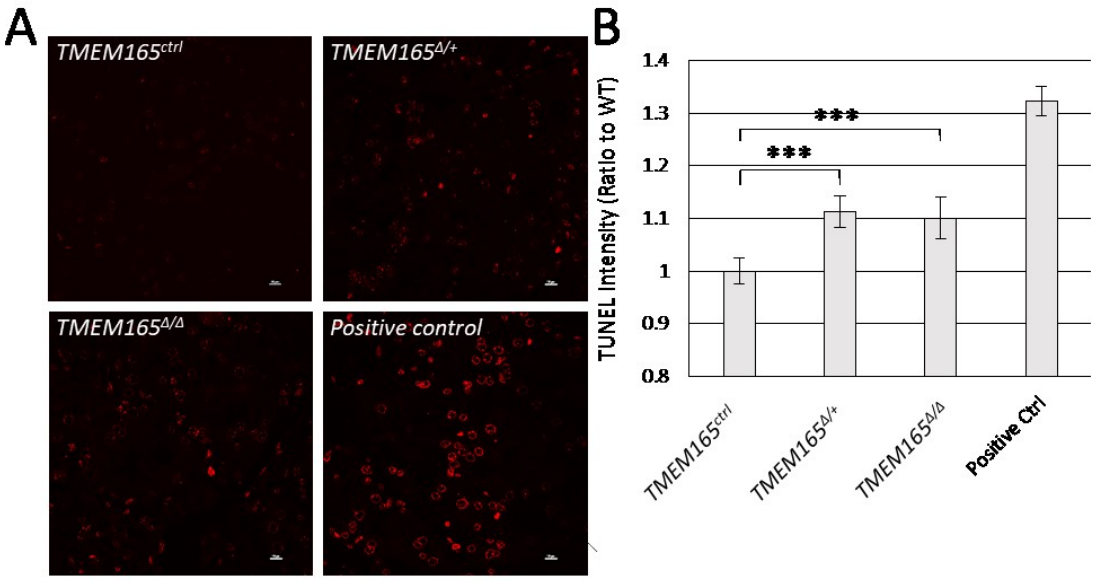

Figure 3.2: *TMEM165*$^{\Delta/\Delta}$ Tissue Exhibits Premature Cell Death.

TUNEL staining (A) of the tissues identifies cells that have undergone cell death. Analysis of the intensity (B) shows a statistically significant increase in TUNEL-positive cells in both heterozygous and homozygous-knockout mice, relative to the wild-type. * $P < 0.05$, ** $P < 0.01$, *** $P < 0.001$ using Student's T-test.

that even a partial decrease in expression of TMEM165 may occasionally affect cell survival in this tissue.

Immunostaining revealed high TMEM165 expression in the Golgi complexes of alveolar epithelial cells that surround the lumen of the *TMEM165*^{ctrl} mammary tissue (Figure 3.3).

Interestingly, the tissue from the *TMEM165*$^{\Delta/\Delta}$ mouse expressed TMEM165 in a patchy mosaic pattern, where a fraction of the alveolar epithelial cells maintained expression and therefore escaped elimination by WAP-Cre (Figure 3.3). One possible reason for the mosaic expression is incomplete deletion of *TMEM165* exons from some cells within the developing mammary gland that later populate a small portion of the tissue. Similar mosaic expression of TMEM165 was seen in mice expressing Cre under control of the MMTV promoter (not shown). These findings demonstrated that WAP-Cre produced a large, yet incomplete, decrease in TMEM165 expression in the milk producing cells of the mammary glands of *TMEM165*$^{\Delta/\Delta}$ animals.

Litters nursed by TMEM165$^{\Delta/\Delta}$ *mothers exhibit low weight gains*

To determine whether TMEM165 deficiency affected the overall quantity or quality of milk production, mothers nursed litters of 6 pups each and litter weight was measured every 2 days for 2 weeks. While all the pups and mothers appeared healthy and behaved normally, pups nursed by *TMEM165*$^{\Delta/\Delta}$ mothers displayed significantly lower litter weights than pups nursed by *TMEM165*^{ctrl} mothers on all days measured (Figure 3.4A). By day 14, litters from *TMEM165*$^{\Delta/\Delta}$ dams weighed only 78% of those from *TMEM165*^{ctrl} dams, suggesting a strong defect in milk quality or quantity.

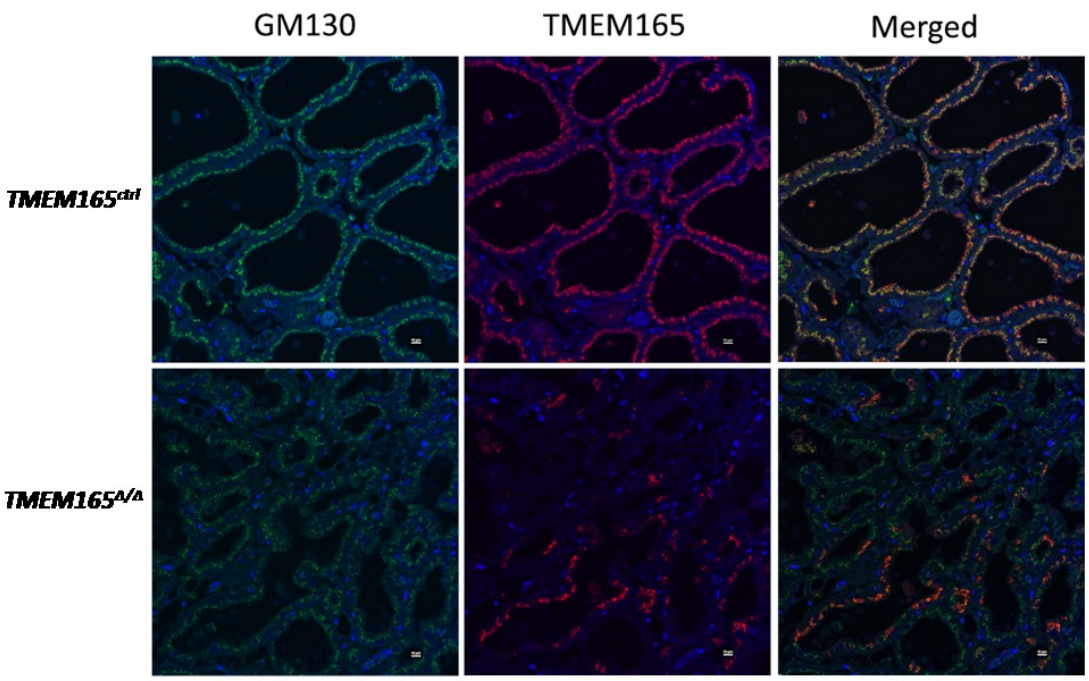

Figure 3.3: *TMEM165*$^{\Delta/\Delta}$ Mammary Tissue has Mosaic Expression.

In situ immunostaining of fixed and sectioned tissue demonstrates that TMEM165 (red) colocalizes with GM130 (green). DAPI (blue) identifies cell nuclei. Some cells within the tissue continue to express TMEM165 in *TMEM165*$^{\Delta/\Delta}$ mice, resulting in mosaicism in these mice.

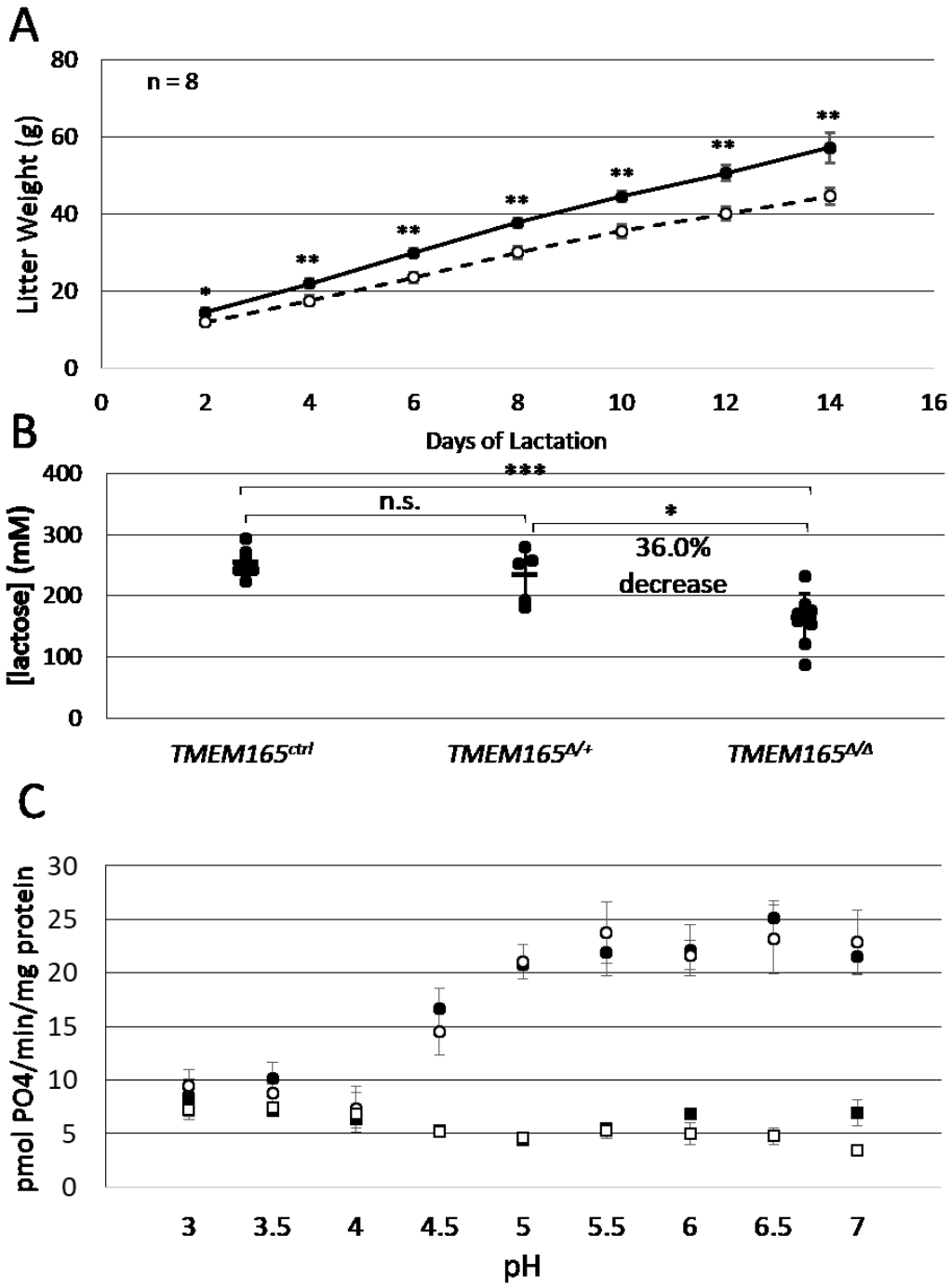

Figure 3.4: Milk from *TMEM165*$^{\Delta/\Delta}$ mothers exhibits low nutritional quality and low lactose.

(A) Litters of 6 pups per mother were weighed every 2 days following birth. Data shown is the average (±S.D.) of litters nursed by 8 mothers of *TMEM165*$^{\Delta/\Delta}$ and *TMEM165*^{ctrl}.

(B) Milk collected from mothers of the specified genotype on day 12 of lactation were assayed for lactose as described in methods. (C) Galactosyltransferase activity, representing β4-GALT-1 subunit of lactose synthase, was measured in detergent-solubilized crude membrane extracts prepared from the indicated nursing mothers on day 12 of lactation. The assay method is described in Methods. * $P < 0.05$, ** $P < 0.01$, *** $P < 0.001$ using Student's T-test.

Lactose deficiency in milk from TMEM165-deficient dams.

Because TMEM165-deficiency leads to deficiencies of glycosylation in humans (Foulquier *et al.* 2012), we hypothesized that *TMEM165*$^{\Delta/\Delta}$ mice may have a deficiency in lactose biosynthesis. To test this possibility, milk samples were collected from dams after 12 days of lactation with 6 pups per dam, and the lactose concentration was measured. Strikingly, we observed a 36% decrease in lactose concentration in the *TMEM165*$^{\Delta/\Delta}$ dams relative to the *TMEM165*$^{\Delta/+}$ and *TMEM165*^{ctrl} dams (Figure 3.4B). The corresponding decline in osmosis would serve to concentrate the residual lactose and thus partially mask a larger decline in the actual rate of lactose biosynthesis.

To determine whether the decline in lactose biosynthesis is caused by a decline in lactose synthase activity, mammary glands from *TMEM165*^{ctrl} and *TMEM165*$^{\Delta/\Delta}$ dams were dissected and homogenized. Crude membrane fractions were isolated by differential centrifugation, washed to remove lactose, permeabilized with non-denaturing detergent, and assayed *in vitro* for galactosyltransferase activity using a protocol that monitors liberation of inorganic phosphate from UDP-galactose in the presence of GlcNAc and added Mn^{2+} (see Materials and Methods). These conditions measure β4-GALT-I activity directly and do not rely on the potentially unstable association of α-lactalbumin and Mn^{2+} with the catalytic subunit of lactose synthase. At physiological pH of 6 for the lumen of the Golgi complex, galactosyltransferase activity was indistinguishable in *TMEM165*^{ctrl} and *TMEM165*$^{\Delta/\Delta}$ samples (Figure 3.4C). Omission of glucose (Figure 3.4C) or UDP-galactose (not shown) resulted in total loss of galactosyltransferase activity, indicating the specificity of the assay method. Galactosyltransferase activity remained constant as pH of the buffer was increased to 7 or

decreased to 5. However, the activity declined to background levels when the pH was lowered to 4 or less (Figure 3.4C). Thus, the *TMEM165*$^{\Delta/\Delta}$ and *TMEM165*^{ctrl} samples appeared to contain equivalent activities of the lactose synthase catalytic subunit when assayed *in vitro* in the presence of excess of Mn^{2+}, and this activity was somewhat sensitive to the acidity of the buffer. These results suggest that lactose synthase enzyme levels are unaffected by TMEM165 deficiency, and instead suggest the activity of enzyme may be severely diminished in the Golgi complexes of *TMEM165*$^{\Delta/\Delta}$ cells. Since TMEM165 is hypothesized to export luminal H^+ in exchange for cytoplasmic Mn^{2+}, TMEM165 deficiency may diminish lactose synthase activity by increasing luminal H^+, decreased luminal Mn^{2+}, or both, resulting in lower lactose production and diminished milk quality.

Lactose deficiency may concentrate other milk components due to lower dilution by osmosis

Lactose concentrations in mouse milk can reach 250 mM and thus serves as the major osmolyte of milk, and perhaps even in the Golgi complex where lactose is synthesized. To investigate the possibility that the deficiency of lactose secretion in TMEM165-deficient mammary glands produced milk with an osmotic defect, milk samples were treated with concentrated nitric acid to eliminate organic components, and then analyzed by inductively coupled plasma mass spectrometry (ICP-MS) alongside calibration standards (see Materials and Methods). Surprisingly, the concentration of calcium did not decline in milk from *TMEM165*$^{\Delta/\Delta}$ dams and actually increased by 23.9% (Figure 3.5A) whereas the concentration of manganese remained constant (Figure 3.5B).

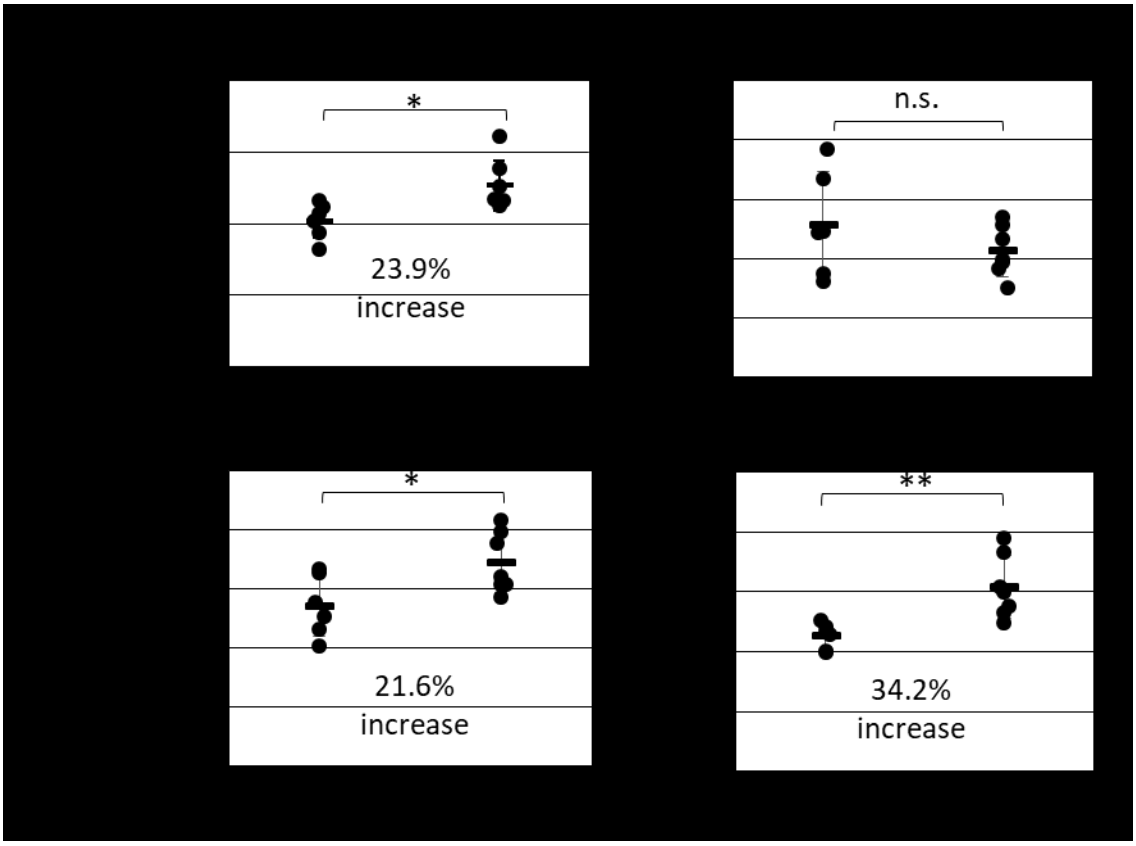

Figure 3.5: Milk from *TMEM165*$^{\Delta/\Delta}$ Mothers has Osmotic Deficiency Causing Increased Metal Concentrations.

Measurements of metal content in milk from *TMEM165*$^{\Delta/\Delta}$ and control mothers were taken. Concentrations of calcium, manganese, iron, and zinc in skimmed milk samples from day 12 of lactation were measured by ICP-MS as described in Methods. * $P < 0.05$, ** $P < 0.01$, *** $P < 0.001$ using Student's T-test.

The concentrations of iron and zinc also increased significantly by 21.6% and 34.2% respectively (Figures 3.5C and 3.5D). Because these metals are mostly bound as ions by milk proteins, we also measured the concentration of total protein in untreated portions of the milk samples. Milk from *TMEM165*$^{\Delta/\Delta}$ dams contained approximately 45% increase in total protein relative to that of *TMEM165*$^{\Delta/+}$ and *TMEM165*^{ctrl} dams (Figure 3.6B). Analysis of milk proteins by SDS-PGE and staining with Coomassie brilliant blue also suggested increased protein concentration in the milk from *TMEM165*$^{\Delta/\Delta}$ dams without any noticeable difference in the pattern of the bands (Figure 3.6A). In addition, we estimated the fat composition of the milk by measuring the creamatocrit composition, which is the percent of milk made up of cream. *TMEM165*$^{\Delta/\Delta}$ dams exhibited a 52% increase in creamatocrit concentration, similar to the increase in total protein concentration (Figure 3.6C). These findings indicate milk from *TMEM165*$^{\Delta/\Delta}$ dams contains significantly higher concentrations of calcium, iron, zinc, total protein, and lipids, none of which are likely to diminish the milk quality. When the metal concentrations were normalized to total protein instead of volume, iron and zinc to protein ratios were similar in milk from *TMEM165*$^{\Delta/\Delta}$ and *TMEM165*^{ctrl} dams (Figures 3.7C and 3.7D). However, milk from *TMEM165*$^{\Delta/\Delta}$ dams did exhibit a significant decrease in the calcium and manganese to protein ratios (Figures 3.7A and 3.7B), which could lower the activity of Mn^{2+}-dependent glycosyltransferases such as lactose synthase, causing a decrease in lactose synthesis and secretion into milk, lower osmosis, and lower dilution of other milk components, including metals and protein.

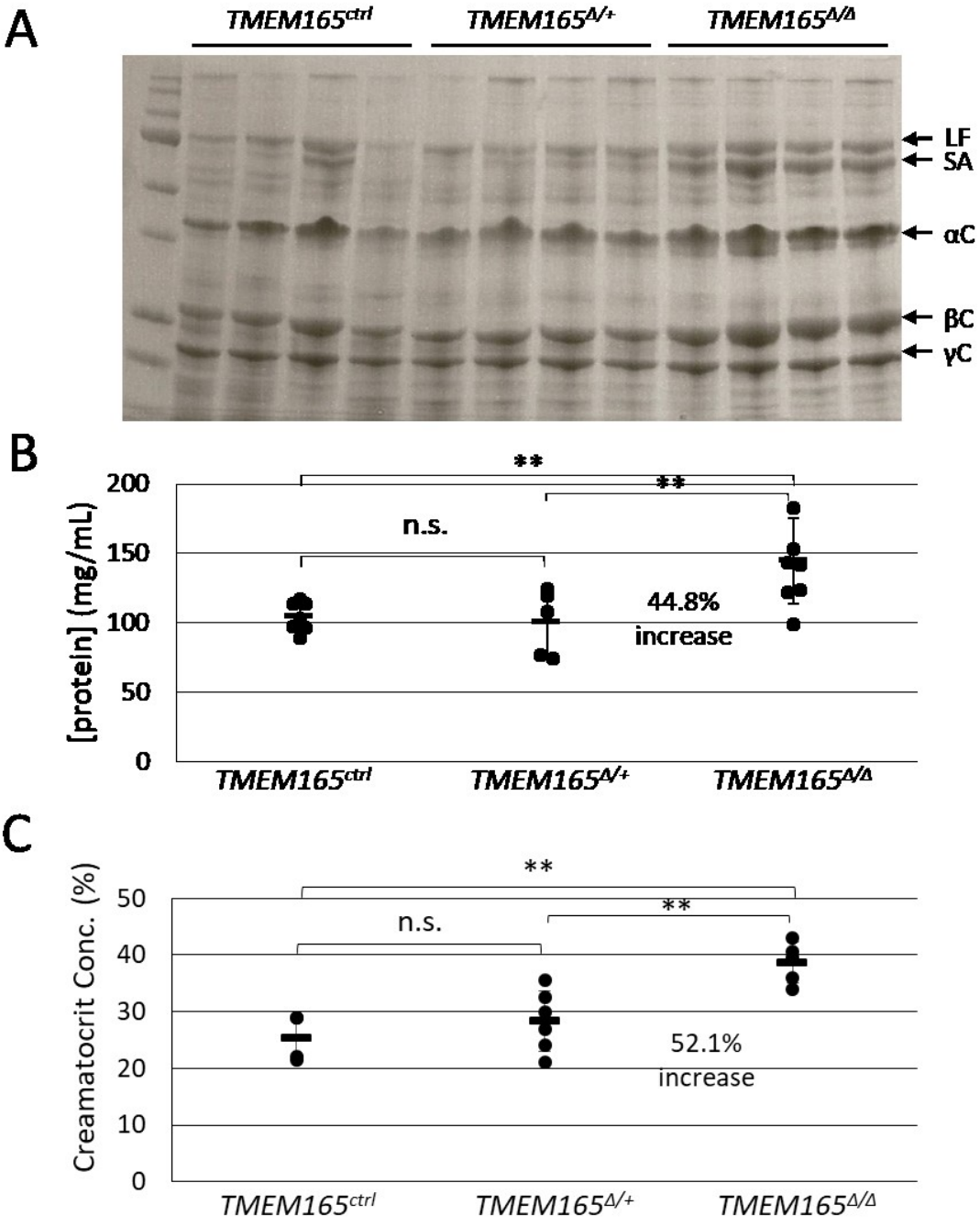
A
TMEM165ctrl
TMEM165Δ/+
TMEM165Δ/Δ
LF
SA
αC
βC
γC
B
[protein] (mg/mL)
200
150
100
50
0
**
**
n.s.
44.8%
increase
TMEM165ctrl
TMEM165Δ/+
TMEM165Δ/Δ
C
Creamatocrit Conc. (%)
50
40
30
20
10
0
**
**
n.s.
52.1%
increase
TMEM165ctrl
TMEM165Δ/+
TMEM165Δ/Δ

Figure 3.6: Protein and Lipid Concentrations in Milk from *TMEM165*$^{\Delta/\Delta}$ Mothers is Increased.

Milk collected from mothers of the specified genotype on day 12 of lactation was skimmed and analyzed by SDS-PAGE and staining with Coomassie blue (A) and quantified using Bradford stain (B). Identified protein bands include lactoferrin (LF), serum albumin (SA), and alpha-, beta-, and gamma-casein (αC, βC, and γC, respectively). Whole milk was also subjected to creamatocrit (lipid) analysis (C). * $P < 0.05$, ** $P < 0.01$, *** $P < 0.001$ using Student's T-test.

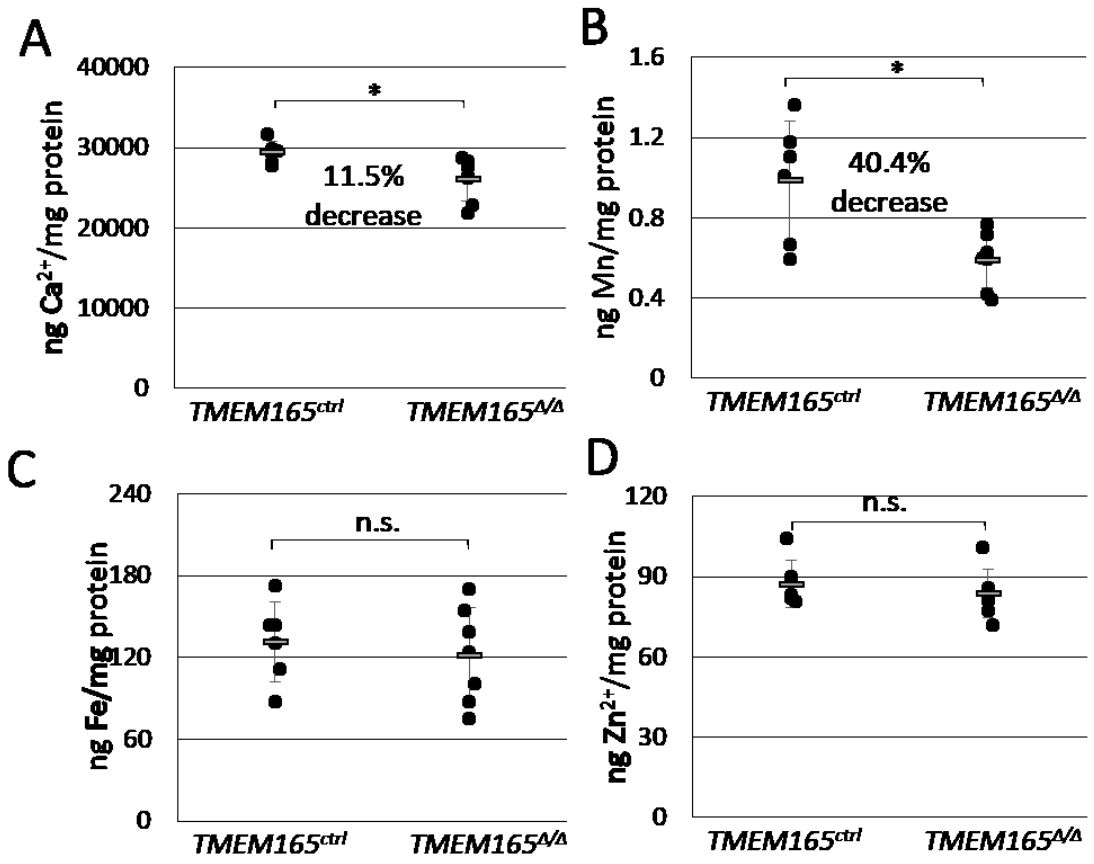

Figure 3.7: Normalized metal content in milk indicates significant deficiency of calcium and manganese from *TMEM165*$^{\Delta/\Delta}$ mothers.

Data from Figure 5 was normalized to total protein levels measured in Figure 6B. * $P < 0.05$, ** $P < 0.01$, *** $P < 0.001$ using Student's T-test.

DISCUSSION

TMEM165 is a Golgi-localized trans-membrane protein that is expressed in virtually all mammalian tissue and is strongly conserved throughout animals, plants, fungi, and even prokaryotes. The data obtained up to now suggest that TMEM165 and its homologs transport H^+, Ca^{2+}, and Mn^{2+} across the Golgi membrane and therefore directly influence the homeostasis of these ions, which indirectly affects the activities of Golgi-localized glycosyltransferases and other enzymes. The strong up-regulation of TMEM165 expression in the alveolar epithelial cells of the mammary gland immediately before parturition when secretory activation is occurring (Stein *et al.* 2003) suggests an important role for this ion exchanger in milk biosynthesis in these prolific secretory cells. Here we show that indeed TMEM165 deficiency in these cells decreases manganese/protein ratio and lactose accumulation in the milk, likely by diminishing Mn^{2+} transport into the Golgi that is critical for lactose synthase activity. This results in lower osmotic dilution of protein, fat, and other constituents and lower milk quality, as detected by growth rates of litters.

Lactose is the major osmolyte in milk (Holt 1983). In addition to this, the process of lactose biosynthesis is carried out by a galactosyl-transferase and therefore requires many of the same substrates and conditions as glycosylation (Figure 3.8, and Berliner and Robinson 1982). Since TMEM165-deficiency is known to cause congenital disorders of glycosylation, it was hypothesized that disruption of expression of TMEM165 during lactation would similarly inhibit the creation of lactose, thereby decreasing the osmotic potential of milk by reducing the lactose composition. This loss of glycosyltransferase activity could result from a decrease in concentration of Mn^{2+}, which is an important

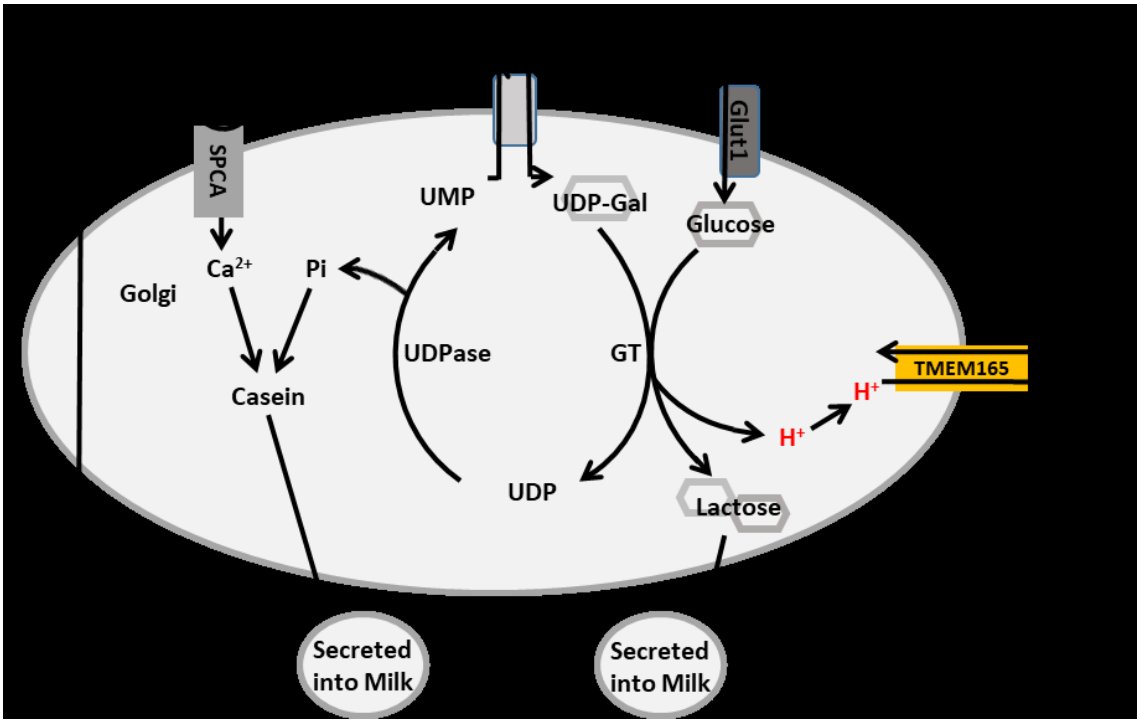

Figure 3.8: Model of Lactose Synthesis in the Golgi Apparatus.

In order to synthesize lactose, UDP-Galactose is transported into the Golgi apparatus in exchange for UMP. A galactosyltransferase (β4-GALT) then covalently links the galactose to glucose, releasing a proton and UDP, the latter of which is cleaved by a phosphatase into inorganic phosphate and UMP. The inorganic phosphate can then be secreted into milk as a part of casein, and the UMP is exchanged for additional UDP-galactose substrate. Once in the milk, lactose serves as the major osmotic driver of water into the milk to provide volume and reduce viscosity.

cofactor in both lactose synthesis and glycosylation (Powell and Brew 1976), and/or a decrease in pH, resultant from accumulation of protons released during lactose synthesis that would otherwise be released to the cytoplasm by TMEM165.

Lactose is synthesized from UDP-galactose and glucose in the Golgi lumen by lactose synthase, an enzyme that depends on Mn^{2+} and is inhibited by acidic pH. Though the expression of the regulatory subunit of lactose synthase (α-lactalbumin) is far greater than the catalytic subunit (β4-GALT-I), the heterozygous knockout mutants of α-lactalbumin exhibited 10 to 30% declines of lactose concentration in milk, which decreased osmolarity and increased total protein concentration by 20-50% (Stinnakre *et al.* 1994, Stacey *et al.* 1995). Milk yield also declined in these heterozygotes (Stacey *et al.* 1995), homozygous knockout mutants produced little milk with no lactose and very high concentration of protein and viscosity. The consequences of TMEM165 deficiency appeared to be similar to the heterozygous α-lactalbumin deficiency, resulting in moderately decreased lactose and increased total protein, fat, and ion concentrations in the milk.

Upon normalizing Ca^{2+}, Mn^{2+}, Zn^{2+}, and Fe^{2+} concentrations in milk to total protein, only Ca^{2+} Mn^{2+} appeared to be significantly decreased in the *TMEM165*$^{\Delta/\Delta}$ animals. The remaining calcium and manganese in milk is probably transported into the Golgi by the secretory pathway Ca^{2+}/Mn^{2+} ATPase SPCA1 (Dürr *et al.* 1998, Ton *et al.* 2002, Lapinskas *et al.* 1995), though SPCA2 may also contribute from a non-Golgi organelle (Xiang *et al.* 2005). These SPCA pumps contribute about 40% of the Ca^{2+} found in milk with the remaining 60% transported by the plasma membrane Ca^{2+} ATPase PMCA2 (Reinhardt *et al.* 2004). As Ca^{2+} is approximately 30,000 times more abundant

in milk than Mn^{2+}, SPCA and TMEM165 likely transport much more Ca^{2+} than Mn^{2+} during lactation. The deficiency of Ca^{2+} transport in *TMEM165*$^{\Delta/\Delta}$ animals was not as great as Mn^{2+} in the milk, possibly because of compensatory effects of the PMCA2 pump which has been shown to be the primary milk calcium transporter (Reinhardt *et al.* 2004). The SPCA pumps appeared unable to fully compensate for the Mn^{2+} transport defects in the *TMEM165*$^{\Delta/\Delta}$ animals, and Mn^{2+} depletion in the Golgi may lower the activity of lactose synthase and potentially other glycosyltransferases responsible for protein glycosylation despite the fact that both are significantly upregulated in lactation (Reinhardt *et al.* 2000). It is not yet clear whether TMEM165 alters the pH of the Golgi of the milk producing cells, but a failure to counter-transport H^+ from the lumen to the cytoplasm in the knockout animals could lead to hyper-acidification and additional loss of lactose synthase and glycosyltransferase activities. H^+ accumulation and Mn^{2+} depletion in the Golgi of these mutant cells could also alter transport of UDP-galactose and other nucleotide-sugars instead of, or in addition to, glycosyltransferase activities. Therefore, defects associated with *TMEM165*$^{\Delta/\Delta}$ Golgi may be broader yet milder than simple deficiency of α-lactalbumin.

TMEM165 is expressed throughout the body of mammals, and humans with homozygous mutations in TMEM165 exhibit a congenital disorder of glycosylation that ultimately manifests with skeletal and growth abnormalities (Foulquier *et al.* 2012, Rosnoblet *et al.* 2016). TMEM165-deficient zebrafish similarly exhibit glycosylation defects and have problems with cartilage development (Bammens *et al.* 2015). Interestingly, supplementation of culture medium with Mn^{2+} was found to partially reverse the glycosylation defects of TMEM165-deficient HeLa cells. The supplemental

Mn^{2+} presumably increases Golgi Mn^{2+} concentration by out-competing Ca^{2+} as a substrate for SPCA's. This rationale was first tested in yeast cells lacking a homolog of TMEM165 known as Gdt1. The residual partial defect in glycosylation in *gdt1*Δ yeast cells was exacerbated by elevated Ca^{2+} and then ameliorated by supplementation with Mn^{2+} in a fashion that depended on the SPCA known as Pmr1 (Potelle *et al.* 2016). Furthermore, when heterologously expressed in bacteria, Gdt1 has been demonstrated to transport Mn^{2+}, though it exhibited a lower affinity for Mn^{2+} than for Ca^{2+} (Thines *et al.* 2018). Presumably, the mechanism of Mn^{2+} transport by Gdt1 is similar to that of Ca^{2+}, which has been demonstrated to be coupled to the pH gradient established by the V-ATPase, the deletion of which causes Gdt1 to function in reverse-mode, instead releasing Ca^{2+} from Golgi lumen (Snyder *et al.* 2017). Transport studies using the purified and reconstituted TMEM165-family proteins will be necessary to ascertain their specific substrate specificities.

In summary, the findings reported here support the hypothesis that TMEM165 exchanges H^+, Mn^{2+}, and Ca^{2+} in the Golgi complex of professional secretory cells and thereby supports glycosyltransferases such as lactose synthase that may be sensitive to H^+ and dependent on Mn^{2+}. The extremely high rates of lactose synthesis could generate H^+ as a byproduct, and thus drive Mn^{2+} and Ca^{2+} uptake into the Golgi via TMEM165. Imbalanced ion homeostasis in TMEM165-deficient cells leads to defects in lactose biosynthesis through increased inhibition or decreased activation of lactose synthase.

MATERIALS AND METHODS

Knockout Mice and Animal Care

Procedures relating to animal care and treatment conformed to Johns Hopkins University Animal Care and Use Committee (ACUC), National Animal Disease Center ACUC, and NIH guidelines. Mice, maintained in a C57BL/6 or mixed C57BL/6 and 129P background, were housed in a standard 12:12 light-dark cycle. Embryonic stem cells (129/SvEv Tac) were transfected with 30 μg of the TMEM165 Knockout First targeting vector (PATHP0001_A_1_B01) from EUCOMM. After insertion of the complete targeting vector was confirmed by PCR of both homology arms, karyotypically normal clones were subjected to blastocyst injection and implantation into pseudopregnant females. The integration of the 5'-homology arm was confirmed using the forward primer 5'-GTGGTGATCAAAGGACACCGTGTGG-3' and the reverse primer 5'-TGTTAGTCCCAACCCCTTCCTCC-3', producing a 5,233 bp band, while the integration of the 3'-homology arm was confirmed using the forward primer 5'-CAACA GCAAGTGGTTTCAGGG-3' and the reverse primer 5'-CTCTGGTCTTGATATAGAC GTGGTCC-3' to produce a 5,177 bp band. The resultant chimeric mice were crossed to C57BL/6 wild-type mice and screened for germ-line transmission of the Knockout First allele by PCR of the resultant progeny, using the forward primer 5'-GTACCGCGTCGA GAAGTTCC-3' and the reverse primer 5'-GATAGCCTAAGCTCGTGTTACAATC-3' to produce a 303 bp band. The wild-type allele was identified by a separate PCR using the same reverse primer but a new forward primer, 5'CCCTGGATTCTACTTAGTCCCC C-3' which produced a 362 bp band.

ROSA-Flp mice were a gift from Dr. Rejji Kuruvilla (Johns Hopkins University). Mice containing the *ROSA-Flp* allele were identified by PCR, using the forward primer 5'-CACTGATATTGTAAGTAGTTTGC-3' and the reverse primer 5'CTAGTGCGAAG

TAGTGATCAGG-3'. These mice were crossed to the mouse containing the Knockout First allele to remove the portions of the cassette contained within the two Frt sites. This resulted in removal of all modifications except the two loxP sites flanking Exon 2 of *TMEM165*. Backcrossing was then conducted to generate mice that tested positive for the floxed allele of *TMEM165*, but not the *ROSA-Flp* allele. Mice were genotyped for the floxed allele of *TMEM165* by PCR using the forward primer, 5'AACTTTGGGGAGGCC AGTTAAG-3' and the reverse primer 5'GATAGCCTAAGCTCGTGTTACAATC-3'. Using these primers, the floxed allele of *TMEM165* produces a 635 bp band while the unfloxed allele produces a 541 bp band. The founder $TMEM165^{fl/+}$ mice were back-crossed multiple times to C57BL/6 and then inbred to generate $TMEM165^{fl/fl}$ before breeding to C57BL/6 bearing WAP-Cre, which were a gift from Dr. Zhe Li (Harvard). WAP-Cre $TMEM165^{fl/+}$ males were bred to $TMEM165^{fl/+}$ and $TMEM165^{fl/fl}$ females and the resulting females were used in experiments.

For experimentation, females bearing WAP-Cre and either $TMEM165^{fl/fl}$, $TMEM165^{fl/+}$, *or* $TMEM165^{+/+}$ were bred, respectively, to males bearing $TMEM165^{+/+}$, $TMEM165^{fl/+}$, *or* $TMEM165^{fl/fl}$ and the resulting litters were equalized to 6 pups per mouse mother on day one of lactation. This breeding program maximized uniformity among the nursing pups. Mice were euthanized at 12 days postpartum for tissue collection, using a 50:50 mix of CO_2:O_2 followed by cervical dislocation. Mammary tissue was removed, flash frozen in liquid nitrogen, and stored at -80°C until membranes were prepared. Some tissue was fixed as described below for microscopy.

Litter Weight Analysis

On the day of birth, litters were adjusted to 6 pups per nursing mother. The litters were then weighed every two days for the first 14 days of lactation.

Histological, Immunofluorescent, and TUNEL Stain Microscopy

Tissue slides were prepared as described previously (Cross *et al.* 2013). Briefly, mammary tissue fixed in Tellyesniczky's fixative (a 20:2:1 ratio of 70% ethanol, formalin, and glacial acetic acid) for 5 hours before being stored in 70% ethanol before paraffin embedding and creation of 4 μm sections. For histological analysis, paraffin-embedded sections were treated with eosin and hematoxylin stain as described in Sheehan and Hrapchak (Sheehan and Hrapchak 1980). Images were obtained using a Leica Aperio AT2 at 20X magnification. For immunofluorescence, methods were conducted as described previously (Reinhardt *et al.* 2014). Briefly, tissue sections were immersed in H-3300 (Vector Laboratories; Burlingame, CA) in a preheated pressure cooker for 20 minutes after pressure normalized. The sections were cooled and washed three times with distilled, deionized water, followed by PBS for 5 minutes. Sections were permeabilized and blocked in PBS containing 0.5% Triton X-100, 0.01 g sodium azide and 50 mg/ml BSA prior to addition of primary antibodies at 4°C overnight. The primary antibodies used were anti-TMEM165-aminoterminal end (Abcam, Cambridge, MA) and anti-GM130 #610822 (BD Transduction Laboratories, San Jose, CA). The sections were washed 3 times with blocking buffer before incubating at 37°C for 2 hours with secondary antibodies, Green antimouse Alexa Fluor A11017 488 F(ab')2 fragment of goat antimouse IgG (H + L), and Red anti-rabbit Alexa Fluor A11070 594 F(ab')2

fragment of goat anti-rabbit IgG (H + L) (Molecular Probes/Life Technologies, Grand Island, NY). Slides were again washed 3 times with blocking buffer and mounted with VectaShield (Vector Laboratories) and DAPI. Finally, TUNEL staining was conducted using the *In Situ* Cell Death Detection Kit, TMR Red (Catalog #12156792910) from Roche (Basel, Switzerland), according to kit instructions. All confocal microscopic analysis was conducted using a Nikon A1+ confocal scanning microscope with 2 GaAsP multi-detector and 2 normal PMTs, utilizing NIS-Elements C imaging software (Nikon, Tokyo, Japan). TUNEL stain images captured using the 561 nm laser and GaAsP detector unit, collecting emissions from 570-620 nm.

Milk Analysis for Lactose, Creamatocrit, and Total Protein

Milk collection was done as described previously (Reinhardt *et al.* 2004). Briefly, on day 12 of lactation, mothers were separated from their size-normalized litters for 4 hours to allow them to produce sufficient milk for collection. The mothers were then anesthetized with avertin prior to being given an intraperitoneal injection of 0.1 IU of oxytocin. After 10 minutes, milk was collected in a 1.5 mL microcentrifuge tube connected by small tubing to a low vacuum that was pulsed. After collection, the pups were returned to their mother. The milk that was collected was centrifuged for 5 minutes at 4000g, and the floating fat layer was removed. The remaining skimmed milk was frozen and stored at -80°C for future analysis. The concentration of lactose in the skimmed milk was determined using the Enzychrom Lactose Assay Kit (ELAC-100) from Bioassay Systems, using the defined protocol from the kit. The concentration of

protein in the skimmed milk was determined with a Bradford assay, using the Coomassie Plus (Bradford) Assay Reagent from Pierce, according to kit instructions.

Determination of Metal Composition by ICP-MS

A 125 µL aliquot of skimmed milk was prepared for metal composition analysis by conducting acid digestion in 300 mm long Pyrex digestion tubes using 5 mL of concentrated (70%) HNO3 and 2 mL of 30% H2O2 as a catalyst. Digestion was conducted by gradually heating the samples to 150°C in a heat block, and allowing the reaction to go to completion (sample became clear and colorless). The samples were then allowed to cool to room temperature before normalizing the volume and adjusting the final HNO3 concentration to 6%. The samples were stored in 15 mL metal-free polypropylene tubes from VWR until the compositions of the identified metals were analyzed using an Agilent 7700x inductively coupled plasma mass spectrometer (Agilent Technologies, Santa Clara, CA). Detection of metals was completed using an octopole reaction system (ORS) cell in He mode to remove interference. The parameters utilized included a radio frequency (RF) power of 1,550 W, an argon carrier gas flow of 1.01 L/min, an argon make-up gas flow of 0.1 L/min, a helium gas flow of 4.3 mL/min, an octopole RF of 200V, and an OctP bias of 18V. Samples were infused using the model 7700X peristaltic pump with a speed of 0.1 rotations per second and micromist nebulizer. Metal concentrations were derived from a calibration curve generated from a dilution series of the atomic absorption standards of each metal (Fluka Analytical, St. Louis, MO), prepared in the same matrix as the samples. Data analysis was performed using Agilent's Mass Hunter software.

Galactosyltransferase Activity Assay

Mammary tissue collected from sacrificed mothers on day 12 of lactation was homogenized by 25 passes with dounce A in 5 mL of a buffer containing 25 mM Tris, 150 mM NaCl, 1% Triton X-100, and 2 mM EDTA at pH 7.5 with a protease inhibitor cocktail (Roche, Basel, Switzerland). The homogenate was transferred to a 15 mL conical tube and centrifuged at 3000g for 10 minutes to remove cellular debris. The supernatant was then centrifuged in a 10kDa filtration tube at 3000g to remove small molecule substrates and products as well as the EDTA. A total of 50 mL of 25 mM Tris-citrate buffer containing 150 mM NaCl, 1% Triton X-100, 5 mM $MgCl_2$, and 5 mM $MnCl_2$, pH 7.5 with a protease inhibitor cocktail (Roche, Basel, Switzerland) was added to the samples over multiple spins in the filtration tube. The samples were then removed from the filtration tube, and appropriately diluted to normalize the total protein concentration, as determined a Bradford assay. The samples were then aliquoted, and the pH was adjusted in individual aliquots by addition of citrate buffer. The volumes were normalized using Tris-citrate buffer that was previously adjusted to the appropriate pH. Samples were then assayed by the methods described in Wu, *et al.* (2011) except UDPase was not added because the samples already expressed excess UDPase activity. Briefly, samples were transferred to a 96-well plate in 25 µL aliquots. Substrates were then added to achieve a final concentration of 1 mM UDP-galactose and 20 mM GlcNAc. Controls had UDP-galactose alone or neither substrate. After 30 minutes, the concentration of free phosphate was determined, using the Malachite Green Phosphate Detection Kit from Cell Signaling Technologies, according to kit instructions.

Gel Electrophoresis and Western Blotting

Mammary gland microsomes were prepared as previously described (Reinhardt *et al.* 2004). Briefly, the tissue was homogenized in 10 volumes of Buffer A (10 mM Tris-HCl, 2 mM $MgCl_2$, 1 mM EDTA and protease inhibitor cocktail (Roche, Basel, Switzerland), pH 7.5). The homogenate was mixed with an equal volume of Buffer B (Buffer A containing 0.3 M KCl) and centrifuged at 10,000g for 10 min. The supernatant was collected, adjusted to 0.7 M KCl by the addition of solid KCl, before centrifugation at 100,000g for 1 h. The supernatant was discarded, and the pellets were resuspended in Buffer C (Buffer A containing 0.15 M KCl). Protein concentrations were determined using the Bio-Rad Protein Assay kit using a bovine serum albumin standard, and buffer was added accordingly to normalize concentration of protein across samples. Equal volumes of microsomes and 2X SDS sample buffer (0.1 M Tris-HCl, pH 6.8, 4% SDS, 0.2% bromophenol blue, 20% glycerol, 2% BME) were combined, and the samples were incubated at room temperature for 30 minutes. Proteins were processed by separation on a 10% SDS/PAGE gel and western blotting, as described previously (Mehta *et al.* 2009). Blots were probed with anti-TMEM165 polyclonal antibodies from rabbit at 1:5,000 dilution (Sigma, HPA038299). Protein standards were probed with anti-α-tubulin polyclonal antibodies from mouse at 1:10,000 dilution (Sigma).

Statistical tests of significance

Student's t-tests were implemented on many datasets, as indicated in the figures (* $P < 0.05$, * $P < 0.01$, *** $P < 0.001$).

REFERENCES

Aoki, T., Yamada, N., Tomita, I., Kako, Y., and Imamura, T., 1987. Caseins are cross-linked through their ester phosphate groups by colloidal calcium phosphate. *Biochimica Et Biophysica Acta - Protein Struct. Mol. Enzym.* 911: 238–243.

Axelsson, M., Karlsson, N. G., Steel, D. M., Ouwendijk, J., Nilsson, T., and Hansson, G. C., 2001. Neutralization of pH in the Golgi apparatus causes redistribution of glycosyltransferases and changes in the O-glycosylation of mucins. *Glycobiology* 11: 633–644.

Bammens, R., Mehta, N., Race, V., Foulquier, F., Jaeken, J., Tiemeyer, M., Steel, R., Matthijs, G., and Flanagan-Steel, H., 2015. Abnormal cartilage development and altered N-glycosylation in Tmem165-deficient zebrafish mirrors the phenotypes associated with TMEM165-CDG. *Glycobiology* 25: 669–682.

Berliner, L. J., and Robinson, R. D., 1982. Structure-function relationships in lactose synthase. Structural requirements of the UDP-galactose binding site. *Biochemistry* 21: 6340–6343.

Colinet, A. S., Sengottaiyan, P., Deschamps, A., Colsoul, M. L., Thines, L., Demaegd, D., Duchene, M. C., Foulquier, F., Hols, P., and Morsomme, P., 2016. Yeast Gdt1 is a Golgi-localized calcium transporter required for stress-induced calcium signaling and protein glycosylation. *Sci. Rep.* 6: 24282.

Cross, B. M., Hack, A., Reinhardt, T. A., and Rao, R., 2013. SPCA2 regulates Orai1 trafficking and store independent Ca^{2+} entry in a model of lactation. *PLoS One* 8: e67348.

Dürr, G., Strayle, J., Plemper, R., Elbs, S., Klee, S. K., Catty, P., Wolf, D. H., and Rudolph, H. K., 1998. The medial-Golgi ion pump Pmr1 supplies the yeast secretory pathway with Ca^{2+} and Mn^{2+} required for glycosylation, sorting, and endoplasmic reticulum-associated protein degradation. *Mol. Biol. Cell* 9: 1149–1162.

Foulquier, F., Amyere, M., Jaeken, J., Zeevaert, R., Schollen, E., Race, V., Bammens, R., Morelle, W., Rosnoblet, C., Legrand, D., Demaegd, D., Buist, N., Cheillan, D., Guffon, N., Morsomme, P., Annaert, W., Freeze, H. H., Van Schaftingen, E., Vikkula, M., and Matthijs, G., 2012. TMEM165 deficiency causes a congenital disorder of glycosylation. *Am. J. Hum. Genetics* 91: 15–26.

Fraser, I., and Mookerjea, S., 1976. Studies on the purification and properties of UDP-galactose glycoprotein galactosyltransferase from rat liver and serum. *Biochem. J.* 156: 347–355.

Holt, C., 1983. Swelling of Golgi vesicles in mammary secretory cells and its relation to the yield and quantitative composition of milk. *J. Theor. Biol.* 101: 247–261.

Kaufman, R. J., Swaroop, M., and Murtha-Riel, P., 1994. Depletion of manganese within the secretory pathway inhibits O-linked glycosylation in mammalian cells. *Biochemistry* 33: 9813–9819.

Kornak, U., Reynders, E., Dimopoulou, A., van Reeuwijk, J., Fischer, B., Rajab, A., Budde, B., Nürnberg, P., Foulquier, F., ARCL Debré-type Study Group, Lefeber, D., Urban, Z., Gruenewald, S., Annaert, W., Brunner, H. G., van Bokhoven, H., Wevers, R., Morava, E., Matthijs, G., Van Maldergem, L., and Mundlos, S., 2007.

Impaired glycosylation and cutis laxa caused by mutations in the vesicular H^+-ATPase subunit ATP6V0A2. *Nat. Genet.* 40: 32-4.

Lapinskas, P. J., Cunningham, K. W., Liu, X. F., Fink, G. R., and Culotta, V. C., 1995. Mutations in PMR1 suppress oxidative damage in yeast cells lacking superoxide dismutase. *Mol. Cell Biol.* 15: 1382–1388.

Mehta, S., Li, H., Hogan, P. G., and Cunningham, K. W., 2009. Domain architecture of the regulators of calcineurin (RCANs) and identification of a divergent RCAN in yeast. *Mol. Cell Biol.* 29: 2777–2793.

Ng, B. G., and Freeze, H. H., 2018. Perspectives on glycosylation and its congenital disorders. *Trends Genet.* 34: 466–476.

Park, J. H., Hogrebe, M., Grüneberg, M., DuChesne, I., von der Heiden, A. L., Reunert, J., Schlingmann, K. P., Boycott, K. M., Beaulieu, C. L., Mhanni, A. A., Innes, A. M., Hörtnagel, K., Biskup, S., Gleixner, E. M., Kurlemann, G., Fiedler, B., Omran, H., Rutsch, F., Wada, Y., Tsiakas, K., Santer, R., Nebert, N. W., Rust, S., and Marquardt, T., 2015. SLC39A8 deficiency: A disorder of manganese transport and glycosylation. *Cell Press* 97: 894-903.

Potelle, S., Morelle, W., Dulary, E., Duvet, S., Vicogne, D., Spriet, C., Krzewinski-Recchi, M. A., Morsomme, P., Jaeken, J., Matthijs, G., De Bettignies, G., and Foulquier, F., 2016. Glycosylation abnormalities in Gdt1p/TMEM165 deficient cells result from a defect in Golgi manganese homeostasis. *Hum. Mol. Genet.* 25: 1489–1500.

Powell, J., and Brew, K., 1976. Metal ion activation of galactosyltransferase. *J. Biol. Chem.* 251: 3645–52.

Reinhardt, T. A., Filoteo, A. G., Penniston, J. T., and Horst, R. L., 2000. Ca^{2+}-ATPase protein expression in mammary tissue. *Am. J. Physiol. Cell Physiol.* 279: C1595–C1602.

Reinhardt, T. A., Lippolis, J. D., Shull, G. E., and Horst, R. L., 2004. Null mutation in the gene encoding plasma membrane Ca^{2+}-ATPase isoform 2 impairs calcium transport into milk. *J. Biol. Chem.* 279: 42369–42373.

Reinhardt, T. A., Lippolis, J. D., and Sacco, R. E., 2014. The Ca^{2+}/H^{+} antiporter TMEM165 expression, localization in the developing, lactating and involuting mammary gland parallels the secretory pathway Ca^{2+} ATPase (SPCA1). *Biochem. Bioph. Res. Comm.* 445: 417–421.

Rosnoblet, C., Legrand, D., Demaegd, D., Hacine-Gherbi, H., de Bettignies, G., Bammens, R., Borrego, C., Duvet, S., Morsomme, P., Matthijs, G., and Foulquier, F., 2013. Impact of disease-causing mutations on TMEM165 subcellular localization, a recently identified protein involved in CDG-II. *Hum. Mol. Genet.* 22: 2914–2928.

Sheehan, D. C., and Hrapchak, B. B., 1980. *Theory and Practice of Histotechnology,* 2nd Ed.; The C.V. Mosby Company, St. Louis, MO.

Snyder, N. A., Stefan, C. P., Soroudi, C. T., Kim, A., Evangelista, C., and Cunningham, K. W., 2017. H^{+} and Pi byproducts of glycosylation affect Ca^{2+} homeostasis and are retrieved from the Golgi complex by homologs of TMEM165 and XPR1. *G3* 7: 3913–3924.

Stacey, A., Schnieke, A., Kerr, M., Scott, A., McKee, C., Cottingham, I., Binas, B., Wilde, C., and Colman, A., 1995. Lactation is disrupted by α-lactalbumin

deficiency and can be restored by human α-lactalbumin gene replacement in mice. *Proc. Natl. Acad. Sci.* 92: 2835–2839.

Stein, T., Morris, J. S., Davies, C. R., Weber-Hall, S. J., Duffy, M, Heath, V. J., Bell, A. K., Ferrier, R. K., Sandilands, G. P., and Gusterson, B. A., 2003. Involution of the mouse mammary gland is associated with an immune cascade and an acute-phase response, involving LBP, CD14 and STAT3. *Breast Cancer Res.* 6: R75-R91.

Stinnakre, M., Vilotte, J., Soulier, S., and Mercier, J., 1994. Creation and phenotypic analysis of α-lactalbumin-deficient mice. *Proc. Natl. Acad. Sci.* 91: 6544–6548.

Thines, L., Deschamps, A., Sengottaiyan, P., Savel, O., Stribny, J., and Morsomme, P., 2018. The yeast protein Gdt1p transports Mn^{2+} ions and thereby regulates manganese homeostasis in the Golgi. *J. Biol. Chem.* 293: 8048–8055.

Ton, V. K., Mandal, D., Vahadji, C., and Rao, R., 2002. Functional expression in yeast of the human secretory pathway Ca^{2+}, Mn^{2+}-ATPase defective in Hailey-Hailey disease. *J. Biol. Chem.* 277: 6422–6427.

Wagner, K.U., Wall, R.J., St-Onge, L., Gruss, P., Wynshaw-Boris, A., Garrett, L., Li, M., Furth, P. A., and Hennighausen, L., 1997. Cre-mediated gene deletion in the mammary gland. *Nucleic Acids Res.* 25: 4323–4330.

Wu, Z. L., Ethen, C. M., Prather, B., Machacek, M., and Jiang, W., 2011. Universal phosphatase-coupled glycosyltransferase assay. *Glycobiology* 21: 727–733.

Xiang, M., Mohamalawari, D., and Rao, R., 2005. A novel isoform of the secretory pathway Ca^{2+}, Mn^{2+}-ATPase, hSPCA2, has unusual properties and is expressed in the brain. *J. Biol. Chem.* 280: 11608–11614.

CHAPTER 4

AUXIN-INDUCIBLE DEPLETION OF THE ESSENTIALOME REVEALS INHIBITION OF TORC1 BY AUXINS AND INHIBITION OF VRG4 BY SDZ 90-215, A NATURAL ANTIFUNGAL CYCLOPEPTIDE

Outside contributions:

Adam Kim and Louis Kester generated the collection of AID-tagged yeast, and established preliminary methods for inducing and interpreting AID-dependent protein degradation. The cyclopeptolide SDZ 90-215 was provided by Novartis, courtesy of Christian Studer, Dominic Hoepfner, Silvio Roggo, and Stephen B. Helliwell.

ABSTRACT

Gene knockout and knockdown strategies have been immensely successful probes of gene function, but small molecule inhibitors (SMIs) of gene products allow much greater time resolution and are particularly useful when the targets are essential for cell replication or survival. SMIs also serve as lead compounds for drug discovery. However, discovery of selective SMIs is costly and inefficient. The action of SMIs can be modeled simply by tagging gene products with an auxin-inducible degron (AID) that triggers rapid ubiquitylation and proteasomal degradation of the tagged protein upon exposure of live cells to auxin. To determine the broad effectiveness of this approach, we AID-tagged over 750 essential proteins in *Saccharomyces cerevisiae* and observed over 66% efficiency of growth inhibition by low concentrations of auxin. Polytopic transmembrane proteins in the plasma membrane, Golgi complex, and endoplasmic reticulum were efficiently depleted if the AID-tag was exposed to cytoplasmic OsTIR1 ubiquitin ligase. The auxin analog 1-napthylacetic acid (NAA) was less potent than auxin on AID-tags and, surprisingly, both molecules inhibited TORC1 signaling at high concentrations. Auxin also synergized with known SMIs when acting on the same essential protein, indicating that AID-tagged strains can be useful for SMI screening. A natural cyclic peptide of unknown function (SDZ 90-215) was found to inhibit an essential GMP/GDP-mannose exchanger in the Golgi complex (Vrg4) as determined by auxin synergy, glycosylation assays, and resistance mutations. These findings suggest that AID-tagging can efficiently model the action of SMIs before they are discovered and facilitate their discovery.

INTRODUCTION

One of the most powerful approaches for experimental determination of gene function involves the identification of phenotypes that appear in the cells of interest upon introduction of mutations that decrease function. Such loss-of-function mutations can be produced easily in many eukaryotic cell types using CRISPR/Cas9-based technologies and earlier methods involving homologous recombination, insertional mutagenesis, and random mutagenesis have been very useful in a wide variety of model organisms. Nearly complete arrays of gene knockout mutants have been produced in budding yeast *Saccharomyces cerevisiae* (Winzeler *et al.*, 1999) and the fission yeast *Schizosaccharomyces pombe* (Kim *et al.*, 2010), with several additional species of pathogenic fungi currently in progress (Roemer *et al.*, 2003; Schwarzmuller *et al.*, 2014; Liu *et al.*, 2008). Though such collections offer enormous potential for understanding diverse biological processes, the general approach is hampered by the inability to knockout essential genes, which typically constitute 10-20% of the genome. Most essential genes in *S. cerevisiae* were successfully rendered hypomorphic by introducing knockout mutations in heterozygous diploids or by introducing mutations in the 3' untranslated regions of haploids (Breslow *et al.*, 2008). However, in all these cases the cells are studied long after the mutation was created and therefore discriminating primary defects from secondary adaptations is very challenging. In addition to such epigenetic effects, secondary mutations often arise that compensate for or obscure the phenotypes of primary mutations (Teng *et al.*, 2013).

Conditional knockout or knockdown of gene function can eliminate some of the major limitations of the unconditional gene knockouts described above. In *S. cerevisiae*,

about 75% of essential genes have been mutated in such a way to render the protein product non-functional at high temperature but functional at low temperature (Ben-Aroya *et al.,* 2008; Li *et al.*, 2011). Such temperature-sensitive mutations allow easy and often reversible inactivation of gene function, but are relatively difficult to produce and often difficult to interpret because the level of gene function may be abnormal even at the permissive temperature and incompletely or slowly inactivated at the non-permissive temperature, and it can be difficult to ascertain these problems. Additionally, the temperature shifts themselves may cause undesirable biological consequences that could confound interpretations. Alternatively, essential genes can be placed under control of regulatory systems that enable tight shut-off of gene transcription (for example, glucose-, methionine-, and tetracycline-repressible promoters), which allows phenotypic analyses as the mRNA and protein products decay at their natural rates (Roemer *et al.,* 2003). CRISPRi using dCas9 can achieve similar repression without altering gene sequences (Qi *et al.*, 2013). Other approaches enable ligand-responsive de-capping, de-tailing, or translational frameshifting of targeted mRNAs (Klauser *et al.,* 2015; Anzalone *et al.*, 2016). These mRNA knockdown approaches may be combined for improved performance, but still the long cellular lifespans of many proteins will delay the appearance of phenotypes.

Several approaches have enabled rapid conditional destruction or mislocalization of targeted proteins. One approach involves N-terminal tagging of the proteins of interest with a temperature-sensitive degron that enables misfolding, ubiquitylation, and degradation of the fusion protein by the 26S proteasome (Dohmen and Varshavsky, 2005). The tag itself allows quantitation of the rate and extent of protein destruction, but

also may interfere to some extent with protein function even under the permissive condition. Similarly, C-terminal tagging of proteins with the auxin-inducible degron (AID) sequence from plants can enable rapid ubiquitylation and proteasomal degradation of the protein upon addition of a small molecule auxin (indole-3-acetic acid) (Nishimura *et al.*, 2009; Morawska and Ulrich, 2013). This latter approach requires co-expression of an E3 ubiquitin ligase from plants such as OsTir1 that recognizes AID-tagged proteins bound to auxin. Though the AID-tagging and destruction system works very well in plant, animal, and fungal cell types and shows great promise for functional genomics research, it has not yet been implemented genome-wide and its limitations are not fully known.

In this study, we AID-tag the C-termini of 758 essential and 313 non-essential gene products of *S. cerevisiae* and simultaneously introduce the OsTIR1 expression cassette together with a selectable marker. The effects of auxin and a non-metabolizable auxin analog (1-naphthaleneacetic acid; NAA) on cell growth were analyzed carefully. Surprisingly, we find that auxin and especially NAA both have off-target inhibitory effects on the TORC1 protein kinase. At low concentrations, auxin was highly specific for on-target AID-tagged proteins that have C-termini were exposed to the cytoplasm or nucleoplasm, including many transmembrane proteins of endoplasmic reticulum, Golgi complex, plasma membrane, and mitochondrial outer membrane. We then explore the possibility that auxins synergize with other small molecules that are known to bind and inhibit particular target proteins. Finally, we show that SDZ 90-215, a potent antifungal cyclopeptide produced naturally by the filamentous fungus *Septoria*, synergizes with auxins in *VRG4-AID* strains but not control strains and that amino acid substitutions

within the substrate-binding pocked of Vrg4 protein confer strong resistance to the compound. These findings validate the use of AID-tagged strains for functional genomics research and for discovery of novel SMIs and antifungals.

RESULTS

High concentrations of auxin and NAA can inhibit TORC1 signaling in S. cerevisiae.

To study the effectiveness of AID-tagging as a tool for functional genomics, we first converted the C-terminal TAP-tags (Ghaemmaghami *et al.,* 2003) on 758 essential genes and 313 non-essential genes of *S. cerevisiae* into AID-tags using a one-step gene replacement strategy (Figure 4.1A). Briefly, the stop codon, transcription terminator, and *HIS3* selectable marker in each TAP-tagged strain was replaced with a short spacer, a minimal AID-tag, a 6xFLAG-tag with stop codon, a transcription terminator, an OsTIR1 expression cassette, and a *URA3* selectable marker. Each AID-tagged strain was purified, validated, arrayed in 96-well dishes, and stored frozen until use. To determine sensitivity to auxin and NAA, the arrayed collection was grown overnight at room temperature in SCD medium containing 0, 25, 100, or 400 μM auxin or 100 μM NAA (a non-metabolizable auxin analog) and the optical density was quantified in a microplate reader at 650 nm after 20 hr and 40 hr incubation at room temperature. At 25 μM auxin, growth was significantly inhibited in approximately 66% of essential and 16% of non-essential AID-tagged proteins relative to 0 μM auxin (Figure 4.1B), and these percentages increased slightly as auxin was increased to 100 or 400 μM or when instead 100 μM NAA was used (Figure 4.1C). This finding suggests that 25 μM auxin was sufficient to

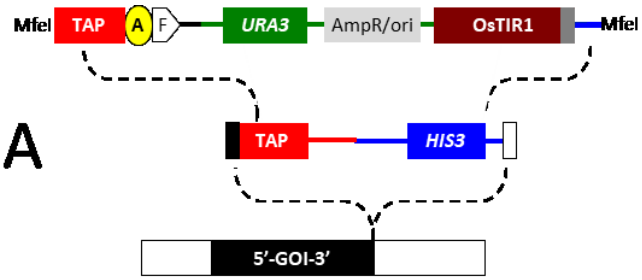
MfeI
TAP
A
F
URA3
AmpR/ori
OsTIR1
MfeI
A
TAP
HIS3
5'-GOI-3'

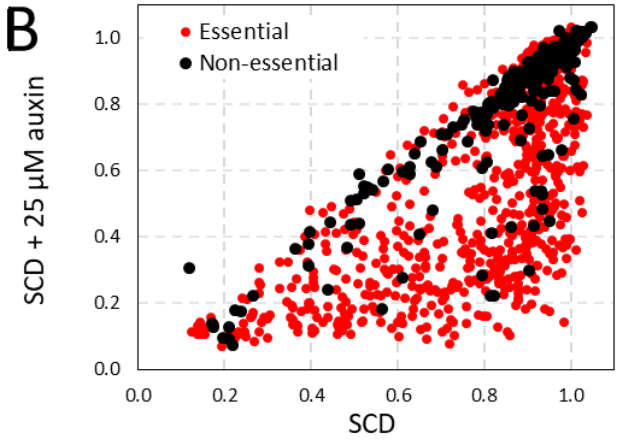
B
Essential
Non-essential
SCD + 25 µM auxin
SCD
0.0
0.2
0.4
0.6
0.8
1.0

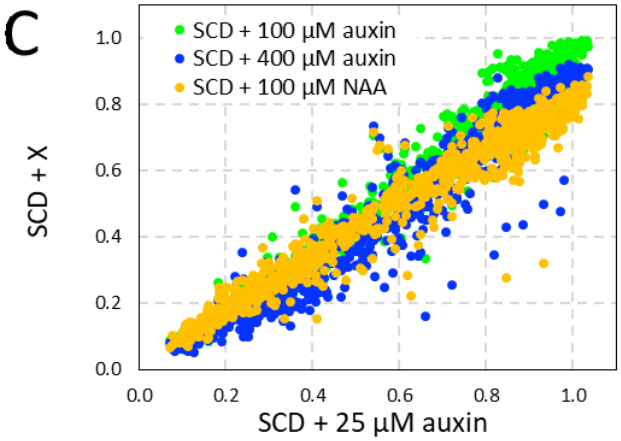
C
SCD + 100 µM auxin
SCD + 400 µM auxin
SCD + 100 µM NAA
SCD + X
SCD + 25 µM auxin
0.0
0.2
0.4
0.6
0.8
1.0

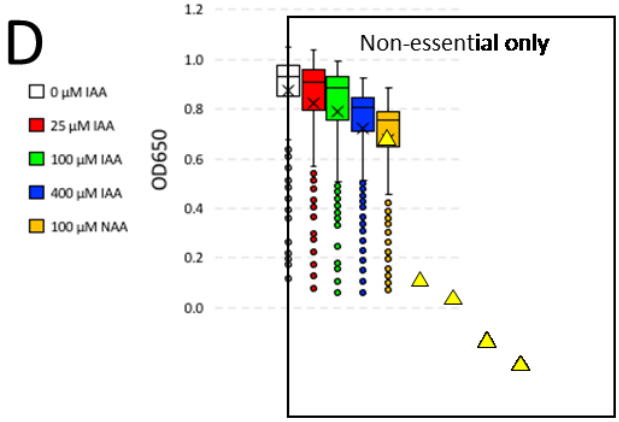
D
0 µM IAA
25 µM IAA
100 µM IAA
400 µM IAA
100 µM NAA
OD650
Non-essential only
0.0
0.2
0.4
0.6
0.8
1.0
1.2

Figure 4.1: AID-tagging and growth defects caused by auxin and NAA.

(A) Schematic of the MfeI-linearized pAIDA2(6FLAG) plasmid that was transformed into individual strains of *S. cerevisiae* with a TAP-tag already present in the gene of interest (GOI). The minimal AID-tag and 6xFLAG-tag are labeled "A" and "F" and the OsTIR1 expression cassette is also indicated. (B) Optical densities of 756 essential (red) and 315 non-essential (black) AID-tagged strains after diluting stationary phase 36-fold into fresh SCD medium with and without 25 μM auxin and incubating for 20 hr at 23°C. (C) Optical densities of AID-tagged strains after culturing in 100 or 400 μM auxin or 100 μM NAA as compared to 25 μM auxin. (D) Box plots of non-essential AID-tagged strains grown in different conditions (centerline = median, X = average, box = middle quartiles, whiskers = middle deciles, circles = outliers, triangles = *GTR1-AID* strain).

deplete most essential AID-tagged proteins and higher concentrations or analogs of auxin only rarely increased susceptibility.

By focusing first on just the non-essential AID-tagged proteins, we noticed that 25, 100, and 400 μM auxin progressively lowered the final cell density in the stationary phase cultures, with 100 μM NAA as the most toxic of all. After a 20 hr growth period, the median optical densities declined by 2, 5, 13, and 19% (Figure 4.1D). These declines persisted even after 40 hr growth period (data not shown). Similar declines were seen in the wild-type parental strain that lacked AID-tag and the OsTIR1 expression cassette, and yet there was no detectable change in its exponential growth rate in any of the conditions (data not shown). These findings confirm earlier results (Nishimura *et al.,* 2009; Morawska and Ulrich, 2013) that auxin and NAA have little effect on growth rate at these concentrations, and also suggest possible off-target effects can become significant as cultures approach the stationary phase.

To explore the possible off-target effects of auxin and NAA, we examined the median-normalized dataset for clear instances of selective toxicity to only the highest concentrations of auxin or to NAA. Four non-essential AID-tagged proteins (Gtr1, Gtr2, Ego1, Ego3) exhibited unusual hypersensitivity to 100 μM NAA and 400 μM auxin relative to 25 μM auxin, a pattern that was not observed elsewhere in the collection of AID-tagged strains. All four proteins bind to each other and function together as positive regulators of the rapamycin-sensitive protein kinase known as TORC1 (Loewith and Hall, 2011). A negative regulator of this GTR-EGO complex (Npr2) exhibited significant resistance to high auxin and NAA when AID-tagged. One potential explanation for these findings is that TORC1 itself can be inhibited by auxin and NAA,

and depletion of the GTR-EGO proteins thus causes hypersensitivity to inhibitors of TORC1. To test this idea, the sensitivities of *gtr1*Δ, *gtr2*Δ, *ego1*Δ, and *ego3*Δ knockout mutants to auxin and NAA were evaluated in growth assays spanning a large range of concentrations (Figure 4.2A). All four EGO-GTR-deficient knockout mutants exhibited strong hypersensitivity to auxin (3.7- to 4.7-fold) and NAA (8.6- to 10.5-fold) relative to the wild-type parent strain BY4741. These effects of auxin and NAA were similar to those of caffeine, a direct inhibitor of TORC1 activity (Reinke *et al.*, 2006). A single amino acid substitution (Tor1-S1954L) that hyperactivates TORC1 (Kim and Cunningham, 2015) largely reversed the hypersensitivity of *gtr1*Δ mutants to auxin, NAA, and caffeine in *gtr1*Δ strains to almost the same level as the strain expressing Gtr1 (Figure 4.2A). Auxin and NAA probably do not inhibit Pib2, an activator of TORC1 that operates independent of GTR-EGO (Kim and Cunningham, 2015; Michel *et al.*, 2017; Tanigawa and Maeda, 2017; Varlakhanova *et al.*, 2017), because the *pib2*Δ knockout mutants still exhibited mild hypersensitivity to auxin, NAA, as well as caffeine (Figure 4.2A) as expected for mildly reduced TORC1 activity. To test whether auxin and NAA can inhibit TORC1 function, the phosphorylation of two indirect targets of TORC1 (Rps6 and Par32) was measured by western blotting after 1 hr incubation of wild-type cells with these compounds. Auxin and NAA strongly decreased phosphorylation of Rps6 similar to caffeine and rapamycin (Figure 4.2B) as shown previously (Gonzalez *et al.*, 2015). Auxin increased phosphorylation of Par32-HA similar to caffeine and rapamycin as expected (Huber *et al.*, 2009) but NAA was seemingly less effective than auxin (Figure 4.2C). Collectively, these findings suggest that auxin and NAA can inhibit TORC1 itself or TORC1-dependent proliferation.

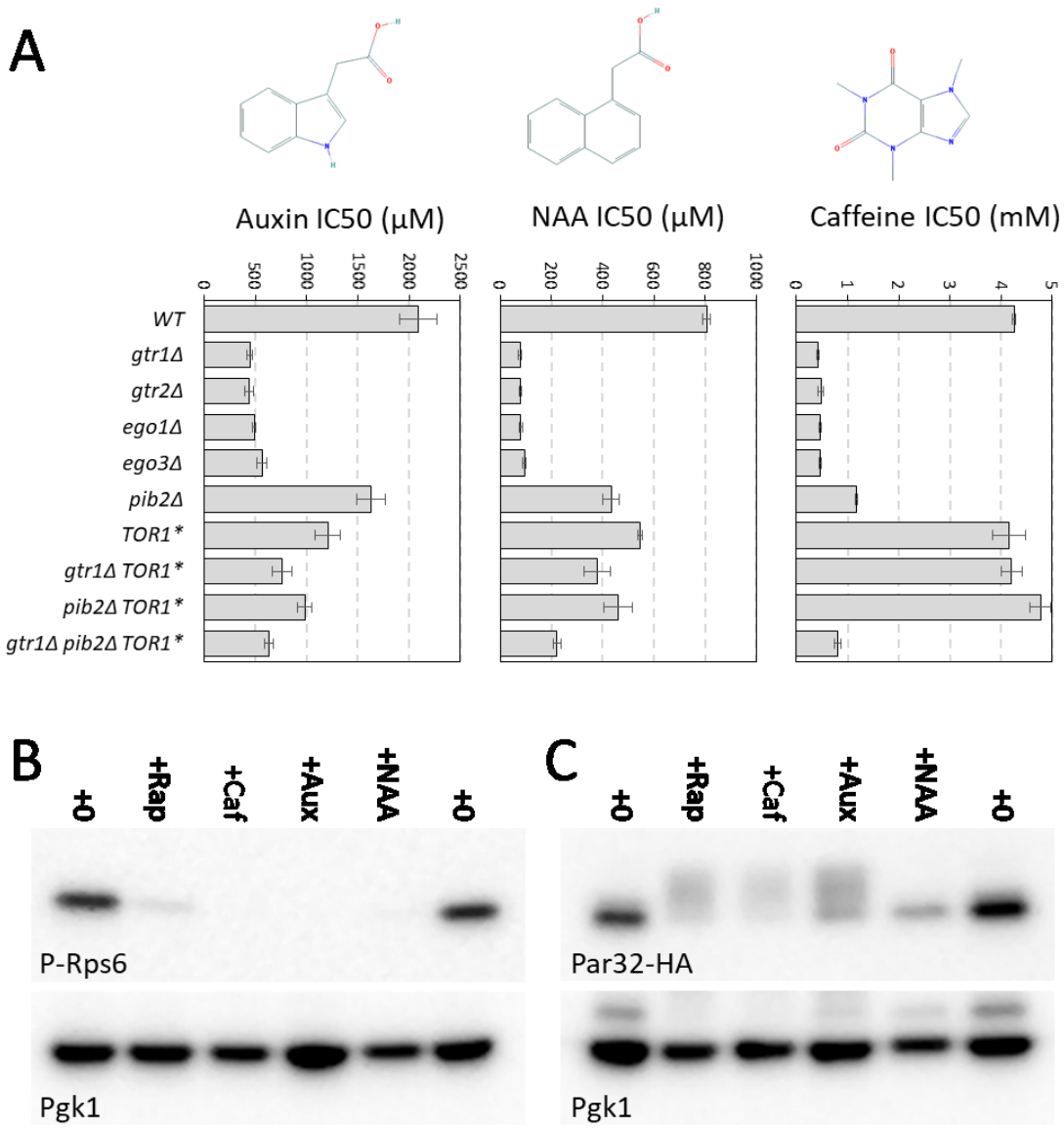

Figure 4.2: Auxin and NAA inhibit TORC1 signaling.

(A) The concentrations of auxin, NAA, and caffeine that cause 50% inhibition of growth (IC50) of the indicated strains in SCD medium are shown as bars (average ± SD of 3 biological replicates). Chemical structures are shown as insets. Crude cell lysates of a wild-type (B) and wild-type expressing Par32-3xHA from plasmid pMS034 [31] (C) strains were prepared from log-phase cultures that had been exposed for 1 hr to 0.2 µg/mL rapamycin, 8 mM caffeine, 4 mM auxin, or 1.6 mM NAA and analyzed by

western blotting using polyclonal antibodies that recognize phospho-eEF1B-□ (B) or monoclonal antibodies that recognize HA (C). Blots were stripped and re-exposed to antibodies recognizing Pgk1 as a measure of gel loading.

While off-target effects of auxin and NAA on TORC1 can explain why several non-essential AID-tagged proteins were susceptible to growth inhibition, 44 additional non-essential AID-tagged proteins exhibited growth inhibition at 25 μM auxin and there was little additional effect of higher concentrations and of NAA. Interestingly, many of these responders can be grouped by function and structure. For example, seven proteins required for biosynthesis of cysteine, serine, and threonine (Cys3, Cys4, Hom2, Hom3, Hom6, Ser2, Thr4) exhibited slow growth rate when AID-tagged and exposed to auxin even though these amino acids were present in SCD culture medium. Additionally, eight of eleven AID-tagged proteins that form the non-essential V-ATPase exhibited slow growth in low auxin. Last, the COG complex consists of three essential subunits (Cog2, Cog3, Cog4) and five non-essential subunits (Cog1, Cog5, Cog6, Cog7, Cog8), and surprisingly 25 μM auxin strongly inhibited growth of AID-tagged Cog1 and Cog8 in addition to Cog4 strains. These observations may reveal additional off-target effects of auxin and NAA that are independent of TORC1, or alternatively suggest the possibility of acute growth inhibition upon rapid depletion of specific non-essential proteins that lasts until compensatory adaptive processes become fully engaged.

When the AID-tag is sequestered within membrane-bound organelles, the tagged protein is expected to be inaccessible to the ubiquitin proteasome system and thus insensitive to auxin. Of 32 essential proteins with C-termini localized within mitochondria, only 2 AID-tagged strains (Tim50, Tim17) were significantly sensitive to low auxin. Of 16 essential proteins with C-termini localized within the lumens of the endoplasmic reticulum or Golgi complex, 5 strains (Brr6, Stt3, Cdc1, Tre2, Smx3) were sensitive to auxin when AID-tagged. The few exceptions may become susceptible to

depletion at some point during biogenesis before the C-terminus is sequestered, or may have incorrectly assigned topologies. When these 48 proteins are excluded, the overall susceptibility of essential proteins to depletion with auxin rose from 66% to 70%.

Interestingly, 42 out of 53 essential transmembrane proteins of the secretory pathway with C-termini facing the cytoplasm (79%) exhibited significant sensitivity to auxin after AID-tagging. This group includes polytopic transmembrane proteins that localize to the plasma membrane (Alr1, Pma1, Hip1), the Golgi complex (Vrg4, Kei1, Lsm8), the nuclear pore complex that spans the nuclear envelope (Nup192), in addition to the endoplasmic reticulum which contains numerous essential proteins that participate in biosynthesis of lipids and glycoproteins. Additionally, 3 essential proteins associated with the mitochondrial outer membrane and with C-termini exposed to the cytoplasm (Sen2, Sen54, Sam35) also conferred sensitivity to auxin when AID-tagged while 2 others (Tom20, Tom22) did not. Excluding the secretome and mitochondriome, we find 450 out of 652 (69%) of the remaining AID-tagged essential proteins exhibited significant sensitivity to auxin, a population that included proteins in the cytoplasm, nucleus, nucleolus, spindle pole body, as well as peripheral associations with the membrane-bound organelles listed earlier. These data show that auxin can frequently induce depletion of essential AID-tagged proteins to levels that become growth limiting as long as the tag is exposed to the cytoplasm or nucleoplasm. A minority of AID-tagged essential proteins did not exhibit growth inhibition by auxin in these conditions for unknown reasons.

TAP-tags and AID-tags can dampen protein expression and function

The effects of auxin on expression of several AID-tagged and TAP-tagged essential transmembrane proteins involved in sphingolipid biosynthesis (Figure 4.3A) were investigated by western blotting (Figures 4.3B and 4.3C). Surprisingly, in the absence of auxin, AID-tagging slightly, but reproducibly, diminished log-phase expression of Lcb1, Lcb2, Aur1, Kei1, and Vrg4 relative to the TAP-tagged parent strains. The addition of 100 μM auxin for 60 minutes strongly depleted the AID-tagged variants but not the TAP-tagged proteins. These findings suggest that AID-tags confer sensitivity to auxin even for transmembrane proteins in the endoplasmic reticulum (Lcb1, Lcb2) and Golgi complex (Aur1, Kei1, Vrg4) and can slightly dampen expression of the attached protein relative to the parental TAP-tags.

To investigate the degree of functional damping by AID-tags, we quantitatively measured the hypersensitivities of AID-tagged and TAP-tagged strains to known on-target inhibitors. Myriocin blocks the essential enzyme serine palmitoyltransferase that is composed of essential proteins Lcb1 and Lcb2 (Nagiec *et al.*, 1994) and *lcb1*Δ/+ and *lcb2*Δ/+ heterozygous diploid strains are more sensitive to myriocin than +/+ wild-type diploid strains in growth assays (Hillenmeyer *et al.,* 2008; Hoepfner *et al.*, 2014; Lee *et al.*, 2014). Interestingly, the concentration of myriocin that causes a 50% decrease in growth (the IC50) was diminished slightly (by 1.3- and 1.2-fold) in Lcb1-TAP and Lcb1-AID strains and diminished strongly (by 3.8- and 7.3- fold) in Lcb2-TAP and Lcb2-AID strains, respectively, relative to the wild-type parent strain (Figure 4.4A). Similarly, resistance to aureobasidin A was diminished moderately (by 1.4- and 2.6-fold) in Aur1-TAP and Aur1-AID strains and diminished very strongly (by 17- and 29-fold) in Kei1-TAP and Kei1-AID strains, respectively (Figure 4.4A). Aureobasidin A inhibits the

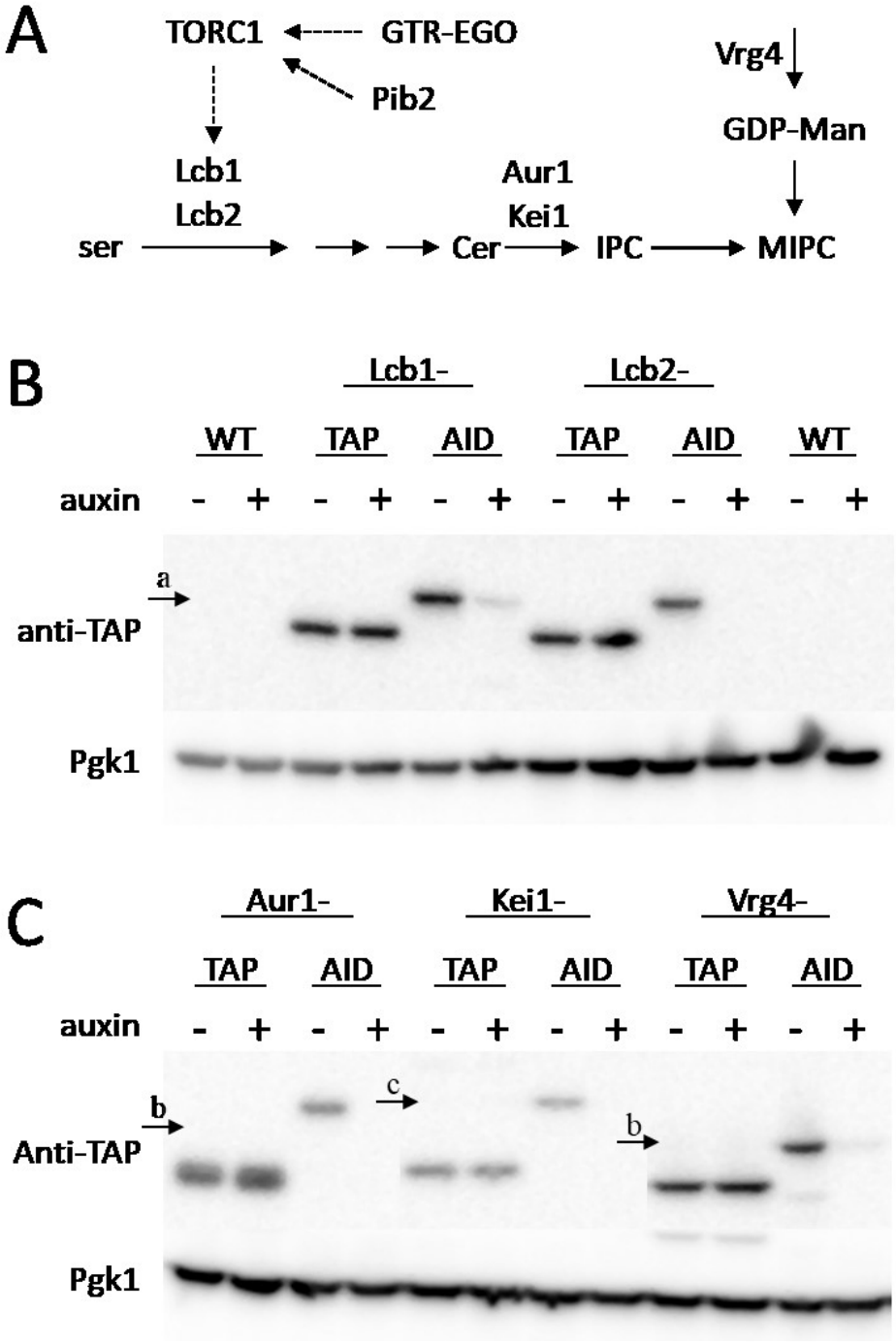

Figure 4.3: Transmembrane proteins involved in sphingolipid biosynthesis are susceptible to depletion.

(A) Schematic representation of sphingolipid biosynthesis pathway from serine (ser) to ceramide (Cer) to inositolphosphoryl-ceramide (IPC) to mannosyl-IPC (MIPC) from

luminal GDP-mannose is depicted along with proteins that catalyze the reactions and their regulators (TORC1, Pib2, GTR-EGO). (B,C) A polyclonal antibody that recognizes a common segment of TAP- and AID-tags was used in western blot analyses of the indicated strains that had been grown to log phase and exposed to 100 μM auxin for 1 hr as indicated.

Footnotes:

[a] Marks relative position of 100 kDa protein molecular weight marker

[b] Marks relative position of 75 kDa protein molecular weight marker

[c] Marks relative position of 50 kDa protein molecular weight marker

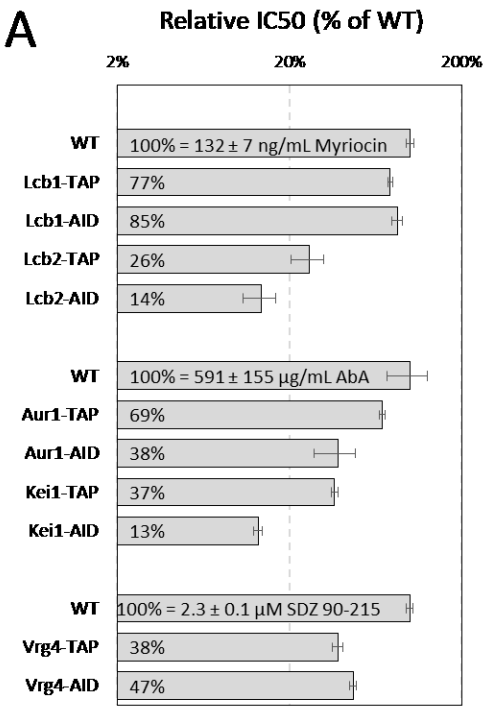

B

	Myr +Aux (CI)	AbA +Aux (CI)	SDZ 90-215 +Aux (CI)	Aux IC50 (µM)
Lcb1-AID	0.16	0.46	0.38	430.1
Lcb2-AID	0.83	1.51	1.01	0.3
Aur1-AID	1.11	0.43	0.48	12.0
Kei1-AID	1.22	0.82	0.72	1.3
Vrg4-AID	1.11	1.23	0.36	68.3

Figure 4.4: TAP- and AID-tagged become hypersensitive to on-target inhibitors that can synergize.

(A) Three replicate cultures of the indicated strains were diluted into fresh SCD medium containing varying concentrations of myriocin, aureobasidin A (AbA) or SDZ 90-215 and average IC50 was charted relative to the wild-type control strain (±SD). (B) The IC50 for auxin was determined for several AID-tagged strains, and the combination index (CI) with myriocin, aureobasidin A, and SDZ 90-215 was determined from checkerboard assays. Synergy is evident when CI is less than 1. Shaded boxes indicate on-target inhibition when synergy was expected.

enzyme inositolphosphoryl-ceramide synthase of the Golgi complex that is composed of essential Aur1 and Kei1 proteins (Hashida-Okado *et al.*, 1996; Sato *et al.*, 2009). Last, resistance of Vrg4-TAP and Vrg4-AID strains to SDZ 90-215, a novel compound that targets the essential GDP-mannose transporter of the Golgi complex (see next section), was moderately diminished (by 2.6- and 2.1-fold). In summary, TAP-tagging alone caused hypersensitivity to on-target inhibitors by 1.3- to 17-fold while AID-tagging conferred additional hypersensitivity of ~1.8-fold in three of five instances. Though C-terminal TAP-tagging was shown to have little effect on expression of client proteins (Ghaemmaghami *et al.*, 2003), our findings suggest the TAP-tag often diminishes their function. Thus, TAP-tagged and AID-tagged proteins often behave like untagged "DAmP" strains that lack a 3' transcription terminator (Breslow *et al.*, 2008), which usually decreases mRNA stability and thus protein expression.

The AID-tagged essential proteins generated here may allow tunable damping of expression at sub-phenotypic concentrations of auxin, and thus may offer new opportunities for discovery and characterization of novel on-target small molecule inhibitors. We tested this possibility using AID-tagged variants of Lcb1, Lcb2, Aur1, Kei1, and Vrg4 that were simultaneously exposed to varying concentrations of auxin and varying concentrations of myriocin, aureobasidin A, and SDZ 90-215 that span the IC50 for each strain. From these checkerboard assays, the IC50 of each drug alone can be measured for each strain and also the degree of synergism can be estimated by calculating the combination index (CI; see Methods). A CI less than 1 indicates synergism, a CI equal to 1 indicates additivity, and a CI greater than 1 indicates antagonism between the two tested compounds. For myriocin and auxin, strong synergism was observed for the

Lcb1-AID strain (CI = 0.16), weak synergism was observed for the Lcb2-AID strain (CI = 0.83), and no synergism was observed for the Aur1-, Kei1-, and Vrg4-AID strains (CI > 1; Figure 4.4B). Aureobasidin A and auxin synergized on the Aur1- and Kei1-AID strains (CI = 0.43 and 0.82) but not the Lcb2- and Vrg4-AID strains (CI = 1.51 and 1.23). SDZ 90-215 synergized with auxin on the Vrg4-AID strain (CI = 0.36) and not the Lcb2-AID strain (CI = 1.01). Though aureobasidin A and SDZ 90-215 both synergized with auxin for several off-target AID-tagged proteins, all three molecules synergized with auxin for all their on-target AID-tagged strains. Thus, low concentrations of auxin can be used to sensitize many AID-tagged strains to on-target inhibitors.

SDZ 90-215 targets Vrg4

Peptolide SDZ 90-215 is a cyclic peptide secreted by *Septoria* species that exhibits strong antifungal activity toward several pathogenic yeasts (Emmer *et al.*, 1994) but the essential target of SDZ 90-215 has not been identified. In a large chemical genomics screen involving thousands of compounds and a panel of heterozygous knockout mutants (Hoepfner *et al.,* 2014), only the *vrg4*Δ/+ and *yor1*Δ/+ diploid strains of *S. cerevisiae* were significantly hypersensitive to SDZ 90-215 (Figure 4.5A). Yor1 is a non-essential multidrug transporter in the plasma membrane that mediates export of many different organic anions from the cytoplasm. The *yor1*Δ/Δ diploids were also extremely hypersensitive to SDZ 90-215 (Hoepfner *et al.,* 2014) probably caused by defects in export of the compound from the cytoplasm. Vrg4 is an essential GDP-mannose transporter in the Golgi complex (Dean *et al.,* 1997) and a good candidate for inhibition by SDZ 90-215. In growth assays, a haploid Vrg4-TAP strain was

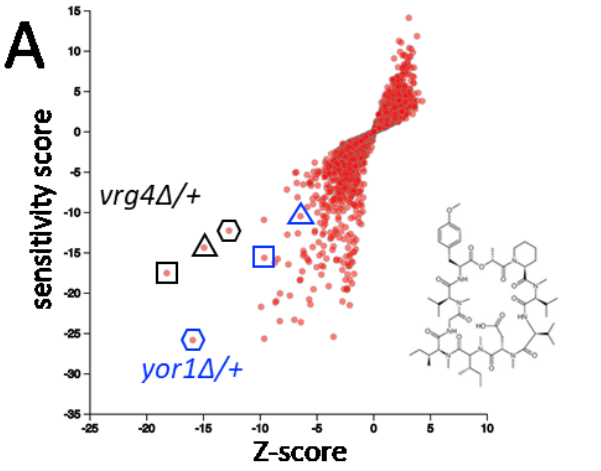
A
sensitivity score
Z-score
vrg4Δ/+
yor1Δ/+

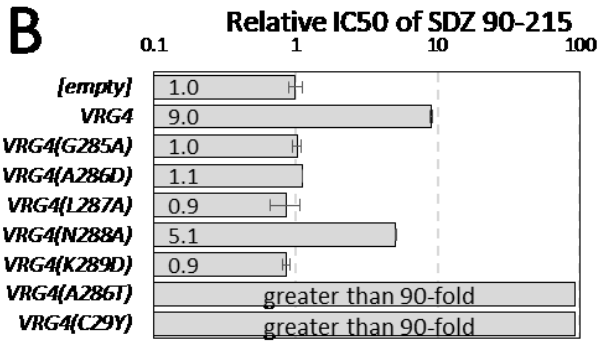
B
Relative IC50 of SDZ 90-215
0.1
1
10
100
[empty]
VRG4
VRG4(G285A)
VRG4(A286D)
VRG4(L287A)
VRG4(N288A)
VRG4(K289D)
VRG4(A286T)
VRG4(C29Y)
1.0
9.0
1.0
1.1
0.9
5.1
0.9
greater than 90-fold
greater than 90-fold

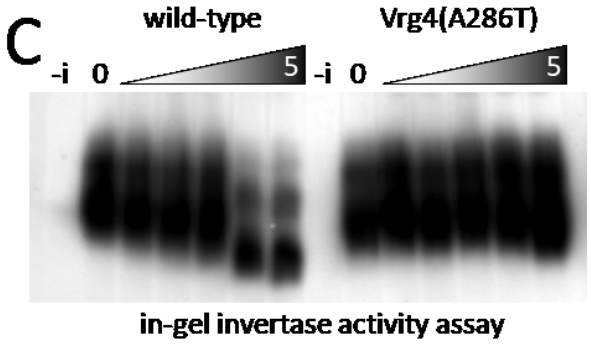
C
wild-type
Vrg4(A286T)
-i
0
5
-i
0
5
in-gel invertase activity assay

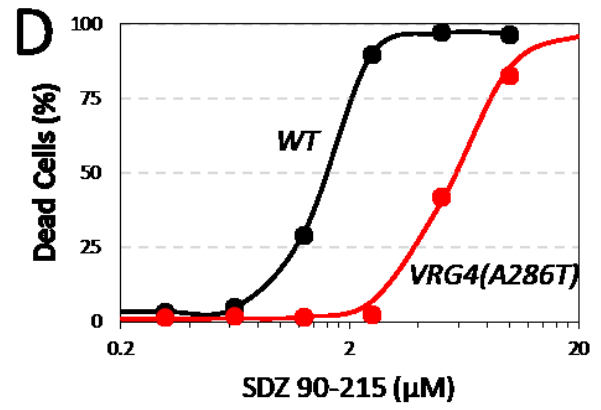
D
Dead Cells (%)
100
75
50
25
0
WT
VRG4(A286T)
0.2
2
20
SDZ 90-215 (µM)

Figure 4.5: SDZ 90-215 targets Vrg4.

(A) The responses of each heterozygous knockout mutant of *S. cerevisiae* to 3, 4, and 6 μg/mL SDZ 90-215 (inset) was charted as a function of Z-score and sensitivity score as described previously (Hoepfner *et al.*, 2014). The heterozygous *vrg4*Δ/+ and *yor1*Δ/+ mutant strains are circled. (B) A wild-type strain was transformed with high-dosage plasmids bearing *VRG4* or several derivatives and the relative IC50 to SDZ 90-215 was determined (empty plasmid set to 1.0). Bars represent the average ±SD from three biological replicates. (C) The SDZ 90-215-resistant Vrg4-A286T strain and wild-type control strain were grown to log phase in SCD medium, then shifted to the same medium (-i) or to invertase-inducing medium containing sucrose instead of glucose that also contained 0 to 5 μM SDZ 90-215. After 3 hr, lysates were prepared, subjected non-denaturing PAGE, and stained for invertase activity. Faster migrating bands represent hypo-glycosylated forms. (D) The wild-type and Vrg4-A286T strains were diluted into fresh SCD medium containing the indicated concentrations of SDZ 90-215, incubated for 24 hr at 30°C, then stained with propidium iodide and analyzed by flow cytometry for live and dead cells. Dots represent average of 3 biological replicates and best-fit curves represent non-linear regression to the standard sigmoid equation. The 50% lethal dose differed by almost 4-fold.

hypersensitive to SDZ 90-215 (Figure 4.4A) and a haploid Vrg4-AID strain was synergistically affected by auxin and SDZ 90-215 but not Myriocin or Aureobasidin (Figure 4.4B). Additionally, overexpression of Vrg4 from a high dosage plasmid (YEpGAP-VRG4) increased resistance to SDZ 90-215 by 9-fold relative to an empty control plasmid (YEpGAP) whereas overexpression of catalytically inactive variants of Vrg4 (G285A, A286D, L287A, K289D substitutions) (Gao *et al.*, 2001) did not alter resistance and a partially inactive variant (N288A) caused weak resistance (Figure 4.5B).

If SDZ 90-215 directly inhibits Vrg4, it may be possible to isolate Vrg4 variants that are catalytically active but resistant to SDZ 90-215. To test this possibility, a haploid yeast strain lacking Yor1 and seven other drug-resistance proteins was mutagenized and plated on medium containing 2.5 μM SDZ 90-215. Of 60 independent colonies that proved resistant to SDZ 90-215, 24 expressed a C29Y variant of Vrg4 and 36 expressed a A286T variant of Vrg4. When integrated into the high-copy plasmid-based *VRG4* gene, the overexpressed C29A and A286T variants increased resistance to SDZ 90-215 by over 10-fold relative to the wild-type Vrg4 plasmid (Figure 4.5B). Integration of the A286T substitution mutation into the *VRG4* locus of wild-type cells increased resistance to SDZ 90-215 by 9.0-fold (not shown). SDZ 90-215 also caused a dose-dependent inhibition of outer chain mannosylation of a secreted protein (invertase) in wild-type cells, but not in Vrg4-A286T mutant cells, as indicated by alterations in native gel mobility (Figure 4.5C). The Vrg4-A286T was also nearly 4-fold more resistant to SDZ 90-215 in measurements of cell death (Figure 4.5D). Collectively, these findings suggest that SDZ 90-215 directly engages Vrg4 from the cytoplasm and inhibits its essential functions.

An X-ray crystal structure of Vrg4 shows a large central substrate-binding cavity that opens to the Golgi lumen (Parker and Newstead, 2017). In this structure, C29 and A286 were positioned near each other in the middle of transmembrane helices 1 and 9 near the base of the cavity. C29 is adjacent to a conserved and functionally critical Y28 residue that makes direct contact with the ribose portion of the substrate GDP-mannose deep within the cavity (Parker and Newstead, 2017). A286 is one turn of helix 9 away from K289, which contacts the second phosphate of GDP-mannose and is part of the signature GALNK motif conserved among mannose-selective nucleotide sugar transporters. In transport assays, the A286D substitution exhibited a 6-fold higher apparent Km for GDP-mannose and no change in Vmax (Gao *et al.*, 2001). The A286T and C29Y substitutions possibly cause resistance to SDZ 90-215 by diminishing affinity of the inhibitor without diminishing affinity of substrates. The conformation of Vrg4 that opens to the cytoplasm where SDZ 90-215 is likely to bind has not been determined experimentally, but it is predicted to contain a substrate-binding cavity that is similar in size and shape owing to an internal duplication and topological inversion of a domain within the protein (Parker and Newstead, 2017). To determine whether the large SDZ 90-215 (1,126 D) can plausibly fit within this cavity, the structures of SDZ 90-215 and Vrg4 were uploaded into SwissDock and modeled. SwissDock generated models of SDZ 90-215 occupying nearly all of the central cavity of Vrg4 (Figure 4.6A) with a favorable free energy ($\Delta G = -9.04$). SwissDock generated similarly favorable models of GDP-mannose (605 D) deep within the central cavity of Vrg4 ($\Delta G = -9.35$) that closely resembled the experimentally determined structure. Therefore, SDZ 90-215 likely binds the central cavity of Vrg4 and prevents binding and transport of its substrates, resulting in

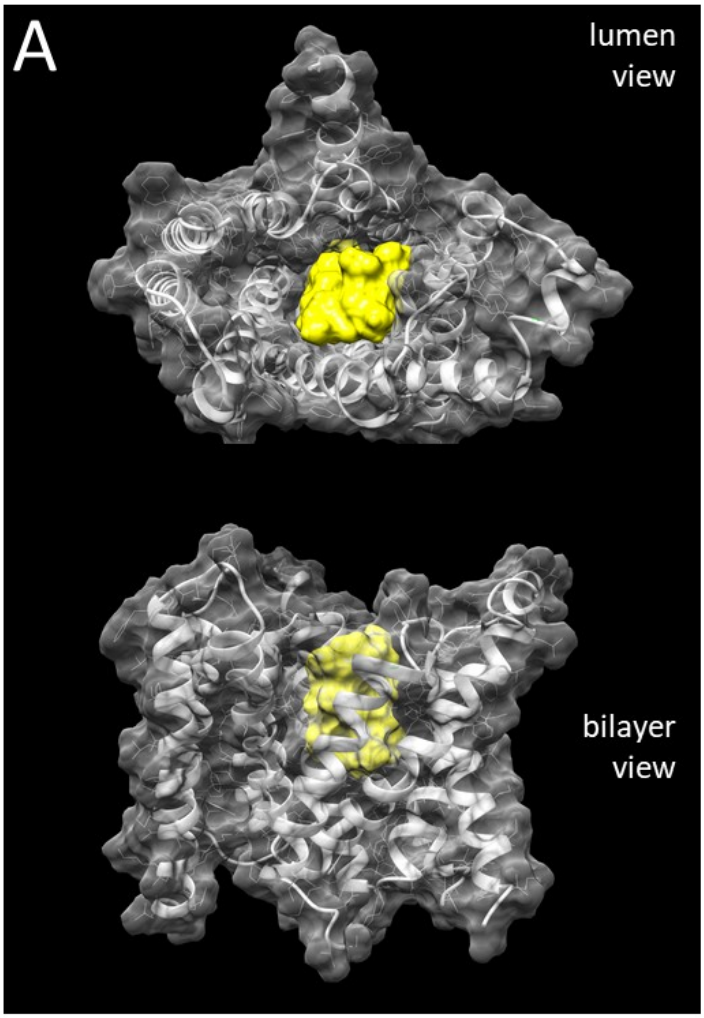
A
lumen
view
bilayer
view

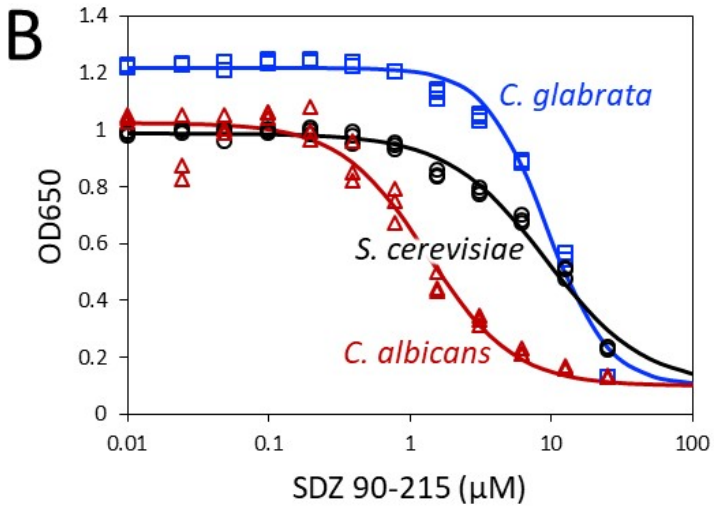
B
1.4
1.2
1
0.8
0.6
0.4
0.2
0
OD650
0.01
0.1
1
10
100
SDZ 90-215 (µM)
C. glabrata
S. cerevisiae
C. albicans

Figure 4.6: CMB402 can dock onto Vrg4 from S. cerevisiae and inhibit growth of pathogenic Candida species.

(A) A model of SDZ 90-215 (yellow) docked into the large central cavity of Vrg4 (translucent gray) was generated using SwissDock and viewed from the Golgi lumen or the plane of the bilayer. (B) Wild-type strains of *S. cerevisiae* (BY4741), *C. glabrata* (BG2) (Cormack and Falkow, 1999), and *C. albicans* (CAI4) (Fonzi and Irwin, 1993) were diluted into fresh YPD containing the indicated concentrations of SDZ 90-215 then optical density at 650 nm was measured after 24 hr. The symbols represent 3 biological replicates and the best-fit curves were obtained by non-linear regression to the standard sigmoid equation.

decreased mannosylation of sphingolipids and N-glycans, slowed cell proliferation, and eventual cell death.

SDZ 90-215 was found previously to inhibit *in vitro* growth of the pathogenic yeasts *Candida albicans*, *C. tropicalis*, *C. guilliermondii,* and *C. krusei* and also to cure several types of *C. albicans* infections in mouse models without toxicity to the animals (Emmer *et al.*, 1994). To compare and extend those findings, we determined the IC50's of SDZ 90-215 on *S. cerevisiae* (strain BY4741) and *C. glabrata* (strain BG2) in addition to *C. albicans* (strain CAI4). In YPD culture medium at 30°C, both *S. cerevisiae* and *C. glabrata* exhibited approximately 7-fold increase in IC50 relative to that of *C. albicans* (IC50 = 1.33 μM). Thus, SDZ 90-215 may be useful as a lead compound for treatment of yeast infections.

DISCUSSION

This study provides strong evidence that auxin-induced depletion of AID-tagged target proteins is a broadly effective strategy for analyzing protein function on a proteome-wide scale. At least 70% of essential proteins with C-termini exposed to the cytoplasm or nucleoplasm could be depleted functionally, as detected by slower growth of cultures, when tagged with AID and exposed to low concentrations of auxin (25 μM). The susceptible proteins included non-transmembrane proteins as well as polytopic transmembrane proteins in the plasma membrane, Golgi complex, endoplasmic reticulum, and mitochondrion. When C-terminal AID-tags are sequestered within these organelles, functional depletion was almost always abolished as expected due to OsTir1 localization in the cytoplasm and nucleoplasm. Among five susceptible AID-tagged

essential transmembrane proteins that we studied carefully, the IC50 for auxin ranged from 0.3 to 430 μM, spanning more than 1,000-fold. The source of the variation likely involves unexpected complexity in the microenvironments surrounding AID-tags, which could vary substantially among targets. Different genes may require very different levels of depletion to produce a growth phenotype. For instance, even before adding auxin, the sensitivity of Lcb1-AID and Lcb2-AID strains to an on-target inhibitor (myriocin) was increased 1.2-fold and 7.3-fold, respectively, relative to untagged wild-type strain. Thus, the latter strain was likely to be closer to the phenotypic threshold. Very low auxin concentrations might deplete Lcb2-AID below the point where it limits growth while being insufficient to deplete Lcb1-AID to the phenotypic level because of its near wild-type level of function. Similar reasoning could explain why the IC50s of Kei1-AID strains for auxin and an on-target inhibitor (aureobasidin A) are 9-fold and 6-fold lower than those of Aur1-AID strains. The amount of auxin required to observe a growth defect in any given AID-tagged strain will depend in part on the degree of depletion required to become limiting for growth, which is target specific.

Interestingly, we observed that TAP-tagging alone diminished resistance to on-target inhibitors by 1.3-fold to 2.7-fold for the five strains studied in detail. TAP-tagging had little or no reported effect on expression (Ghaemmaghami *et al.*, 2003), but clearly can have significant effects on protein function. About 25% of essential proteins could not survive with just a C-terminal TAP-tag (Ghaemmaghami *et al.*, 2003) and were not studied here. About 8% of TAP-tagged essential proteins could not be AID-tagged here, possibly due to the ~2-fold lower expression we observed for most AID-tagged proteins relative to TAP-tagged parent strains. A codon-optimized AID-tag improved basal

expression (unpublished results) and therefore may enable AID-tagging of proteins with less perturbation. These findings suggest that many TAP- and AID-tagged essential proteins have significantly damped function, providing a useful alternative to the collection of untagged proteins with damped expression (Breslow *et al.*, 2008).

Here we report that auxin and NAA both have off-target effects as inhibitors of TORC1 signaling, especially at high concentrations. Knockout mutants lacking positive regulators of TORC1 became hypersensitive to known on-target inhibitors (rapamycin and caffeine) as well as auxin and NAA, while hyperactivating mutations in Tor1 largely reversed these hypersensitivities. Additionally, just 1 hr exposure to auxin or NAA altered phosphorylation of downstream effectors of TORC1. Because NAA had greater activity against TORC1 and lesser activity against AID-tagged proteins than auxin, extra caution should be used when interpreting results with high concentrations of NAA. While novel inhibitors of TORC1 and its mammalian ortholog mTORC1 are potentially useful as immunosuppressants, the AID-tagged strains generated here may useful for discovering auxin-like analogs that have decreased off-target activities and increased selectivity for AID-tags.

Acute depletion of AID-tagged proteins with auxin can be instrumental in deciphering gene function before secondary responses and compensatory effects become manifest (Holland *et al.,* 2012). Mild depletion of AID-tagged proteins can sensitize cells to on-target inhibitors, and thus facilitate screening and discovery of small molecule inhibitors (SMIs) akin to earlier sensitization strategies that involve haploinsufficiency or damped expression. A screen of 1,776 compounds using complete collections of homozygous and heterozygous gene knockout mutants identified the essential GDP-

mannose transporter Vrg4 as a possible target of SDZ 90-215 and the ABC-family transporter Yor1 as a possible SDZ 90-215 efflux pump (Hoepfner *et al.*, 2014). Here we present additional data confirming that SDZ 90-215 targets Vrg4: (1) Vrg4-TAP and Vrg4-AID strains were hypersensitive to SDZ 90-215, (2) auxin synergized with SDZ 90-215 only on the latter strain, (3) overexpression of Vrg4 caused resistance to SDZ 90-215, (4) amino acid substitutions near the substrate-binding sites of Vrg4 caused resistance to SDZ 90-215, (5) the biological function of Vrg4 in mannosylation of a secretory protein was inhibited by exposure of cells to SDZ 90-215, and (6) SDZ 90-215 can be accommodated within the large central cavity observed in an X-ray crystal structure of Vrg4. Though the central cavity was open to the lumen of the Golgi complex in this conformation of Vrg4, the conformation that opens to the cytoplasm where SDZ 90-215 likely binds is predicted to be similar due to the internal duplication and topological inversion of a five-transmembrane domain to generate the full-length ten-transmembrane polytopic protein (Parker and Newstead, 2017).

Vrg4 is essential in *S. cerevisiae*, *C. glabrata*, and *C. ablicans* for mannosylation reactions in the Golgi complex, and hence for normal synthesis of mannan in the cell wall and sphingolipids in the cell membrane (Nishikawa *et al.*, 2002). Because these functions are unique to fungi, Vrg4 inhibitors are expected to exhibit antifungal properties. SDZ 90-215 was found previously to have potent antifungal activity against several pathogenic yeasts with low toxicity in mouse (Emmer *et al.*, 1994). As a natural product synthesized by a species of filamentous fungus in the genus *Septoria*, SDZ 90-215 and related cyclopeptides may be natural antifungals that are optimized to target Vrg4 or other members of the SLC35 family of nucleotide sugar transporters.

MATERIALS AND METHODS

Plasmids, Yeast strains, and genetic screens

TAP-tagged strains of *S. cerevisiae* in the BY4741 background (Ghaemmaghami *et al.*, 2003) were purchased from Dharmacon Inc., grown to log phase in YPD medium, transformed with the MfeI-digested linearized plasmid pAIDA2(6FLAG) depicted in Figure 4.1 using the lithium acetate method, and plated onto synthetic complete medium lacking uracil and containing 2% dextrose (SCD-ura agar medium) to select for transformants using conventional procedures (Sherman *et al.*, 1986). From each transformation, four independent colonies were picked, purified by streaking onto SCD-ura agar medium, and tested for correct AID-tagging of by assessing growth on SCD-his agar medium. Three validated colonies from each transformation were then arrayed in 96-well culture dishes and tested for growth defects in SCD medium containing 100 μM auxin. The concordance rate among the three isolates was over 99%, and therefore a single representative was chosen and arrayed into the master set of 96-well dishes. The master set containing 15% glycerol was frozen and stored at -80°C. Additional strains of *S. cerevisiae*, *C. glabrata*, and *C. albicans* are listed in Table 4.1.

The pAIDA2(6FLAG) plasmid was derived from plasmid pNHK53 (Morawska and Ulrich, 2013) which bears the URA3 selectable marker and OsTIR1 expression cassette as follows. pNHK53 was digested with XmaI plus AscI to remove a 8 bp segment of the polylinker and then ligated to a similarly digested 1,519 bp fragment of synthetic DNA that contained the transcription terminator from the *HIS3* homologous gene of *Schizosaccharomyces pombe*, a unique MfeI cleavage site, a TAP-AID*-6FLAG coding segment identical to a portion of pHYG-AID*-6FLAG (Morawska and Ulrich,

2013), a stop codon and unique AflII cleavage site, and a transcription terminator from the *CYC1* gene of *S. cerevisiae* (see Figure 4.1A). The AID* segment within pAIDA2(6FLAG) was later removed and replaced with a codon-optimized AID* segment by digestion with BsiWI plus AflII and ligation of a synthetic DNA fragment. Both plasmids and their sequences are available upon request.

To identify mutants of *S. cerevisiae* that confer resistance to SDZ 90-215, the haploid BY4741Δ8 strain (Hoepfner *et al.*, 2012) lacking eight genes involved in drug resistance (*SNQ2, PDR5, YOR1, PDR1, PDR2, PDR3, YAP1, YRM1*) was mutagenized with 2.5% ethylmethanesulfonate to 20% viability and then $2x10^7$ viable cells were plated onto SCD agar medium containing 2.5 μM SDZ 90-215. After 2 days incubation at 30°C, sixty independent colonies were picked, re-tested, and subjected to whole genome sequencing as described previously (Hoepfner *et al.*, 2012). Single-end reads were mapped to the S288C reference genome using BWA. All sixty SDZ 90-215-resistant strains contained either the C29Y or A286T substitution mutations in the gene encoding Vrg4.

Determination of IC50 and synergy.

All chemical compounds were obtained from Sigma-Aldrich Inc. apart from aureobasidin A (Takara Inc.) and SDZ 90-215 (Novartis Inc.). The IC50 of *S. cerevisiae* strains was determined by diluting stationary phase cultures 1000-fold into fresh SCD medium containing 2-fold serial dilutions of the indicated compounds in 96-well dishes (200 μL final volume), incubating at 30°C for 24 hr, then resuspending and measuring optical density at 650 nM using a Thermomax microplate reader (Molecular Devices).

Raw data were fit to the standard sigmoid equation y = ODmin + (ODmax – ODmin)/(1+(x/IC50)^slope) by non-linear regression with Kaleidagraph™ software. The four parameters were tabulated and the IC50s from three replicate experiments were averaged. In checkerboard assays where strains were exposed to two serially diluted compounds simultaneously, the IC50's for each compound alone were determined as described above and then the combination index (CI) was calculated as the IC50 from the diagonal of optical densities that contain approximately 1:1 ratio of the two compounds in terms of IC50 units (Lehar *et al.*, 2009). When CI equals 1, the two compounds behave additively as if they were the same compound acting on the same target. When CI is significantly less than 1, the two compounds exhibit synergy. Compounds with the same target or different targets within a single pathway often exhibit synergy (Lehar *et al.*, 2007).

Western blotting and in-gel invertase assays.

For western blotting, cells were lysed via fast alkaline lysis in 0.5 M NaOH with 1.85% β-mercaptoethanol (BME) in ice water for 10 minutes. The protein was then precipitated by addition of trichloroacetic acid (TCA) to a final concentration of 10% (w/w) and washed once with water. Protein pellets were suspended in SDS sample buffer (0.1 M Tris-HCl, pH 6.8, 4% SDS, 0.2% bromophenol blue, 20% glycerol, 2% BME), incubated at 37 °C for 30 minutes, separated on 10% polyacrylamide gels with SDS, transferred to Hybond, and then blocked and probed with antibodies as described previously (Mehta *et al.*, 2009). Primary antibodies were used as follows: anti-TAP rabbit polyclonal antibodies (ThermoFisher, CAB1001) at 1:10,000 dilution, anti-

hemagglutinin (HA) mouse monoclonal antibodies (Covance, Princeton, NJ) at 1:10,000 dilution, or anti-phospho S6 (Ser-235/236) mouse monoclonal antibodies (Cell Signaling, Danvers, MA) at 1:5000 dilution, anti-PGK1 mouse monoclonal antibodies (Abcam) at 1:10,000.

In-gel invertase assays were adapted from (Huffaker and Robbins, 1982). Briefly, log-phase cultures in YPD medium plus 500 mM KCl were pelleted, washed, and suspended in the same medium but with reduced glucose (0.05%) to induce invertase expression. SDZ 90-215 was added to varying concentrations and cultures were incubated at 30°C for 3 hr. The cells were pelleted, washed once with 20mM sodium azide and once with TPB buffer (8.25 mM Tris-HCl pH 7, 30 mM diethylbarbituric acid, 0.1 mM phenylmethanesulfonyl fluoride) before being resuspended in 20 µL TPB buffer. Acid-washed glass beads were added to the cells before vortexing to break the cells before 50 µL of TPB buffer containing 15% glycerol and 0.01% bromophenol blue was added. The samples were centrifuged, and the supernatant was loaded onto pre-cast 10% polyacrylamide gel lacking SDS (Bio-Rad). After electrophoresis with Tris-borate buffer (8.25 mM Tris base, 80 mM boric acid, pH 7.5), the gel was incubated for 10 minutes in cold sucrose solution (0.1 M sucrose in 0.1 M sodium acetate, pH 5.1) at 4°C. The gel was then transferred to sucrose solution at 37°C and incubated for another 10 min. The gel was rinsed twice with water, and transferred to a Pyrex dish, where TTC solution (1 mg/mL 2,3,5-triphenyltetrazolium chloride in 0.5 M NaOH) was added and brought to boiling on a hot plate in the hood until color developed. Finally, the gel was washed with water and then 10% acetic acid.

Docking of SDZ 90-215 to Vrg4.

The structures of SDZ 90-215 (CID=158437) and Vrg4 (PDB=5OGE) were downloaded from NCBI databases and uploaded into SwissDock (Grosdidier *et al.*, 2011). The lowest free energy models were visualized using UCSF Chimera v1.13 (Petterson *et al.*, 2004).

Statistical tests of significance.

Student's T-tests were implemented on many datasets, as indicated in the figures (* = $p < 0.05$, ** = $p < 0.01$, *** = $p < 0.001$).

Table 4.1: Strains used in Chapter 4

Strain	Background	Genotype	Source
K1251	BY4741[a]	*MATa*	Gaiver et al. (2002)
AK060	BY4741	*MATa gtr1::NatR*	Kim and Cunningham (2015)
AK061	BY4741	*MATa gtr2::NatR*	Kim and Cunningham (2015)
AK062	BY4741	*MATa ego1::NatR*	Kim and Cunningham (2015)
AK063	BY4741	*MATa ego3::NatR*	Kim and Cunningham (2015)
AK018	BY4741	*MATa pib2::NatR*	Kim and Cunningham (2015)
AK104	BY4741	*MATx TOR1(I954S)*	Kim and Cunningham (2015)
AK102	BY4741	*MATx gtr1::NatR TOR1(I954S)*	Kim and Cunningham (2015)
AK106	BY4741	*MATx pib2::KanR TOR1(I954S)*	Kim and Cunningham (2015)
AK108	BY4741	*MATx gtr1::NatR pib2::KanR TOR1(I954S)*	Kim and Cunningham (2015)
NS269	BY4741	*MATa LCB1-TAP::HIS3*	This Study
NS270	BY4741	*MATa LCB1-TAP-AID-6XFLAG::TIR1::URA3*	This Study
NS271	BY4741	*MATa LCB2-TAP::HIS3*	This Study
NS272	BY4741	*MATa LCB2-TAP-AID-6XFLAG::TIR1::URA3*	This Study
NS273	BY4741	*MATa Aur1-TAP::HIS3*	This Study

NS274	BY4741	*MATa AUR1-TAP-AID-6XFLAG::TIR1::URA3*	This Study
NS275	BY4741	*MATa KEI1-TAP::HIS3*	This Study
NS276	BY4741	*MATa KEI1-TAP-AID-6XFLAG::TIR1::URA3*	This Study
NS283	BY4741	*MATa VRG4-TAP::HIS3*	This Study
NS284	BY4741	*MATa VRG4-TAP-AID-6xFLAG::TIR1::URA3*	This Study
NS250	BY4741	*MATa VRG4(A286T)::URA3*	This Study
BG2	*C. glabrata*		Cormack and Falkow (1999)
CAI4	*C. albicans*		Fonzi and Irwin (1993)
NS277	BY4741	*MATa MCD4-TAP::HIS3*	This Study
NS278	BY4741	*MATa MCD4-TAP-AID-6XFLAG::TIR1::URA3*	This Study
NS279	BY4741	*MATa ALR1-TAP::HIS3*	This Study
NS280	BY4741	*MATa ALR1-TAP-AID-6XFLAG::TIR1::URA3*	This Study
NS281	BY4741	*MATa PMA1-TAP::HIS3*	This Study
NS282	BY4741	*MATa PMA1-TAP-AID-6XFLAG::TIR1::URA3*	This Study
NS285	BY4741	*MATa HIP1-TAP::HIS3*	This Study

NS286	BY4741	*MATa HIP1-TAP-AID-6XFLAG::TIR1::URA3*	This Study
NS287	BY4741	*MATa VHT1-TAP::HIS3*	This Study
NS288	BY4741	*MATa VHT1-TAP-AID-6XFLAG::TIR1::URA3*	This Study
NS289	BY4740	*MATa CKA1-TAP::HIS3*	This Study
NS290	BY4741	*MATa CKA2-TAP::HIS3*	This Study
K2025	BY4741	*MATa CKA1-TAP-AID-6XFLAG::TIR1::URA3 CKA2-TAP-AID-6XFLAG::HygR*	This Study

Footnote

[a] background mutations in BY4741 (his3Δ1 leu2Δ0 met15Δ0 ura3Δ0)

REFERENCES

Anzalone, A.V., A.J. Lin, S. Zairis, R. Rabadan, and V.W. Cornish, 2016. Reprogramming eukaryotic translation with ligand-responsive synthetic RNA switches. Nat Methods 13(5):453-8.

Ben-Aroya, S., C. Coombes, T. Kwok, K.A. O'Donnell, J.D. Boeke, and P. Hieter, 2008. Toward a comprehensive temperature-sensitive mutant repository of the essential genes of Saccharomyces cerevisiae. Mol Cell 30(2):248-58.

Breslow, D.K., D.M. Cameron, S.R. Collins, M. Schuldiner, J. Stewart-Ornstein, H.W. Newman, S. Braun, H.D. Madhani, N.J. Krogan, and J.S. Weissman, 2008. A comprehensive strategy enabling high-resolution functional analysis of the yeast genome. Nat Methods 5(8):711-8.

Cormack, B.P., and S. Falkow, 1999. Efficient homologous and illegitimate recombination in the opportunistic yeast pathogen Candida glabrata. Genetics 151(3):979-87.

Dean, N., Y.B. Zhang, and J.B. Poster, 1997. The VRG4 gene is required for GDP-mannose transport into the lumen of the Golgi in the yeast, Saccharomyces cerevisiae. J Biol Chem 272(50):31908-14.

Dohmen, R.J., and A. Varshavsky, 2005. Heat-inducible degron and the making of conditional mutants. Methods Enzymol 399:799-822.

Emmer, G., M.A. Grassberger, J.G. Meingassner, G. Schulz, and M. Schaude, 1994. Derivatives of a Novel Cyclopeptide. 1. Synthesis, Antifungal Activity, and Structure-Activity Relationships. J Med Chem 37:1908-17.

Fonzi, W.A., and M.Y. Irwin, 1993. Isogenic strain construction and gene mapping in Candida albicans. Genetics 134(3):717-28.

Gao, X.D., A. Nishikawa, and N. Dean, 2001. Identification of a conserved motif in the yeast golgi GDP-mannose transporter required for binding to nucleotide sugar. J Biol Chem 276(6):4424-32.

Ghaemmaghami, S., W.K. Huh, K. Bower, R.W. Howson, A. Belle, N. Dephoure, E.K. O'Shea, and J.S. Weissman, 2003. Global analysis of protein expression in yeast. Nature 425(6959):737-41.

Giaever, G., A.M. Chu, L. Ni, C. Connelly, L. Riles, S. Veronneau, S. Dow, A. LucauDanila, K. Anderson, B. Andre, A.P. Arkin, A. Astromoff, M. El-Bakkoury, R. Bangham, R. Benito, S. Brachat, S. Campanaro, M. Curtiss, K. Davis, A. Deutschbauer, K.D. Entian, P. Flaherty, F. Foury, D.J. Garfinkel, M. Gerstein, D. Gotte, U. Güldener, J.H. Hegemann, S. Hempel, Z. Herman, D.F. Jaramillo, D.E. Kelly, S.L. Kelly, P. Kötter, D. LaBonte, D.C. Lamb, N. Lan, H. Liang, H. Liao, L. Liu, C. Luo, M. Lussier, R. Mao, P. Menard, S.L. Ooi, J.L. Revuelta, C.J. Roberts, M. Rose, P. Ross-Macdonald, B. Scherens, G. Schimmack, B. Shafer, D.D. Shoemaker, S. Sookhai-Mahadeo, R.K. Storms, J.N. Strathern, G. Valle, M. Voet, G. Volckaert, C.Y. Wang, T.R. Ward, J. Wilhelmy, E.A. Winzeler, Y. Yang, G. Yen, E. Youngman, K. Yu, H. Bussey, J.D. Boeke, M. Snyder, P. Philippsen, R.W. Davis, and M. Johnston, (2002). Functional profiling of the Saccharomyces cerevisiae genome. Nature 418, 387–391.

Gonzalez, A., M. Shimobayashi, T. Eisenberg, D.A. Merle, T. Pendl, M.N. Hall, and T. Moustafa, 2015. TORC1 promotes phosphorylation of ribosomal protein S6 via the AGC kinase Ypk3 in Saccharomyces cerevisiae. PLoS One 10(3):e0120250.

Grosdidier, A., V. Zoete, and O. Michielin, 2011. SwissDock, a protein-small molecule docking web service based on EADock DSS. Nucleic Acids Res 39(Web Server issue):W270-7.

Hashida-Okado, T., A. Ogawa, M. Endo, R. Yasumoto, K. Takesako, and I. Kato, 1996. *A*UR1, a novel gene conferring aureobasidin resistance on Saccharomyces cerevisiae: a study of defective morphologies in Aur1p-depleted cells. Mol Gen Genet 251(2):236-44.

Hillenmeyer, M.E., E. Fung, J. Wildenhain, S.E. Pierce, S. Hoon, W. Lee, M. Proctor, R.P. St Onge, M. Tyers, D. Koller, R.B. Altman, R.W. Davis, C. Nislow, and G. Giaever, 2008. The chemical genomic portrait of yeast: uncovering a phenotype for all genes. Science 320(5874):362-5.

Hoepfner, D., C.W. McNamara, C.S. Lim, C. Studer, R. Riedl, T. Aust, S.L. McCormack, D.M. Plouffe, S. Meister, S. Schuierer, U. Plikat, N. Hartmann, F. Staedtler, S. Cotesta, E.K. Schmitt, F. Petersen, F. Supek, R.J. Glynne, J.A. Tallarico, J.A. Porter, M.C. Fishman, C. Bodenreider, T.T. Diagana, N.R. Movva, and E.A. Winzeler, 2012. Selective and specific inhibition of the plasmodium falciparum lysyl-tRNA synthetase by the fungal secondary metabolite cladosporin. Cell Host Microbe 11(6):654-63.

Hoepfner, D., S.B. Helliwell, H. Sadlish, S. Schuierer, I. Filipuzzi, S. Brachat, B. Bhullar, U. Plikat, Y. Abraham, M. Altorfer, T. Aust, L. Baeriswyl, R. Cerino, L. Chang,

D. Estoppey, J. Eichenberger, M. Frederiksen, N. Hartmann, A. Hohendahl, B. Knapp, P. Krastel, N. Melin, F. Nigsch, E.J. Oakeley, V. Petitjean, F. Petersen, R. Riedl, E.K. Schmitt, F. Staedtler, C. Studer, J.A. Tallarico, S. Wetzel, M.C. Fishman, J.A. Porter, and N.R. Movva, 2014. High-resolution chemical dissection of a model eukaryote reveals targets, pathways and gene functions. Microbiological research 169(2-3):107-20.

Holland, A.J., D. Fachinetti, J.S. Han, and D.W. Cleveland, 2012. Inducible, reversible system for the rapid and complete degradation of proteins in mammalian cells. Proc Natl Acad Sci U S A. 109(49):E3350-7.

Huber, A., B. Bodenmiller, A. Uotila, M. Stahl, S. Wanka, B. Gerrits, R. Aebersold, and R. Loewith, 2009. Characterization of the rapamycin-sensitive phosphoproteome reveals that Sch9 is a central coordinator of protein synthesis. Genes Dev 23(16):1929-43.

Huffaker, T.C., and P.W. Robbins, 1982. Temperature-sensitive yeast mutants deficient in asparagine-linked glycosylation. J Biol Chem 257(6):3203-10.

Kim, A., K.W. Cunningham, 2015. A LAPF/phafin1-like protein regulates TORC1 and lysosomal membrane permeabilization in response to endoplasmic reticulum membrane stress. Mol Biol Cell 26(25):4631-45.

Kim, D.U., J. Hayles, D. Kim, V. Wood, H.O. Park, M. Won, H.S. Yoo, T. Duhig, M. Nam, G. Palmer, S. Han, L. Jeffery, S.T. Baek, H. Lee, Y.S. Shim, M. Lee, L. Kim, K.S. Heo, E.J. Noh, A.R. Lee, Y.J. Jang, K.S. Chung, S.J. Choi, J.Y. Park, Y. Park, H.M. Kim, S.K. Park, H.J. Park, E.J. Kang, H.B. Kim, H.S. Kang, H.M. Park, K. Kim, K. Song, K.B. Song, P. Nurse, and K.L. Hoe, 2010. Analysis of a

genome-wide set of gene deletions in the fission yeast Schizosaccharomyces pombe. Nat Biotechnol 28(6):617-23.

Klauser, B., J. Atanasov, L.K. Siewert, and J.S. Hartig, 2015. Ribozyme-based aminoglycoside switches of gene expression engineered by genetic selection in S. cerevisiae. ACS Synth Biol 4(5):516-25.

Lehar, J., G.R. Zimmermann, A.S. Krueger, R.A. Molnar, J.T. Ledell, A.M. Heilbut, G.F. Short, 3rd, L.C. Giusti, G.P. Nolan, O.A. Magid, M.S. Lee, A.A. Borisy, B.R. Stockwell, and C.T. Keith, 2007. Chemical combination effects predict connectivity in biological systems. Mol Syst Biol 3:80.

Lee, A.Y., R.P. St Onge, M.J. Proctor, I.M. Wallace, A.H. Nile, P.A. Spagnuolo, Y. Jitkova, M. Gronda, Y. Wu, M.K. Kim, K. Cheung-Ong, N.P. Torres, E.D. Spear, M.K. Han, U. Schlecht, S. Suresh, G. Duby, L.E. Heisler, A. Surendra, E. Fung, M.L. Urbanus, M. Gebbia, E. Lissina, M. Miranda, J.H. Chiang, A.M. Aparicio, M. Zeghouf, R.W. Davis, J. Cherfils, M. Boutry, C.A. Kaiser, C.L. Cummins, W.S. Trimble, G.W. Brown, A.D. Schimmer, V.A. Bankaitis, C. Nislow, G.D. Bader, and G. Giaever, 2014. Mapping the cellular response to small molecules using chemogenomic fitness signatures. Science 344(6180):208-11.

Lehar, J., A.S. Krueger, W. Avery, A.M. Heilbut, L.M. Johansen, E.R. Price, R.J. Rickles, G.F. Short, 3rd, J.E. Staunton, X. Jin, M.S. Lee, G.R. Zimmermann, and A.A. Borisy, 2009. Synergistic drug combinations tend to improve therapeutically relevant selectivity. Nat Biotechnol 27(7):659-66.

Li, Z., F.J. Vizeacoumar, S. Bahr, J. Li, J. Warringer, F.S. Vizeacoumar, R. Min, B. Vandersluis, J. Bellay, M. Devit, J.A. Fleming, A. Stephens, J. Haase, Z.Y. Lin,

A. Baryshnikova, H. Lu, Z. Yan, K. Jin, S. Barker, A. Datti, G. Giaever, C. Nislow, C. Bulawa, C.L. Myers, M. Costanzo, A.C. Gingras, Z. Zhang, A. Blomberg, K. Bloom, B. Andrews, and C. Boone, 2011. Systematic exploration of essential yeast gene function with temperature-sensitive mutants. Nat Biotechnol 29(4):361-7.

Liu, O.W., C.D. Chun, E.D. Chow, C. Chen, H.D. Madhani, and S.M. Noble, 2008. Systematic genetic analysis of virulence in the human fungal pathogen Cryptococcus neoformans. Cell 135(1):174-88.

Loewith, R., and M.N. Hall, 2011. Target of rapamycin (TOR) in nutrient signaling and growth control. Genetics 189(4):1177-201.

Michel, A.H., R. Hatakeyama, P. Kimmig, M. Arter, M. Peter, J. Matos, C. De Virgilio, and B. Kornmann, 2017. Functional mapping of yeast genomes by saturated transposition. Elife 6.

Morawska, M., and H.D. Ulrich, 2013. An expanded tool kit for the auxin-inducible degron system in budding yeast. Yeast 30(9):341-51.

Nagiec, M.M., J.A. Baltisberger, G.B. Wells, R.L. Lester, and R.C. Dickson, 1994. The LCB2 gene of Saccharomyces and the related LCB1 gene encode subunits of serine palmitoyltransferase, the initial enzyme in sphingolipid synthesis. Proc Natl Acad Sci U S A 91(17):7899-902.

Nishikawa, A., J.B. Poster, Y. Jigami, and N. Dean, 2002. Molecular and phenotypic analysis of CaVRG4, encoding an essential Golgi apparatus GDP-mannose transporter. J Bacteriol 184(1):29-42.

Nishimura, K., T. Fukagawa, H. Takisawa, T. Kakimoto, and M. Kanemaki, 2009. An auxin-based degron system for the rapid depletion of proteins in nonplant cells. Nat Methods 6(12):917-22.

Parker, J.L., and S. Newstead, 2017. Structural basis of nucleotide sugar transport across the Golgi membrane. Nature 551(7681):521-4.

Pettersen, E.F., T.D. Goddard, C.C. Huang, G.S. Couch, D.M. Greenblatt, E.C. Meng, and T.E. Ferrin, 2004. UCSF Chimera--a visualization system for exploratory research and analysis. J Comput Chem 25(13):1605-12.

Qi, L.S., M.H. Larson, L.A. Gilbert, J.A. Doudna, J.S. Weissman, A.P. Arkin, and W.A. Lim, 2013. Repurposing CRISPR as an RNA-guided platform for sequence-specific control of gene expression. Cell 152(5):1173-83.

Reinke, A., J.C. Chen, S. Aronova, and T. Powers, 2006. Caffeine targets TOR complex I and provides evidence for a regulatory link between the FRB and kinase domains of Tor1p. J Biol Chem 281(42):31616-26.

Roemer, T., B. Jiang, J. Davison, T. Ketela, K. Veillette, A. Breton, F. Tandia, A. Linteau, S. Sillaots, C. Marta, N. Martel, S. Veronneau, S. Lemieux, S. Kauffman, J. Becker, R. Storms, C. Boone, and H. Bussey, 2003. Large-scale essential gene identification in Candida albicans and applications to antifungal drug discovery. Mol Microbiol 50(1):167-81.

Sato, K., Y. Noda, and K. Yoda, 2009. Kei1: a novel subunit of inositolphosphorylceramide synthase, essential for its enzyme activity and Golgi localization. Mol Biol Cell 20(20):4444-57.

Schwarzmuller, T., B. Ma, E. Hiller, F. Istel, M. Tscherner, S. Brunke, L. Ames, A. Firon, B. Green, V. Cabral, M. Marcet-Houben, J.D. Jacobsen, J. Quintin, K. Seider, I. Frohner, W. Glaser, H. Jungwirth, S. Bachellier-Bassi, M. Chauvel, U. Zeidler, D. Ferrandon, T. Gabaldon, B. Hube, C. d'Enfert, S. Rupp, B. Cormack, K. Haynes, and K. Kuchler, 2014. Systematic phenotyping of a large-scale Candida glabrata deletion collection reveals novel antifungal tolerance genes. PLoS Pathog 10(6):e1004211.

Sherman, F., J.B. Hicks, and G.R. Fink, 1986. Methods in Yeast Genetics. Cold Spring Harbor, N.Y.: Cold Spring Harbor Laboratory.

Tanigawa, M., and T. Maeda, 2017. An In Vitro TORC1 Kinase Assay That Recapitulates the Gtr-Independent Glutamine-Responsive TORC1 Activation Mechanism on Yeast Vacuoles. Mol Cell Biol 37(14).

Teng, X., M. Dayhoff-Brannigan, W.C. Cheng, C.E. Gilbert, C.N. Sing, N.L. Diny, S.J. Wheelan, M.J. Dunham, J.D. Boeke, F.J. Pineda, and J.M. Hardwick, 2013. Genome-wide consequences of deleting any single gene. Mol Cell 52(4):485-94.

Varlakhanova, N.V., M.J. Mihalevic, K.A. Bernstein, and M.G.J. Ford, 2017. Pib2 and the EGO complex are both required for activation of TORC1. J Cell Sci 130(22):3878-90.

Winzeler, E.A., D.D. Shoemaker, A. Astromoff, H. Liang, K. Anderson, B. Andre, R. Bangham, R. Benito, J.D. Boeke, H. Bussey, A.M. Chu, C. Connelly, K. Davis, F. Dietrich, S.W. Dow, M. El Bakkoury, F. Foury, S.H. Friend, E. Gentalen, G. Giaever, J.H. Hegemann, T. Jones, M. Laub, H. Liao, N. Liebundguth, D.J. Lockhart, A. Lucau-Danila, M. Lussier, N. M'Rabet, P. Menard, M. Mittmann, C.

Pai, C. Rebischung, J.L. Revuelta, L. Riles, C.J. Roberts, P. Ross-MacDonald, B. Scherens, M. Snyder, S. Sookhai-Mahadeo, R.K. Storms, S. Veronneau, M. Voet, G. Volckaert, T.R. Ward, R. Wysocki, G.S. Yen, K. Yu, K. Zimmermann, P. Philippsen, M. Johnston, and R.W. Davis, 1999. Functional characterization of the S. cerevisiae genome by gene deletion and parallel analysis. Science 285(5429):901-6.

CHAPTER 5

CONCLUDING REMARKS

The Golgi apparatus plays a crucial cellular role by providing a centralized location for glycosylation and the sorting and processing of proteins and lipids in eukaryotes. In order for these processes to function normally, a homeostatic balance of all components of all reactions within the Golgi must be carefully maintained. Alteration of the composition of proteins, cofactors, substrates, or byproducts within the Golgi can have downstream consequences in the fates of the cell. This is evidenced by the numerous human disorders that arise from deregulation of Golgi homeostasis. In this dissertation, we have characterized two proteins, Erd1 and Gdt1, which provide important roles in the maintenance of homeostasis of the Golgi apparatus in yeast, supporting the crucial cellular process of glycosylation. Based on the data presented in Chapter 2, both of these genes have the potential to relieve stress from glycosylation via the removal of byproducts.

Erd1 is required for the recycling of inorganic phosphate (Pi), released from nucleotide phosphates after the transfer of glycosyl groups from nucleotide sugars during glycosylation. This phosphate cleavage is required to prepare the nucleotide for exchange with additional nucleotide sugars, which can be used for additional glycosylation reactions (Capasso and Hirschberg 1984). The existence of a phosphate exporter in the Golgi membrane has been long hypothesized, but the protein responsible has never been identified. While the data presented in Chapter 2 provides strong evidence that Erd1 is functioning *in vivo* as the transporter of phosphate across the Golgi membrane, it still remains possible that it is only functioning in a regulatory role of this activity. Therefore, additional research must be conducted to establish the mechanism of transport and

determine how the kinetics of transport effects the rate of reaction of glycosyltransferases.

The future study of Erd1 should begin with purification of the protein for the purposes of *in vitro* transport studies and structural determination. Generation of a crystal structure for this protein could help determine key amino acids within the active site of the protein that could be mutated and assessed for relevance to the activity of the protein. Furthermore, this could enable the generation of co-crystals with Pi groups in order to establish the ability of the protein to bind Pi. The purified protein could also be reconstituted into liposomes for the purpose of transport studies, which could definitively demonstrate the ability to transport Pi across a membrane and the kinetics of this activity. The mechanism of action, such as dependency of a proton or metal gradient or membrane charge could be determined in these transport assays as well.

Interestingly, the absence of *ERD1* in yeast resulted in secretion of the Pi into the media. Previous reports demonstrated that *erd1Δ* yeast have deficiencies of glycosylation, but since there are no homologs to Erd1 in metazoan species, it is possible that this activity is conducted by an as yet undiscovered transporter that is unrelated to Erd1. Another possibility is that, for metazoans, the normal course of action for these species is to eliminate excess Pi via secretion into the bloodstream, where it can be reabsorbed into other cells by plasma membrane transporters. If this is the case, it is likely that the concentration of Pi in the *trans* Golgi significantly exceeds that of the *cis* Golgi.

To test this hypothesis, future experiments could be conducted on mammalian cell culture utilizing fluorescence indicator protein for inorganic phosphate (FLIPPi) sensors. These sensors were originally developed for *in vitro* use, but modified for use in live

plants, to create live-cell imaging of localized concentrations of Pi (Sun *et al.* 2008; Mukherjee *et al.* 2015). This technology utilizes an inorganic phosphate binding protein (PiBP) from cyanobacteria fused to two fluorescent proteins to create a FRET-based Pi-sensor (Sun *et al.* 2008). Transgenic strains may then be generated that express the Pi sensor within different cellular compartments, such as the Golgi complex. Combining ratiometric analysis with confocal microscopy can then enable the determination of relative concentrations of Pi in various cellular compartments (Sun *et al.* 2008). This technology has not yet been implemented in mammalian cells, and may require some modification before it can be successfully utilized.

This work also characterized the Golgi protein Gdt1, which has also been demonstrated to be important for glycosylation (Colinet *et al.* 2016; Potelle *et al.* 2016). Importantly, Gdt1, similarly to the vacuolar protein Vcx1, was determined to function as a reversible exchanger of H^+ and Ca^{2+} that is regulated by calcineurin. This is in agreement with other publications that have demonstrated that Gdt1 is able to undergo pH-dependent transport Ca^{2+} and Mn^{2+} when heterologously expressed in the membranes of bacteria (Potelle *et al.* 2016; Thines *et al.* 2018). Additionally, it has been previously reported that loss of TMEM165, the mammalian homolog of Gdt1, disrupts pH homeostasis in addition to causing glycosylation deficiencies that can be rescued through supplementation with Mn^{2+} (Potelle *et al.* 2016). When combined with a knockout of SPCA1, loss of TMEM165 results in synthetic lethality (Blomen *et al.* 2015).

The revelation that there is a highly conserved H^+/Ca^{2+} exchanger in the Golgi was unexpected, since there is presumably no need for it. The reversibility of the exchange activity may indicate that Gdt1/TMEM165 is one of if not the primary source

of a proton leak that has been identified in the Golgi when the V-ATPase is inactivated (Schapiro and Grinstein 2000). The exchanger could continue transporting Ca^{2+}/Mn^{2+} into the Golgi in exchange for H^+ until the pH gradient between the Golgi and cytoplasm is neutralized. The reversibility of Gdt1 may also provide insight into the evolutionary purpose of the protein. Due to the importance of homeostatic regulation of Ca^{2+}, Mn^{2+} and the pH of the Golgi, Gdt1/TMEM165 may be conserved to function as a sensor of these factors. If any one of the three factors reach a concentration too high or too low, the reversible exchange activity of Gdt1/TMEM165 could enable correctional adjustment, without requiring degradation or synthesis of other proteins. For example, if the concentration of Mn^{2+} becomes too high in the Golgi lumen, Gdt1/TMEM165 would become more likely to transport Mn^{2+}, along with H^+, into the cytoplasm while still transporting Ca^{2+} into the Golgi lumen. In this way, exchangers like Gdt1/TMEM165 are incredibly important in maintaining homeostasis of ion concentrations within organelles.

It had previously been shown that expression of TMEM165 was upregulated during lactation, but the effects of loss of this expression had not been studied (Reinhardt *et al.* 2014). The work presented in Chapter 3 provides the first insight into the importance of TMEM165 in the process of lactation. Loss of TMEM165 in the lactating mammary gland results in deficiencies of lactose synthesis that decreases the osmotic potential of the milk. This decreases the volume and nutritious quality of the milk itself, ultimately resulting in low weight gain of the pups that are nursing from the TMEM165-deficient mother. The Ca^{2+} and Mn^{2+} composition of the milk suggests that loss of TMEM165 decreased the transport of these metals into the Golgi and therefore the secretory network, consistent with previous models of TMEM165 activity.

Generation of crystal structures and determination of the kinetics of transport of both TMEM165, and its yeast homolog, Gdt1, still remains to be completed in the future. The stoichiometry of transport will be particularly important in determining whether the activity of Gdt1/TMEM165 contributes to a charge imbalance that would have to be corrected by some other mechanism. Movement of only one proton out of the Golgi while moving a divalent cation like Ca^{2+} or Mn^{2+} make the Golgi lumen more positive. Alternatively, if two protons are transported to the cytoplasm for every metal transported into the lumen, the net charge would remain unchanged. The mechanism by which calcineurin regulates the activity of Gdt1, as well as Vcx1, remains to be identified. Further genetic screening is required to find the direct target of calcineurin that influences the activity of these exchangers. Since calcineurin is required for response to pH-induced stress in fungi (Nakamura *et al.* 1993), it is possible that it inhibits Gdt1 and Vcx1 by modulating the pH of the cytoplasm or Golgi, thereby modifying the pH gradient.

A recent study determined that when V-ATPase activity is lost, calcineurin is required for the rapid internalization of the proton pump Pma1, which is responsible for removal of protons from the cytoplasm, from the plasma membrane. This occurs via a mechanism mediated by Rim8 and Rsp5 (Velivela and Kane 2017). This study also provided evidence that internalization of Pma1 not only prevents cellular loss of protons, but it also compensates for loss of V-ATPase activity by re-distributing Pma1 to acidify other cellular compartments, such as the endosome (Velivela and Kane 2017). As the data presented in Chapter 2 show, loss of V-ATPase activity causes Vcx1 and Gdt1 to function in reverse-mode, acidifying the vacuole and Golgi at the expense of Ca^{2+}, provided by Pmc1 and Pmr1. This would result in an increase in the cytoplasmic

concentration of Ca^{2+}, activating the calcineurin response pathway, and triggering internalization of Pma1 to compensate. This model would be consistent with the data presented in Chapter 2, as calcineurin activation during high Ca^{2+} stress would internalize Pma1, and decrease the pH of the cytoplasm, limiting the pH gradient by which Gdt1 and Vcx1 function.

Additionally, it has not yet been determined whether calcineurin similarly effects TMEM165 in mammalian cells. Since some studies have shown that supplementation with galactose or Mn^{2+} can restore glycosylation to TMEM165-deficient cells and/or patients, similar analyses should also be conducted in mice to determine if similar supplementations can restore normal lactose synthesis and litter weight gain to nursing pups. Supplementation can be achieved by providing the mice with high-galactose food or regular injections.

A potentially versatile tool provided in this dissertation is the establishment of a method for screening the collection of auxin inducible degron (AID) tagged essential genes to find specific targets of small molecule inhibitors, described in Chapter 4. The study of essential genes is difficult, since the inability to eliminate the genes requires generation and analysis of point mutations, which can be very arduous, or analysis of heterozygous strains, which has limited efficacy due to the presence of one functional allele in the strain. The AID-tagged collection of yeast enables the user to rapidly and reversibly target a given protein for degradation by addition of auxin. This enables the strain to be analyzed for acute effects of protein loss. An example of this method being utilized is presented in Chapter 2, where an AID-tagged version of Vrg4 was utilized to inhibit glycosylation by blocking transport of GDP-mannose into the Golgi apparatus,

thus eliminating the source of the Pi secreted in the absence of Erd1. Due to the essential nature of Vrg4, this experiment would have otherwise been unachievable, as glycosylation would not be sufficiently blocked in a strain that was heterozygous for *VRG4*.

The further versatility of the system was established in Chapter 4, where it was shown that the AID tag sufficiently dampened the expression of a protein to increase the sensitivity of the strain to an inhibitor of the tagged protein. This means that the whole collection can be screened for hypersensitivity to a drug to identify candidate genes and pathways that may be targeted by the drug. Further analysis can be conducted using the checkerboard assays outlined in Chapter 4, which look for synergism or antagonism between auxin and a given drug when used in combination on an AID-tagged strain. When the two drugs display synergism, they are likely targeting similar proteins or pathways, and thus, this method may be utilized to elucidate targets and mechanisms of drugs and antifungals, as demonstrated with SDZ 90-215 being confirmed as an inhibitor of Vrg4.

While the AID collection and the methods described in Chapter 4 may be utilized identifying targets of new antifungals and inhibitors for future use in research and medicine, they may also be adapted for use in other scientific pursuits. For example, a longstanding question, regarding essential genes, is how to distinguish between genes that are required for cell survival and those that are required for cell proliferation. This may be more easily distinguished by introducing auxin to the collection and screening for strains that have an increased incidence of cell death, such as through the use of staining with propidium iodide, which is only permeable to yeast after cell death has occurred

(Madeo *et al.* 1997). If the auxin-induced depletion of an essential protein does not exhibit increased cell death, it is likely that the protein is required for growth, but not survival. Similarly to the use of the AID-tagged Vrg4 strain in Chapter 2, individual strains from this collection, even ones with known and fully characterized functions, may be analyzed in the presence of auxin to elucidate pathways and mechanisms that are otherwise masked or blocked by the activity of essential genes with no commercial inhibitors. This potentially opens the door for numerous lines of research and experimentation that would otherwise be prevented by the inability to block the activity of an essential gene.

Glycosylation has been well characterized during the decades-long study of the process and the hundreds of genes involved. However, an increasing number of congenital disorders of glycosylation have been identified in the recent past (Scott *et al.* 2014), emphasizing the requirement for additional research into the pathways that influence glycosylation and treatments that could aid the growing number patients with these congenital disorders. The data presented in this dissertation provide insight into some of the genes that influence glycosylation. The methods presented may be utilized in the future for further mechanistic analysis of the pathways involved in glycosylation and potentially for the discovery of treatments that could support patients with glycosylation disorders.

REFERENCES

Blomen, V. A., P. Májek, L. T. Jae, J. W. Bigenzahn, J. Nieuwenhuis *et al.*, 2015. Gene essentiality and synthetic lethality in haploid human cells. Science 350: 1092–1096.

Capasso, J., and C. Hirschberg, 1984. Mechanisms of glycosylation and sulfation in the Golgi apparatus: evidence for nucleotide sugar/nucleoside monophosphate and nucleotide sulfate/nucleoside monophosphate antiports in the Golgi apparatus membrane. Proc National Acad Sci 81: 7051–7055.

Colinet, A.-S., P. Sengottaiyan, A. Deschamps, M.-L. Colsoul, L. Thines *et al.*, 2016. Yeast Gdt1 is a Golgi-localized calcium transporter required for stress-induced calcium signaling and protein glycosylation. Sci Rep-uk 6: 24282.

Madeo, F., E. Fröhlich, and K.-U. Fröhlich, 1997. A Yeast Mutant Showing Diagnostic Markers of Early and Late Apoptosis. J Cell Biology 139: 729–734.

Mukherjee, P., S. Banerjee, A. Wheeler, L. A. Ratliff, S. Irigoyen *et al.*, 2015. Live Imaging of Inorganic Phosphate in Plants with Cellular and Subcellular Resolution. Plant Physiol 167: 628–638.

Nakamura, T., Y. Liu, D. Hirata, H. Namba, S. Harada *et al.*, 1993. Protein phosphatase type 2B (calcineurin)-mediated, FK506-sensitive regulation of intracellular ions in yeast is an important determinant for adaptation to high salt stress conditions. Embo J 12: 4063–4071.

Potelle, S., W. Morelle, E. Dulary, S. Duvet, D. Vicogne *et al.*, 2016. Glycosylation abnormalities in Gdt1p/TMEM165 deficient cells result from a defect in Golgi manganese homeostasis. Hum Mol Genet 25: 1489–1500.

Reinhardt, T. A., J. D. Lippolis, and R. E. Sacco, 2014. The Ca^{2+}/H^{+} antiporter TMEM165 expression, localization in the developing, lactating and involuting mammary gland parallels the secretory pathway Ca^{2+} ATPase (SPCA1). Biochem Bioph Res Co 445: 417–421.

Schapiro, F. B., and S. Grinstein, 2000. Determinants of the pH of the Golgi Complex. J Biol Chem 275: 21025–21032.

Scott, K., T. Gadomski, T. Kozicz, and E. Morava, 2014. Congenital disorders of glycosylation: new defects and still counting. J Inherit Metab Dis 37: 609–617.

Sun, H., A. Scharff-Poulsen, H. Gu, I. Jakobsen, J. M. Kossmann *et al.*, 2008. Phosphate sensing by fluorescent reporter proteins embedded in polyacrylamide nanoparticles. Acs Nano 2: 19–24.

Thines, L., A. Deschamps, P. Sengottaiyan, O. Savel, J. Stribny *et al.*, 2018. The yeast protein Gdt1p transports Mn^{2+} ions and thereby regulates manganese homeostasis in the Golgi. J Biol Chem 293: 8048–8055.

Velivela, S., and P. M. Kane, 2017. Compensatory Internalization of Pma1 in V-ATPase Mutants in Saccharomyces cerevisiae Requires Calcium- and Glucose-Sensitive Phosphatases. Genetics 208: genetics.300594.2017.

Intended to be blank.

Nathan Snyder

ns1438@gmail.com

(812)-230-1727

Personal Statement

As a dedicated scientist, I am seeking to expand my expertise in the field of molecular and cellular biology.

Skills

Cellular - Cell/bacterial/fungal culture, Drug/ion tolerance screening, Mating/sporulating yeast (tetrad dissections), Yeast strain generation, Inducible degron systems, Sucrose fractionation gradients, Transport assays, Beta-galactosidase activity assays

Molecular - RNA/DNA extraction/isolation, Primer design, Plasmid cloning, Restriction digests, Ligation, DNA sequencing, PCR, RT-PCR, qPCR, Agarose gels, Genomic integration/tagging

Microscopy - Light microscopy, Fluorescence microscopy, Confocal microscopy, SEM, FISH, In situ

Animal - Mouse handling/breeding/dissection, Genotyping, Frozen tissue sectioning (Cryostat)

Protein/Immunological – protein isolation, SDS-PAGE, Western blotting, TLC

Computational - UNIX and Python coding, ImageJ

General – Lab maintenance, Media preparation, Radioactivity, Buffer preparation, Gas chromatography

Education

Johns Hopkins University

Ph.D. in Biology

July 2012 – Present

Shippensburg University of Pennsylvania

Bachelor of Science in Biology

August 2008 – May 2012

Employment History

Ph.D. Candidate

Lab of Dr. Kyle Cunningham

Johns Hopkins University

May 2013 - Present

Safety Committee

- Biology representative for the Homewood Research Safety Committee
- Head organizer of the Biology Safety Committee
- Safety Coordinator for the lab of Dr. Kyle Cunningham

Teaching Assistantship

- Genetics Lab (2013)
- Cell Biology Lab (2014)
- Advanced Cell Biology (2014, 2015, 2016)
- Cell Biology lecture (2015, 2016, 2017)
- Biochemistry Lecture (2016, 2017)
- Genetics Lecture (2017)

Student Mentoring

- 8 undergraduates (2013-2017)
- 7 graduate rotation students (2015-18)

Conferences/Posters

- 28th International Conference on Yeast Genetics and Molecular Biology (2017) - poster

- Pennsylvania Academy of Sciences (2011) – presented poster
- Celebration of Student Research (2012) – presented poster
- Johns Hopkins CMDB Annual Department Retreat (2015 ,2017) – presented poster
- Colloquium for Kyle Cunningham (2017) – presented poster
- Annual progress report for Johns Hopkins CMDB Department (2015, 2016, 2017) – 30 minute PowerPoint presentation

Publications

Snyder, Nathan A., Stefan, Christopher P., Soroudi, Camille T., et al. (2017). H^+ and Pi byproducts of glycosylation affect Ca^{2+} homeostasis and are retrieved from the Golgi complex by homologs of TMEM165 and XPR1. G3 (Bethesda) 7(12):3913-3924.

Jiang, Linghuo, Wang, Junjun, Asghar, Faiza, Snyder, Nathan A., and Cunningham, Kyle W. (2018). CaGdt1 plays a compensatory role for the calcium pump CaPmr1 in the regulation of calcium signaling and cell wall integrity signaling in Candida albicans. Cell Commun. Signal 16:33.

Snyder, Nathan A., Kim, Adam, Kester, Louis, et al. (2018). Auxin-inducible depletion of the essentialome reveals inhibition of TORC1 by auxins and inhibition of Vrg4 by SDZ 90-215, a natural antifungal cyclopeptide. G3 (Bethesda). [submitted]

Snyder, Nathan A., Palmer, Mitchell V., Reinhardt, Timothy A, et al. (2018). Milk biosynthesis requires TMEM165, a Golgi cation exchanger. JBC. [submitted]

Special Awards

Dean's List

Shippensburg University of PA

Fall 2008, 2009, 2010, 2011

Spring 2009, 2010, 2011, 2012

References

Dr. Kyle Cunningham
Advisor/Professor of Biology
Johns Hopkins University
kwc@jhu.edu
(410) 516-7844

Dr. Trina Schroer
Professor of Biology
Johns Hopkins University
schroer@jhu.edu
(410) 516-5373

Dr. William Patrie
Associate Professor of Biology
Shippensburg University of PA
wjpatr@ship.edu
(717) 477-1400